Valley Widening and the Composite Nature of Valley Margin Sequence Boundaries: Evidence from the Neilson Wash Compound Valley Fill, Cretaceous Ferron Sandstone, Utah

---

A Thesis Presented to

the Faculty of the Department of Earth and Atmospheric Sciences

University of Houston

In Partial Fulfillment

of the Requirements for the Degree

Master of Science

By

Christopher Eric Campbell

May 2013

Valley Widening and the Composite Nature of Valley Margin Sequence Boundaries: Evidence from the Neilson Wash Compound Valley Fill, Cretaceous Ferron Sandstone, Utah

Christopher Eric Campbell

APPROVED:

Dr. Janok P. Bhattacharya, Chairman

Dr. William Dupre

William Hill

Dr. Dan Wells, Dean
College of Natural Sciences and Mathematics

Acknowledgements

I would like to thank Dr. Janok P. Bhattacharya both for his guidance and for his seemingly unending patience. To my thesis committee members William Dupre and William “Bill” Hill, I would also like for their advice and support over the years. To everyone at BP that helped me, from the managers who gave me the time off to go to the field, to all of the geoscientists who encouraged me to pursue my Master’s degree, thank you. I would also like to thank BP, Anadarko Petroleum Corp., ExxonMobil, Shell, Nexen, BHP Billiton, and Pioneer Natural Resources for their generous support of the Quantitative Sedimentology Laboratories who funded this research. And finally I would like to thank my family and my friends – I’m going to make it up to you for every time I was too busy. And last, but certainly lot least, I would like to thank my brother for I could not have done this without him.

Valley Widening and the Composite Nature of Valley Margin Sequence Boundaries: Evidence from the Neilson Wash Compound Valley Fill, Cretaceous Ferron Sandstone, Utah

---

An Abstract of a Thesis

Presented to

the Faculty of the Department of Earth and Atmospheric Sciences

University of Houston

In Partial Fulfillment

of the Requirements for the Degree

Master of Science

By

Christopher Eric Campbell

May 2013

Abstract

Incised valleys are at the center of a debate about whether sequence boundaries are chronostratigraphically significant. Current research has suggested that the sequence boundary that makes up the floor and walls of an incised valley is constantly being modified throughout the entire relative sea-level cycle. This would imply that sequence boundaries are strongly diachronous composite surfaces. New models of incised valley evolution show that incised valleys continue to widen as they are being filled which is in disagreement with existing models of valley evolution. The Cretaceous Ferron Sandstone in Neilson Wash, located west of Hanksville, Utah, contains a well exposed compound valley fill. The Ferron Sandstone in the study area was deposited as part of the Notom Delta that prograded into the Henry Mountains Basin from the southwest. From measured sections and digital photographs a detailed bedding diagram of the fluvial and facies architecture of the fill was completed. The data shows that the outcrop is one of a compound valley system made up of multiple cut and fill episodes. These terraces were formed by a series of relative sea-level fluctuations over a period of ~ 100,000 years. The oldest valley terraces shows tidal influence and are perched high in the system. Younger valley fill is coarser and shows mostly fluvial deposits. This is interpreted as a stepped forced regressive valley system. The 100,000-year duration of this cycle suggests relative sea-level changes are driven by glacioeustacy. Analysis of the oldest valley reveals that it widened as it was filled. Wheeler analysis of the compound valley fill reveals that the sequence boundary flooring the compound valley is a composite surface with terrace deposits preserved above it. The presence of terrace deposits above

the sequence boundary is significant. During falling relative sea levels fluvial systems extend out over falling stage deposits along the ramp. These falling stage deposits may be younger than the terrace deposits and should lie below the evolving sequence boundary. This relationship, with older deposits above and younger deposits below the sequence boundary, suggests that sequence boundaries are not chronostratigraphically significant.

Contents

Introduction

Incised valleys provide critical information for interpreting regional geologic history, such as tectonic uplift or subsidence, global sea-level changes, climate, and shifts in depositional environments (Ardies et al., 2002; Strong & Paola, 2008; Martin et al., 2011), and are significant hydrocarbon reservoirs (Zaitlin et al., 1994; Ardies et al., 2002; Wellner & Bartek, 2003; Boyd et al., 2006; Gibling, 2006). Knowledge of the internal fluvial architecture of valley fills is critical for understanding how channel connectivity controls fluid flow, which is important for production strategy within this class of reservoir (Miall, 1988, 2006; Zaitlin et al., 1994; Garrison & van den Bergh, 2006). Along with the valleys, the lowstand deltas and associated deepwater facies that valleys convey sediment to, are themselves important hydrocarbon reservoirs (Bhattacharya & Walker, 1992; van Heijst & Postma, 2001; Mattheus et al., 2007; Martin et al., 2011). Because of this, there is interest in understanding what controls the timing of valley incision and valley geomorphology as it relates to the volume and source (i.e. eroded shelf sands) of sediment found in these more distal environments (van Heijst & Postma, 2001; Mattheus et al., 2007; Strong & Paola, 2008; Martin et al., 2011).

Incised valleys also play an important role in sequence stratigraphic interpretations (Van Wagoner et al., 1990). The unconformity that is the floor and sides of the valley is defined as a sequence boundary, which is a key surface to recognize when attempting to interpret the sequence stratigraphy of an area (Van Wagoner et al., 1990; Zaitlin et al., 1994). The sequence statigraphic organization of valley fills is also significant because systems tracts present within valley fills can be used to predict the fluvial architecture (Shanley & McCabe, 1994; Zaitlin et al.,1994; Blum & Aslan, 2006).

Because incised valleys are a link between marine environments and their contemporaneous alluvial plains, they allow geologists to carry sequence stratigraphic interpretation from the marine realm to the non-marine (Shanley & McCabe, 1994; Blum & Aslan, 2006).

Lately, incised valleys have been at the center of an ongoing debate about the time-transgressive nature of sequence boundaries and whether they are chronostratigraphically significant surfaces (Catuneanu et al., 1998; van Heijst and Postma, 2001; Törnqvist et al., 2003; Blum & Aslan, 2006; Korus et al., 2008; Strong & Paola, 2008; Bhattacharya, 2011, Holbrook & Bhattacharya, 2012). Sequence boundaries are defined as regional chronostratigraphically significant surfaces (unconformities and their correlative conformity) formed by a fall in relative sea level, which separate facies that are temporally and physically unrelated (Van Wagoner et al., 1990). However, research has shown that depositional sequence boundaries may be time transgressive and can separate rocks that are contemporaneous (Catuneanu et al., 1998; van Heijst and Postma, 2001; Törnqvist et al., 2003; Strong & Paola, 2008; Bhattacharya, 2011; Martin et al., 2011, Holbrook & Bhattacharya, 2012). Strong and Paola (2008) illustrated through flume modeling experiments that there can be older fluvial terrace deposits above the sequence boundary and younger falling stage deltaic deposits found below it. This violates the definition of a sequence boundary and illustrates that sequence boundaries may not be chronostratigraphically significant (Strong & Paola, 2008; Bhattacharya, 2011; Holbrook & Bhattacharya, 2012). Bhattacharya (2011) points out that in order for sequence boundaries to be chronostratigraphically significant, a horizontal line drawn through the lacuna in time space should separate older deposits below from younger deposits above. This is not the case when older fluvial terrace deposits are preserved above the sequence boundary while younger falling stage deposits are preserved below it (Bhattacharya, 2011). Strong and Paola (2008) also point out that rivers continue to widen their valleys as they fill, illustrating that sequence boundaries evolve throughout an entire cycle of relative sea level change. The interpretation here is that sequence boundaries are in effect composite surfaces formed from many diastems (Bhattacharya, 2011; Holbrook & Bhattacharya, 2012). In an effort to both resolve these issues concerning the defining characteristics of sequence boundaries, and extend sequence stratigraphic interpretation to non-marine environments, researchers have been focusing on the allogenic and autogenic controls on incised valley dimensions (width, depth, and cross sectional area), plan view shape (sinuosity, tributive valleys, drainage patterns, and gullying), geomorphologic evolution, as well as the architecture and type of fill (Posamentier, 2001; Ardies et al., 2002; Blum & Aslan, 2006; Boyd et al., 2006; Plint & Wadsworth, 2006; Mattheus et al., 2007; Strong & Paola, 2008; Martin et al., 2011). These controls are climate, tectonics, drainage basin size, slope of the shelf vs. slope of the alluvial plain, substrate erodibility, eustasy, fluvial style, valley slope, avulsion frequency, tributary junctions, valley bends, sediment supply, discharge, stream power, flood magnitude and frequency, and most importantly time (Shumm and Ethridge, 1994; Ardies et al., 2002; Blum and Törnqvist, 2000; Blum and Aslan, 2006; Mattheus et al., 2007; Strong and Paola, 2008; Martin et al., 2011).

The Ferron Sandstone Member of the Mancos Shale Formation comprises a series of eastward thinning deltaic clastic wedges, each of which show a transition from marine shoreface and deltaic sandstones into fluvial strata (Gardner, 1995; Garrison & van den

Bergh, 2004; Li et al., 2010). In the Henry Mountains Basin (sensu Gardner, 1995; Garrison & van den Bergh, 2004) incised valleys are found within the top of the Ferron Sandstone of the Notom delta (Li et al., 2010). Along Neilson Wash, the extensive valley exposures provide an opportunity to study a compound valley complex in detail. The focus of this research is threefold: First, conduct a detailed study of the fluvial and facies architecture of the valley fills, second, explore fluvial terrace formation and the diachronous nature of sequence boundaries by looking for evidence of valley widening as they are filling, third, investigate the controls on valley widening in an effort to explain how these valleys evolved.

Regional Geology

The Western Interior Basin is a retroarc foreland basin found along the eastern margin of the Sevier fold and thrust belt (DeCelles & Coogan, 2006). This basin was created during the Sevier Orogeny in response to both loading of the crust (thickening) in the Sevier fold and thrust belt, and long wavelength subsidence due to mantle dynamics (Pang & Nummedal, 1995; DeCelles, 2004). The Western Interior Seaway was created by a marine transgression that, by late Albian time, had flooded the Western Interior Basin (Fig. 1) (Plint & Wadsworth, 2003; DeCelles, 2004). At its maximum, the Western Interior Seaway connected the Gulf of Mexico in the south to the Northern Boreal Sea to the north (Plint & Wadsworth, 2003; Bhattacharya & MacEachern, 2009; Zhu et al., 2012). However, the Western Interior Seaway was never very deep, with maximum water depth estimates ranging from 500m to 600m (Pang & Nummedal, 1995).

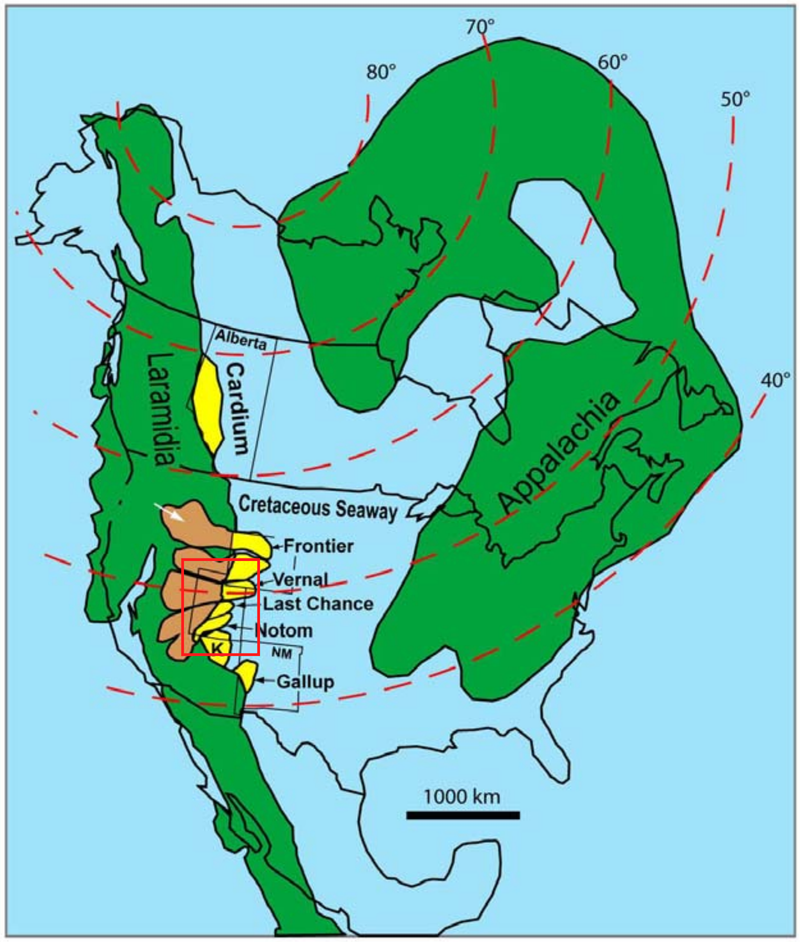

Figure 1. Turonian Paleogeography of North America illustrating the Western Interior Seaway and the major depocenters along its western flank (modified from Bhattacharya and MacEachern, 2009). The red box outlines the location of figure 2.

The Ferron Sandstone Member of the Mancos Shale Formation was deposited during the middle Turonian to late Santonian stages in two deltaic complexes that prograded out into the Western Interior Seaway along its western margin (Fig. 2) (Peterson and Ryder, 1975; Gardner, 1995; Garrison & van den Bergh, 2004; Zhu et al., 2012). These complexes are the Vernal Delta Complex, located in north-central Utah, and the Southern Utah Deltaic Complex in central and southern Utah (Fig. 2) (Garrison &

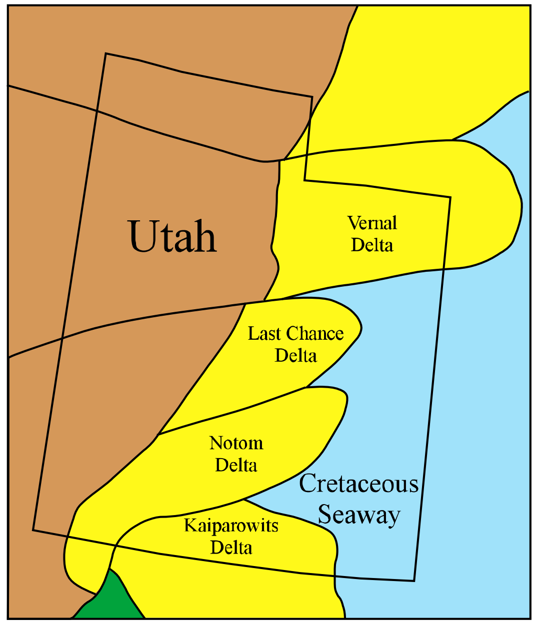

Figure 2. Paleogeography of Utah during the Turonian illustrating the four major deltaic complexes (modified from Bhattacharya and MacEachern, 2009).

van den Bergh, 2004). The Southern Utah Deltaic Complex is composed of the older Notom Delta (the southern lobe) and the younger Last Chance Delta (the northern lobe) (Fig. 2) (Garrison & van den Bergh, 2004). The Ferron Sandstone is a fluvio-deltaic, and upper shoreface sandstone deposited as an eastward thinning clastic wedge composed of sediments derived from the mountains of the Sevier Orogeny to the west (Fig. 3) (Gardner, 1995; Garrison & van den Bergh, 2004; Li et al., 2010; Zhu et al., 2012). The paleolatitude for Utah during the Cretaceous was approximately 45° N to 50° N, and climate at this time is characterized as a greenhouse period (Fig. 1) (Ryer & Anderson, 2004; Gibling, 2006). Climate conditions in Utah at this time were subtropical and humid, as indicated by immature gleysols and abundant coal within the Ferron (Bhattacharya & Tye, 2004; Zhu et al., 2012). The Ferron Sandstone Member divides

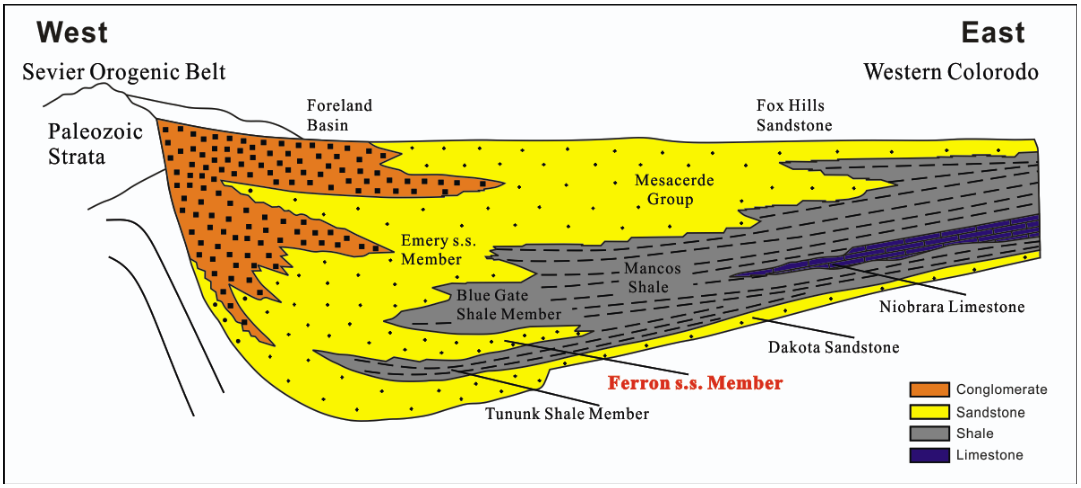

Figure 3. Cross section through the Western Interior Basin illustrating the deposition of various stratigraphic units within the subsiding basin (modified from Montgomery et al., 2004, from Armstrong, 1968).

the Mancos Shale Formation into the Tununk Shale Member below and the Lower Bluegate Shale Member above (Fig. 4) (Garrison & van den Bergh, 2004; Zhu et al., 2012). The Ferron Sandstone is itself divided lithostatigraphically into a lower and upper Ferron (Garrison & van den Bergh, 2004). The upper Ferron Sandstone is considered to be predominately fluvial, while the lower Ferron is composed of shallow marine deposits (Peterson & Ryder, 1975; Ryer & Anderson, 2004). Using flooding surfaces, the upper and lower Ferron Sandstone were placed into two 3rd order composite genetic stratigraphic sequences (Gardner, 1995; Garrison & van den Bergh, 2004). The upper Ferron makes up the *Ferronensis* sequence, and the lower Ferron makes up part of the *Hyatti* sequence (Gardner, 1995; Garrison & van den Bergh, 2004).

The Ferron Sandstone in the study area was deposited in the southwesterly sourced Notom Delta, (Fig. 2) (Garrison & van den Bergh, 2004). The Notom Delta prograded out into a lineament bounded sub-basin of the Western Interior Basin (WIB)

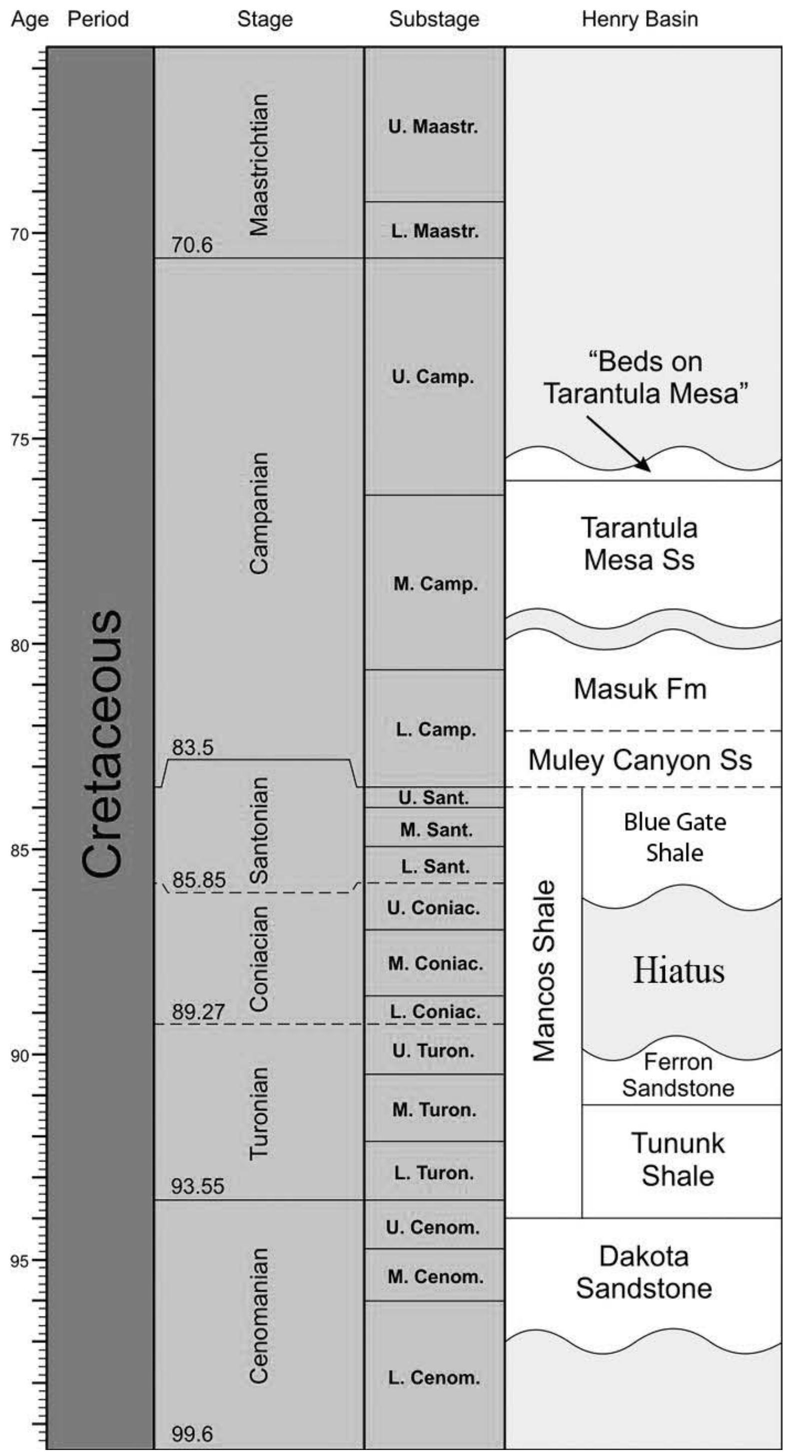

Figure 4. Stratigraphic column of the Henry Mountains Basin (from Zhu et al., 2012, modified from Fielding, 2010).

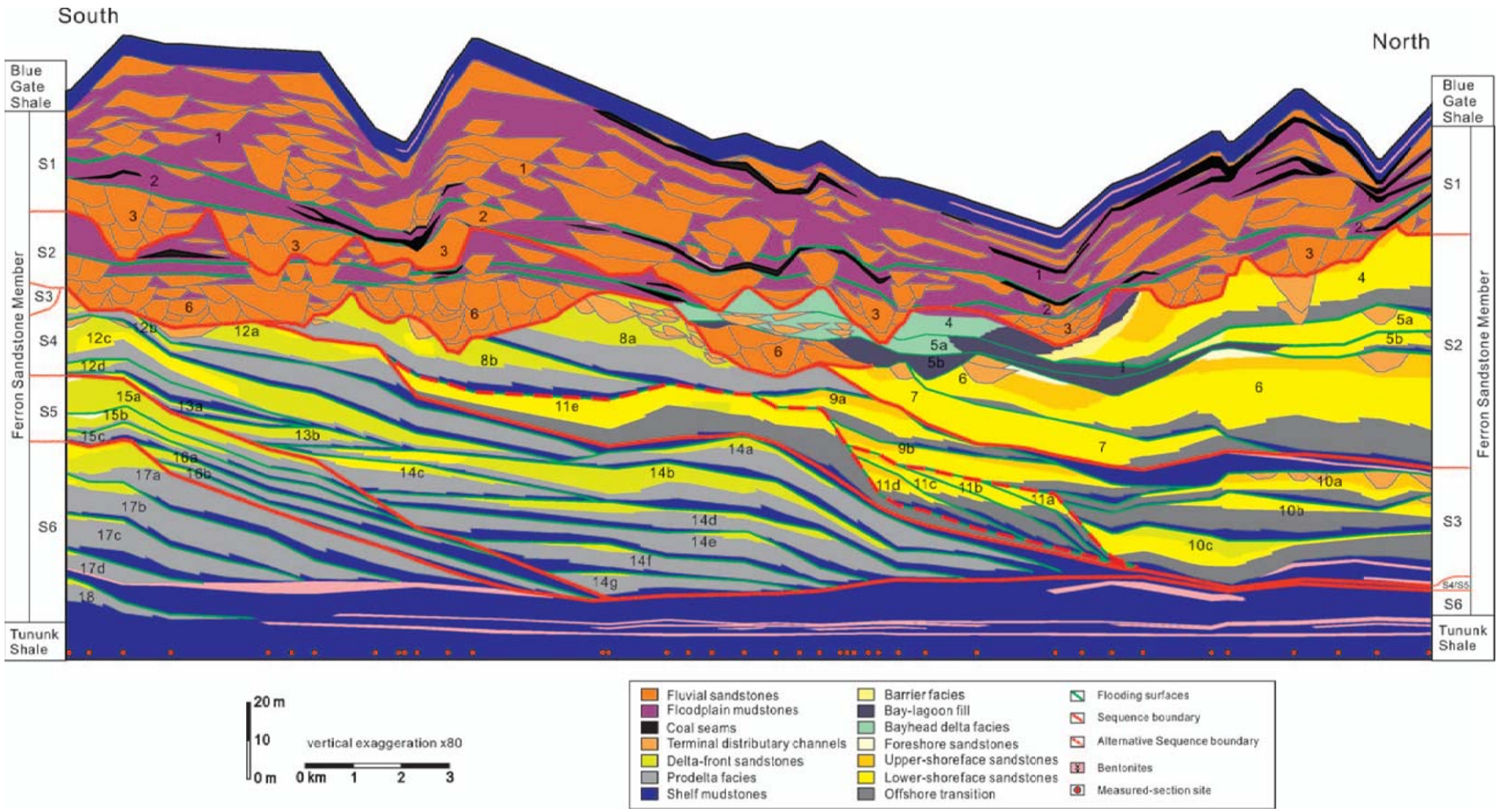

Figure 5. Regional dip section through the Notom Delta illustrating the delta's division into 6 sequences, 18 parasequence sets, and 43 parasequences which were deposited over 640,000 years (from 91.25 to 90.63 ma) (from Zhu et al., 2012).

called the Henry Mountains Basin (HMB) (Gardner, 1995; Garrison & van den Bergh, 2004). $^{40}Ar/^{39}Ar$ age dates from sanidine crystals found in bentonite beds at the base of the Notom Delta indicate that the delta prograded into the area around 91.25 $\pm$ 0.77 Ma (Zhu et al., 2012). The Notom delta is composed of 43 parasequences collected into 18 parasequence sets (Fig. 5) (Zhu et al., 2012). These parasequence sets display degradational, progradational, aggradational, and retrogradational stacking patterns, and are grouped into 6 sequences (Zhu et al., 2012). The Neilson Wash compound incised valley is incised into parasequence 4 and the underlying unconformity at its base is sequence boundary 1 (Li et al., 2010; Zhu et al., 2012). Using radiometric ages it is calculated that the entire Notom delta was deposited over a period of ~ 620,000 years (Zhu et al., 2012). This gives an approximate time span for each of the sequences of approx. 100,000 years (Zhu et al., 2012). The high frequency nature of these cycles suggests that they are driven by variations in global ice volume associated with Milankovitch cycles (Li et al., 2010; Zhu et al., 2012). These high frequency fluctuations in global sea level are overprinted upon the second order regression of the Greenhorn Sea (Sethi & Leithold, 1994). This situation is favorable for the formation of incised valleys formed by multiple cutting and filling events, much like the Quaternary compound valleys observed along the Texas Gulf Coast (Blum & Aslan, 2006).

Study Location, Methods, and Data

Field work conducted intermittently from the summer of 2006 to the fall of 2008 has revealed a well exposed compound incised valley within the Cretaceous Ferron "Notom" Delta in southern Utah. The research area is located within Neilson Wash on

Factory Bench, which lies west of Hanksville, Utah (Fig. 6). Neilson Wash is an arroyo with vertical and near vertical walls up to 35 m high in the study area. In this study area two branches of the wash join together, which allows for mapping of the incised valleys in 3 dimensions (Fig. 6). The main outcrop that is the focus of the proposed research is the easternmost cliff in the study area.

Data collected in the field includes 13 measured sections and hundreds of digital photographs (Fig. 7). Data for the measured sections was collected using a hand lens, tape measure, grain size card, Jacob staff, a Brunton compass, and a rock hammer. Grain size, paleocurrent direction, sedimentary structures, trace fossils, and preserved cross-set thicknesses were measured for the sections. The measured sections were assembled digitally and a cross section was made. The datum used to hang the measured sections isthe base of parasequence 4. Using the digital photographs as a guide, a bedding diagram of the fluvial architecture was made. Using the techniques of Miall (1992) each of the bounding surfaces were ordered from 1st to 8th order surfaces. Again using the measured sections and photographs grain sizes and facies variability were mapped across the cross section. The bedding diagram was then color coded to illustrate grain size and sedimentary structures. Estimates for flow depth were obtained by using the methods of LeClair and Bridge (2001). Paleocurrent measurements were compared to the bedding diagram in order to distinguish between lateral, downstream, and upstream accretion. Using the detailed bedding diagram as a guide, a Wheeler diagram was assembled of the outcrop in order to analyze and illustrate the relative age of the valley fill deposits (Fig. 38).

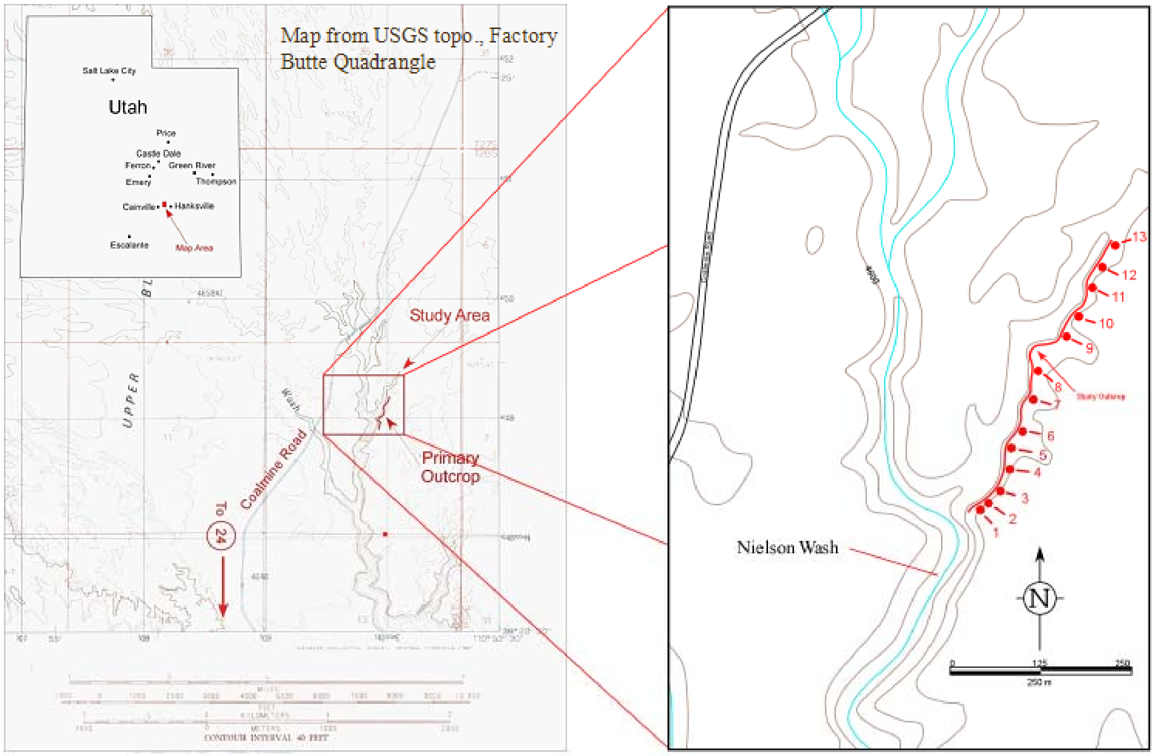

Figure 6. Study location in Neilson Wash west of Hanksville, Utah and locations of measured sections.

Neilson Wash Compound Valley Architecture and Fill

Field research has found that the outcrop exposure is that of a compound valley fill. There are two main trunk valley systems within the field area; valley 1 (younger) and valley 3 (older), as well as tributary valleys 2A and 2B. The criteria used for recognizing these valleys are: (1) there is an abrupt basinward shift in facies across a sharp erosional contact (2) the beds underlying the erosion surface are truncated (3) depths of incision are greater than the channel depths (4) valley fill deposits onlap and downlap onto the valley contact (2) the beds underlying the erosion surface are truncated (3) depths of incision are greater than the channel depths (4) valley fill deposits onlap and downlap onto the valley

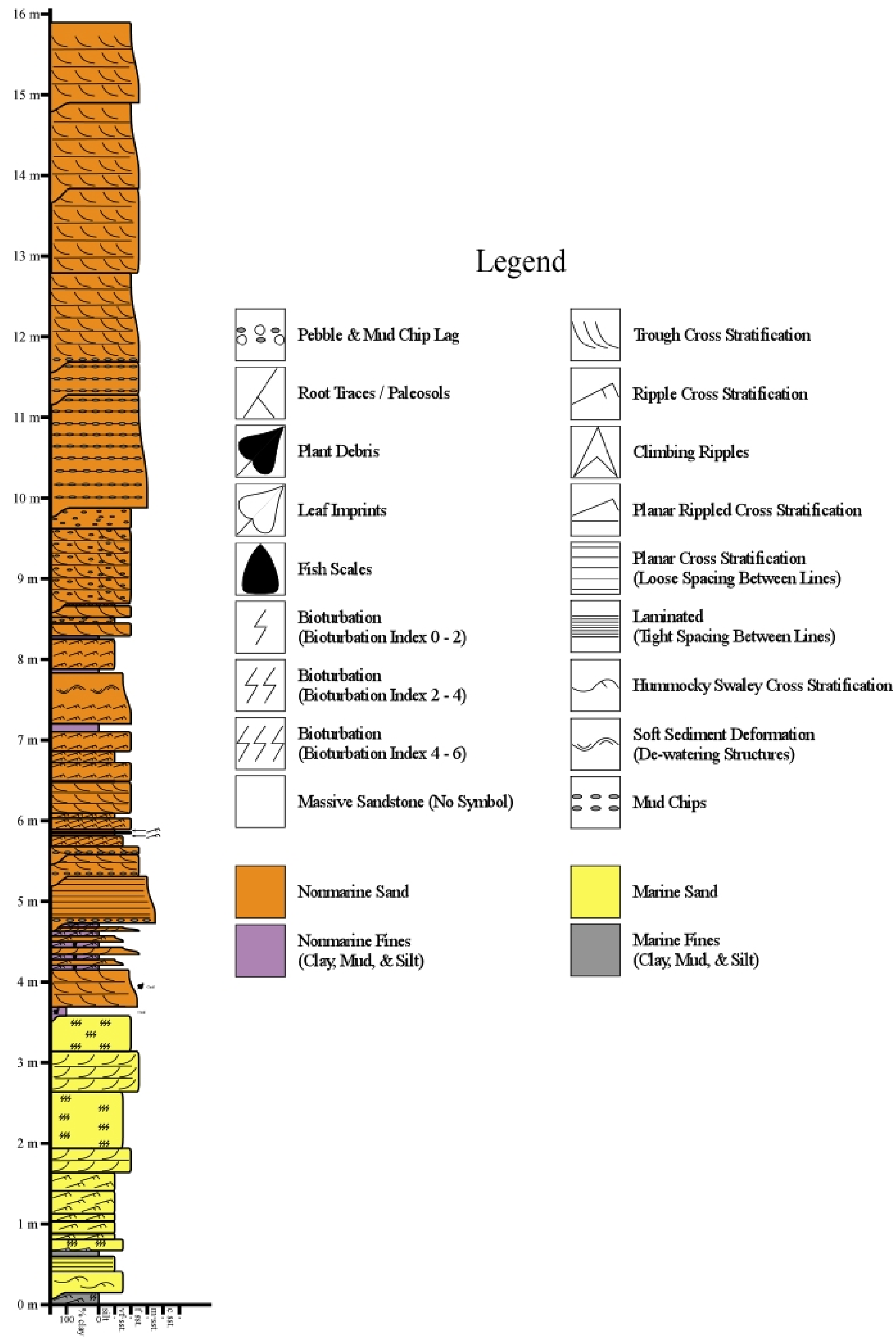

Figure 7. Example measured section (section #2) with symbols.

floor and margins (5) interfluves that can be mapped out regionally (6) the presence of smaller tributary valleys. Furthermore, there is evidence of fluvial terraces. The compound valley is filled with deposits from 4 separate cut and fill events. The valley fill deposits are fluvial (with varying degrees of tidal influence), floodplain, and estuarine deposits. Criteria used to distinguish the separate valley incision and backfilling events are: (1) distinct erosion surfaces cross cutting older cut and fill deposits, (2) the facies of the fill bounded by these erosion surfaces, (3) the degree of tidal influence within the fluvial facies, (4) their depth of incision, (5) observed channel depths, and (6) paleohydraulics.

The valley in the study area is referred to here as the Neilson Wash compound valley system because there are both trunk and tributary stratigraphic valleys and their fills preserved in outcrop. The Neilson Wash compound valley system was incised into the coastal plain in response to multiple fluctuations in relative sea level. These valleys incised into lower shoreface deposits (Facies Mls., Table 1) of parasequence 4. A minimum of five incision and fill episodes went into the formation of this compound valley system. The valley deposits preserved in outcrop are termed here valley 3A (V3A), valley 3B (V3B), valley 2A (V2A), valley 2B (V2B), and valley 1 (V1) (Fig. 8). The paleoshoreline direction during this time, based on the strike of wave ripples, ran approximately north-northwest to south-southeast (Fig. 9a) (Li et al., 2010). These valleys incised into parasequence 4. This parasequence measures 16 meters thick from its base to its top and is primarily composed of lower and upper shoreface deposits.

Facies	Lithology	Biota	Sedimentary Structures
Fluvial Sandstone (Fl)	Very fine- to medium-grained sandstones, few coarse grained sandstones, extrabasinal grains. Pebble lags, mudstone rip up clasts, mud drapes, fining upward.	Logs, plant material, minor amounts of coal, no apparent burrowing.	Dune- and ripple-scale trough cross stratification, planar beds, massive beds, soft sediment deformation, mud rip-up clasts.
Large Scale Inclined Strata (Fls)	Medium- to fine-grained sandstone, fining upward.	No plant material and no apparent burrowing.	Cross beds (avalanch faces) approx. 1 meter thick draped with dune scale trough cross stratification
Tidally Influenced Fluvial (Ft)	Medium- to very fine-grained sandstones interbedded with mudstones, fining upward.	Leaf impressions, some plant material, *Planolites* burrows, *Beakonites.*	Dune- and ripple-scale scale trough cross stratification (some displaying bi-directional paleocurrent indicators), planar cross stratification, climbing ripples, double mud drapes, mud draped dune slipfaces, soft-sediment deformation
Abandoned Channel (Ac)	Very fine-grained sandstones, silt and mudstones.	Plant material and abundant leaf impressions. Coal seams. No apparent burrows.	Ripple-scale cross lamination, rare dune scale cross stratification, planar laminated silt and mud.
Floodplain (Fpl)	Coals, carbonaceous shale, and mudstones. Very fine-grained sandstone crevasse splays, paleosols.	Abundant organic material, leaf imprints, root traces.	Dune and ripple cross stratification (splays), planar lamination, slickensides, massive.
Inclined Heterolithics (Ih)	Very fine- to fine-grained sandstones with abundant silt and mud drapes.	Logs at channel base, plant material, leaf impressions, *Arenicolites* and *Planolites* burrows.	Ripple-scale cross stratification, Dune scale trough cross stratification, climbing ripples, double mud drapes, reactivation surfaces, ladderback ripples, soft-sediment deformation.
Esturine Muddy Facies (Em)	Primarily mudstone and siltstone with few interbedded very fine grained sandstones.	Leaf impressions, plant material, rare fish scales, no apparent burrows.	Massive, planar lamination, ripple cross stratification, siderite nodules.
Marine (Lower Shoreface) (Mls)	Siltstones interbedded with very fine grained to fine grained sandstones.	Fish scales, some plant material, *Ophiomorpha*, *Chrondrites*, *Thalassinoidies*, *Asterosoma*, *Palaeophycus*.	Hummocky-swaley cross stratification, dune-scale trough cross stratification, ripple-scale cross stratification, planar cross stratification, massive.

Table 1. Major facies identified within the Neilson Wash compound valley.

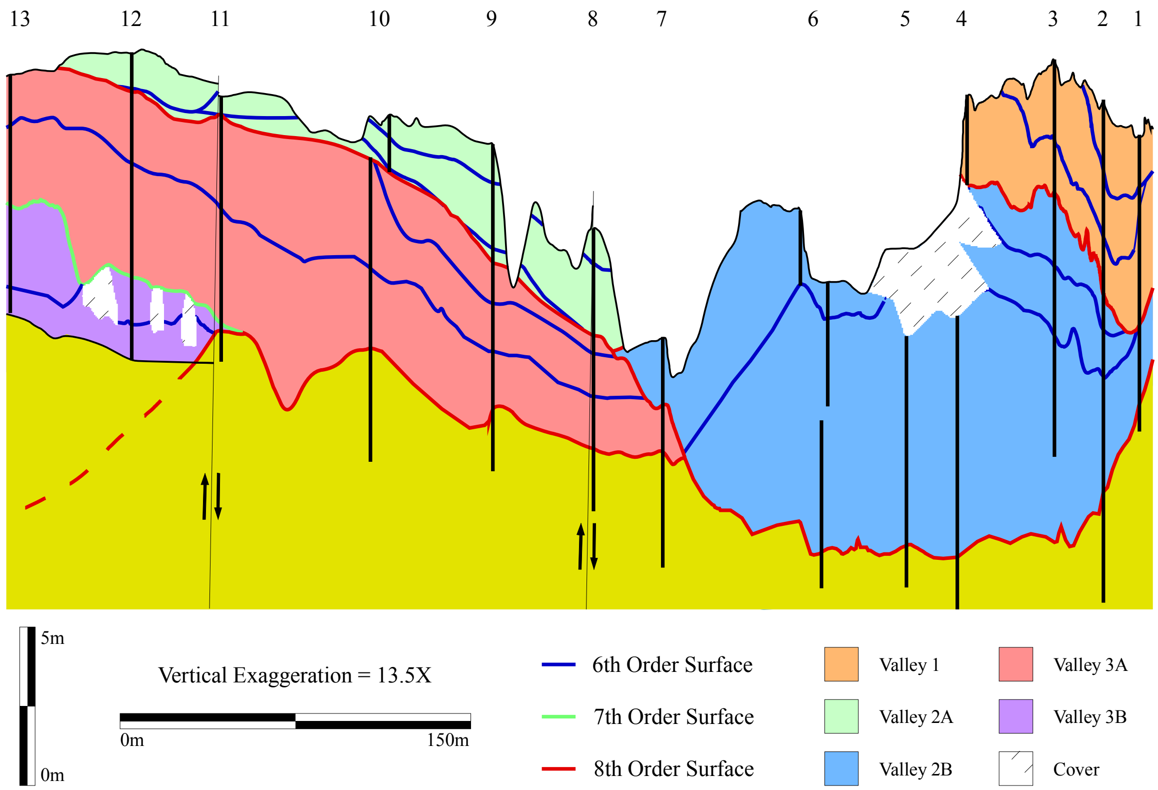

Figure 8. Vertically exaggerated cross section of the study outcrop illustrating the various valley fills. Solid black vertical lines with numbers above mark locations of measured sections. Cross section was structurally restored across the 2 faults.

Valley 3B

Valley 3B (V3B), the oldest valley fill found in the study outcrop, is located in the far northern end of Neilson Wash (Plate 1, Fig. 10). At its thickest there are 4.1 meters of the uppermost portion of the preserved valley fill exposed and its width in outcrop is 91 meters. Only the southern edge of this fill unit is exposed and its basal unconformity dips away northward into the subsurface (Fig. 10). In the study outcrop the top of V3B's deposits lie 19.1 meters above the base of parasequence 4. The base of this exposure, which in this case is the base of the wash, is 15 meters above the base of

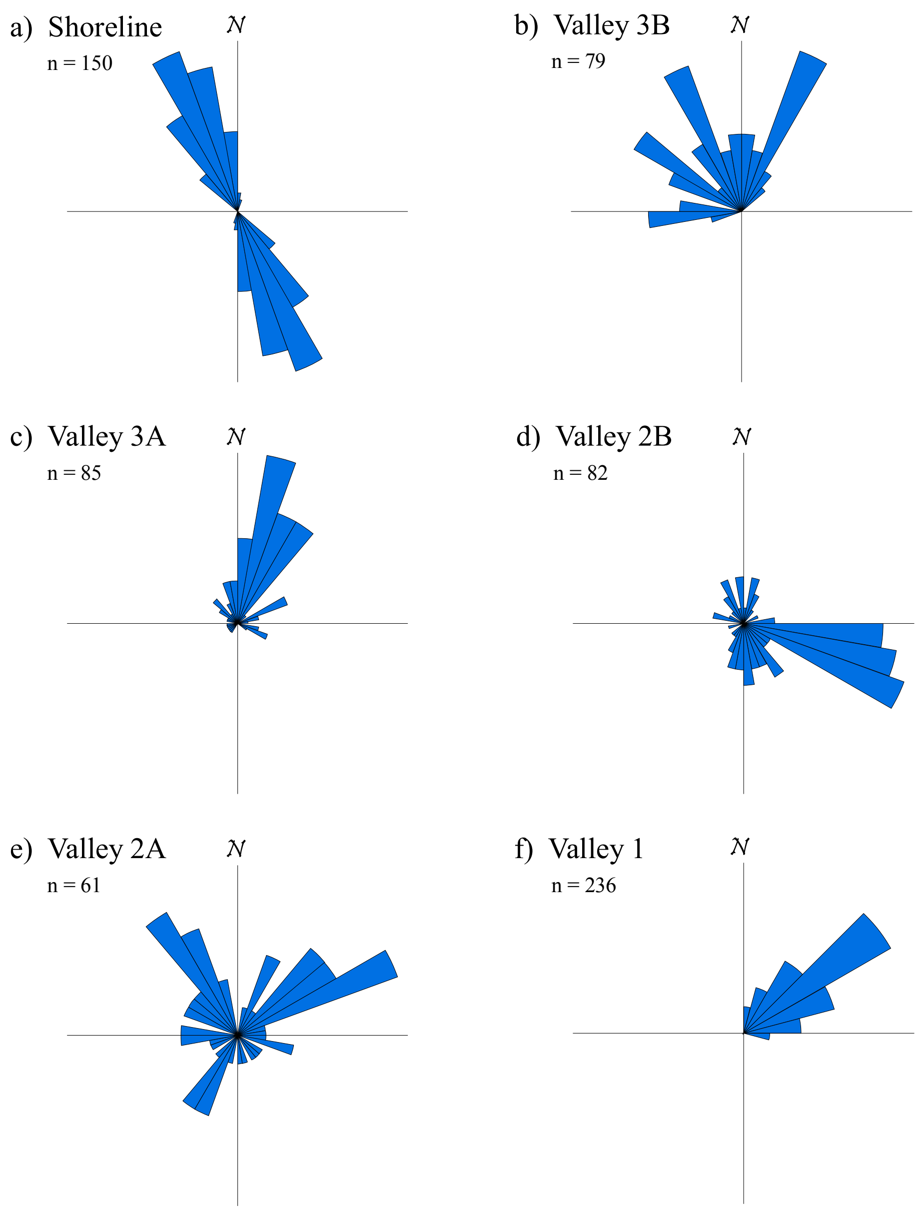

Figure 9. Rose diagrams for the shoreline and valley fills (rose diagrams for valley 1 and shoreline modified from Li et al., 2010).

parasequence 4 (Fig. 10). Across the field area it was observed that the minimum erosional relief for V3B is 10.5 meters, the highest and lowest occurrences are 12.6 m and 2.3 m respectively (above the base of parasequence 4), and the maximum preserved

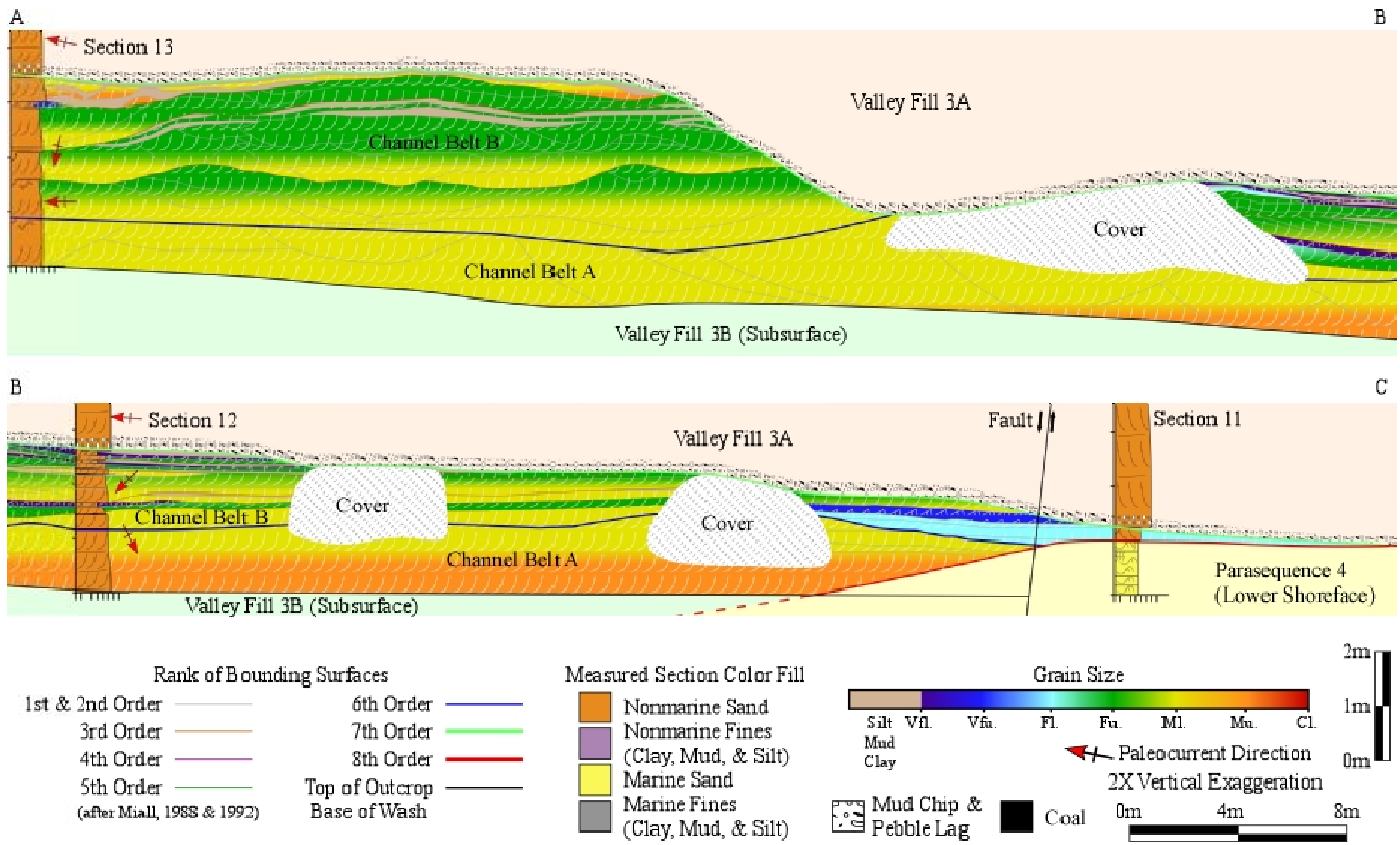

Figure 10. Detailed bedding diagram of valley fill 3B.

thickness is 6.5 meters (Hilton, 2013). The criteria used for identifying this as an incised valley fill are (a) the fill is non-marine (fluvial), (b) it is incised into marine (lower shoreface) deposits of parasequence 4, and (c) there is an abrupt basinward shift in facies across the basal surface (Fig.10). Paleocurrents for both of these channel belts are primarily to the north and the west (Fig. 9b). The basal unconformity underlying V3B is the composite sequence boundary 1 (SB1) (Li et al., 2010; Zhu et al., 2012). This composite sequence boundary is an 8th order surface (*sensu* Miall, 2006) that underlies all of the valley fill throughout the entire field area.

Despite the lack of outcrop exposure there are two very different channel belts exposed (Fig. 10). Only the top one meter of the lower channel belt, channel belt A (CB-A), is exposed above the base of the wash and is found along the width of the valley exposure. The quality of this exposure is somewhat poor and is composed of dune-scale trough cross-stratified sandstones which shows no evidence of tidal influence (Facies Fl., Table 1, Fig 11a and 11b). Grain sizes fine upwards and range from medium upper to medium lower sand. Cross-set thicknesses range from a few centimeters up to 38 cm. Internally there are only 1st order surfaces present separating cross-sets. Channel belt A deposits are bounded on top by a 6th order surface, which is erosive and slightly undulating. This 6th order scour surface is a sharp contact and there is a very high degree of connectivity between the two channel belts (i.e. no mud drapes or floodplain deposits between them).

The upper channel belt, channel belt B (CB-B), is ≤ 2.5 meters thick and runs across the entire width of this exposure (Fig. 10). Trough cross-stratified sandstones make up most of what is preserved in this channel belt with cross-set thickness ranging

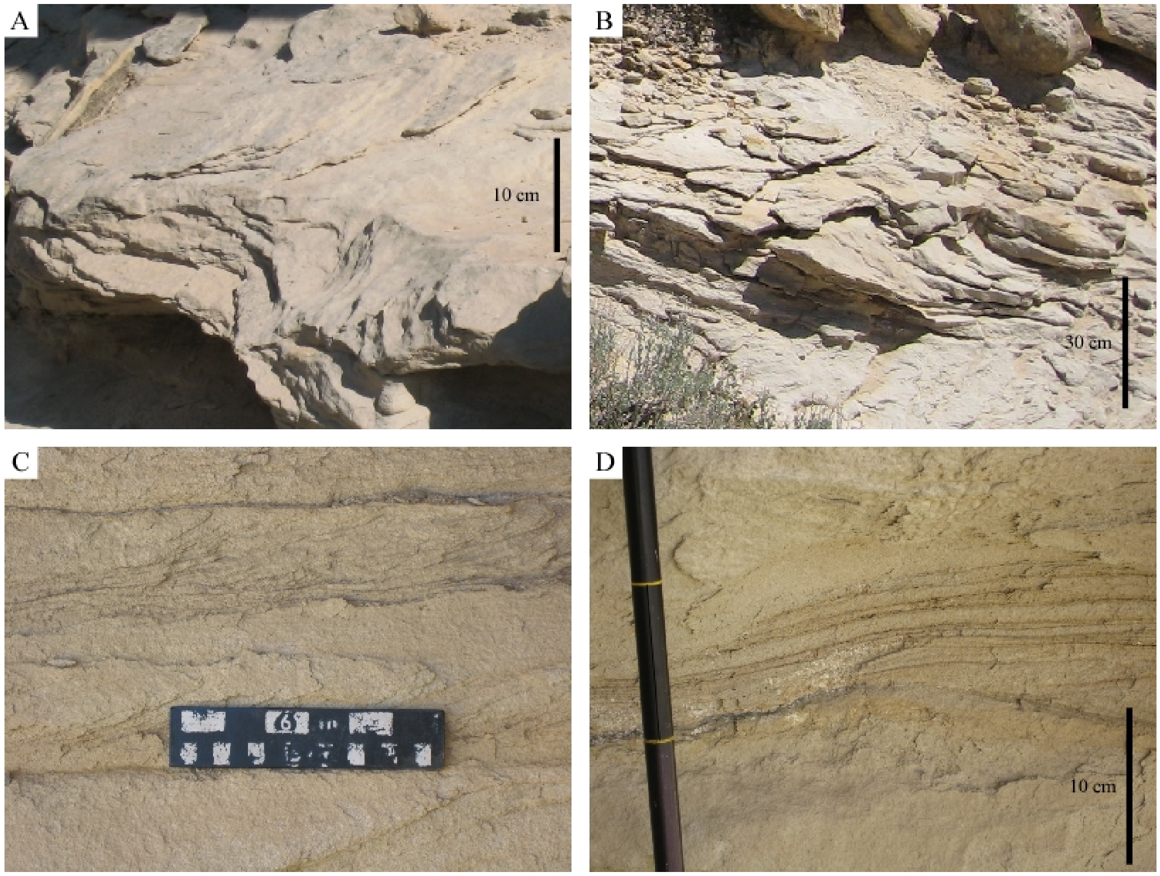

Figure 11. Outcrop close-ups of valley 3B's fill. A&B) Dune scale cross sets of CB-A (Facies Fl). C) Dune scale cross sets of CB-B with mud lamina draping the dune foresets (Facies Ft). D) Double mud drapes within CB-B (Facies Ft).

from 5 to 27 cm. Ripple cross-stratified sandstones are also found capping individual cross-sets. Mudstones are found as either single or double mud drapes, or draping the slipfaces of dune foresets (Facies Ft., Fig. 11c and 11d). Grain sizes for the sands range from medium upper to fine lower-scale in the dune-scale cross-beds, and fine lower to very fine lower in the ripple-scale cross-beds. Flood deposits are upward fining thin units (≤ 1 meter), capped by mud and/or rippled sandstones, and bounded by 3rd order surfaces. These 3rd order surfaces, as well as 2nd, do not have much relief. Not all of this channel belt is preserved as its upper bounding surface is the undulating 7th order surface that was created by the cut and fill episode that is valley 3A. Using cross-set thicknesses from each of the channel belts and the technique of LeClair and Bridge (2001), estimated flow depths for CB-B range from 2.4 to 3.7 meters.

Interpretation

Because of the limited of outcrop it is difficult to make an interpretation regarding the style of formative channels. All that is exposed of CB-A is a single fining upward bed set interpreted as a single flood deposit composed of sinuous crested (3D) dunes. If there were falling stage ripple cross-stratified sands or muds draping this unit, they have been scoured away by the younger channel belt (CB-B). There is a lack of any tidal signature such as flow reversals or double mud drapes within these deposits (Facies Fl, Table 1). Channel belt B is made up of multiple fining upward beds interpreted as flood units that stack to form a compound bar. Each of these flood deposits are downstream accreting sinuous crested dunes that occasionally have ripples preserved on top. The low relief of the 2nd and 3rd order surfaces implies that these 3D dunes were deposited as low relief bars or sand sheets (Holbrook, 2001). Double mud drapes, muddy lamina within dunes, and its heterogeneity suggests that CB-B is a tidally influenced fluvial deposit (Facies Ft, Table 1; Figs. 11c and 11d).

Valley 3A

Valley 3A (V3A) is located along the northern half of the study outcrop and is well exposed throughout the field area (Plate 1, Fig. 12). In the northern limits of

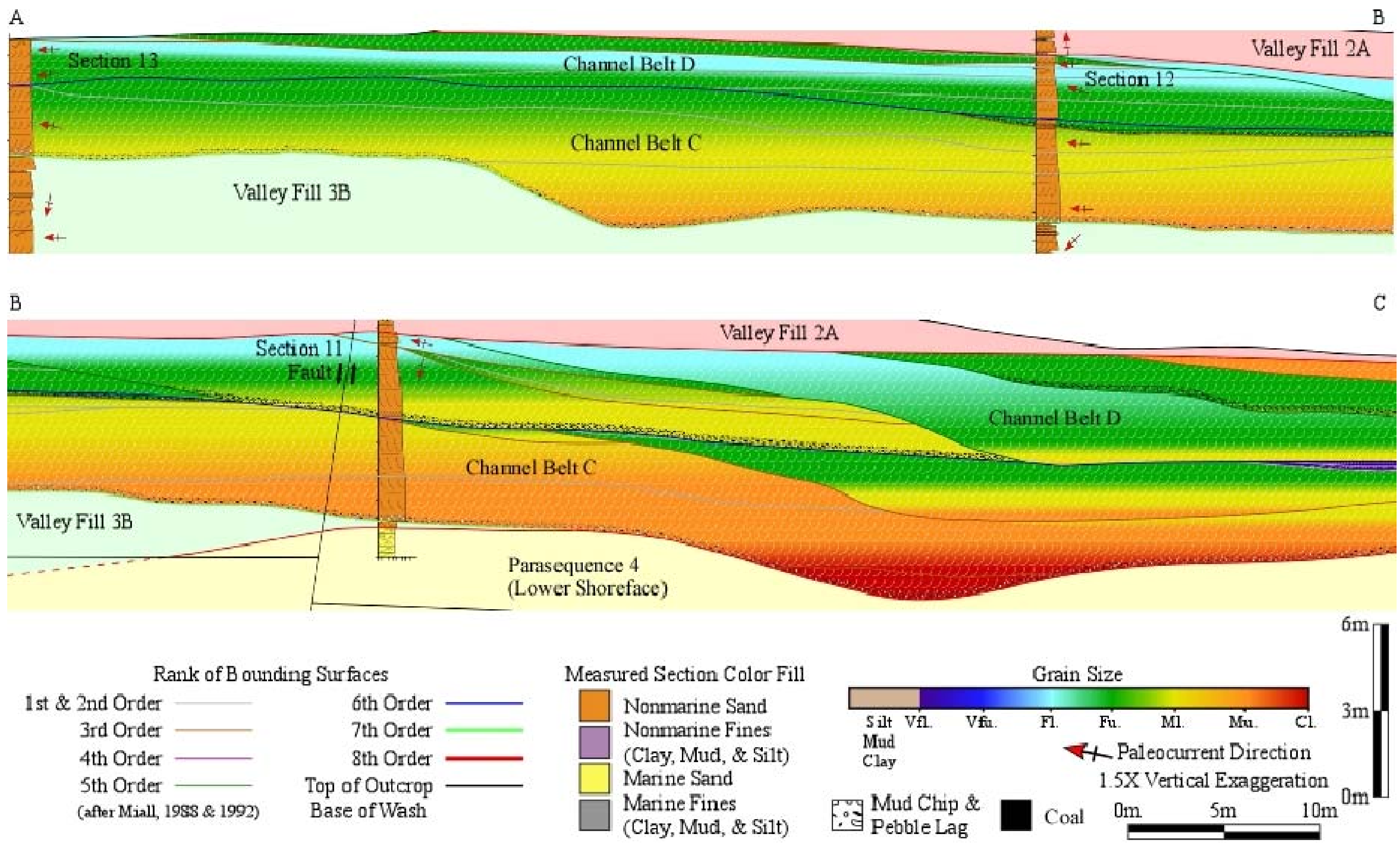

Figure 12. Detailed bedding diagram of the northern half of valley fill 3A.

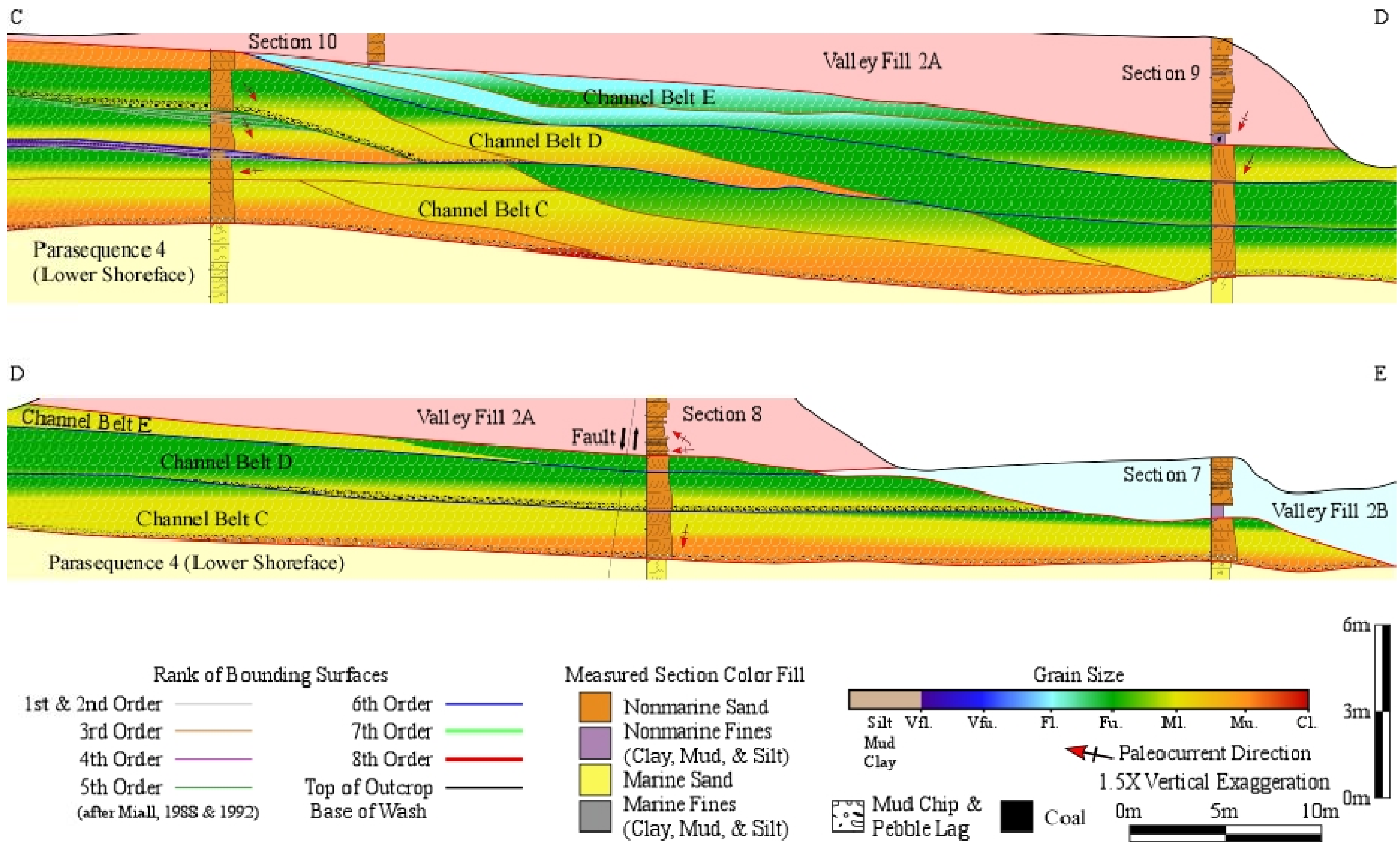

Figure 12 *continued*. Detailed bedding diagram of the southern half of valley fill 3A.

the field area these deposits extend into the subsurface. It is exposed from the northern end of the study outcrop 290 meters south where it is truncated by overlying valley deposits (Plate 1). At its thickest in outcrop it is 8.5 meters high and is made up of three stacked channel belts. In the study outcrop the top of V3A's deposits reach an elevation of 24 meters above the base of parasequence 4. The lowest occurence found in the field area is 4.8 meters above the base of parasequence 4, its highest occurrence is 30.6 meters, its maximum preserved thickness is 16.3 meters, and it has a minimum erosional relief of 7.8 meters (Hilton, 2013). Criteria used to identify this fill as a valley are (a) it truncates the upper portion of the older valley two B as well as marine deposits of parasequence 4 and (b), its erosional relief is greater than one channel depth. The axis of V3A runs roughly north-northeast to south-southwest and paleocurrents are generally north-northeast (Fig. 9c). It is bounded above by an 8th order composite surface and below by a 7th order surface along its northern half, and an 8th order composite surface along its southern exposure (Plate 1, Fig. 12). The 7th and 8th order surface that make up the valley floor is undulating and has a pebble lag, mud chips, and organic material along it (Fig. 13a).

The lowest channel belt of this valleys fill, channel belt C (CB-C), is bounded below by the valley floor already described and above by a 6th order surface that marks the base of the next channel belt. It is present along the entire length of the valley fill and reaches a maximum thickness of 5 meters over the lowest incision point of this valley along the outcrop (Fig. 11). It is composed of facies Fl. (Table 1), and sand grain sizes range from coarse lower to very fine lower, with the majority of the deposits being medium upper to fine upper (Fig. 12). Cross-set thicknesses range from 5 cm to 47 cm (the average is 18 cm) with the thicker cross-sets found at the base of the channel fill. In the northern section of the lower channel belt, paleocurrents are northerly and the 2^{nd} order surfaces within the beds are only slightly undulating (Figs. 12, 13b). Between sections 10 and 11, multiple 3^{rd} order surfaces divide the channel belt into multiple upward fining deposits. The 3^{rd} order surfaces dip towards the south at or less than 19 degrees, and paleocurrents here are westerly (Fig. 12). Individual fining upward units (bounded by 3^{rd} order surfaces) are at least 1 meter in height. Ripple cross stratified sandstone as well as mudstones are present as drapes in the central portion of this channel belt's outcrop (Fig. 13c).

The middle channel belt, channel belt D (CB-D), is also exposed across the entire length of valley 3A's exposure (Plate 1, Fig. 12). Like the lower channel belt (CB-C) it is made up of facies Fl (Table 1). It is bounded below by a 6^{th} order surface that is slightly undulating and has mud chips up to 1 cm in size along it. It is bounded on top by an 8^{th} order composite surface along its northern half, and a 6^{th} order surface along its southern half that marks the base of the next channel belt (Plate 1, Fig. 12). It is found along the entire length of the valley fill (Fig. 12). It reaches a maximum thickness of 4 meters in the center of the valley exposure and tapers at the ends due to erosion (Fig. 12). It has little ripple cross-stratified sands or muds and is made up of trough cross-stratified sandstone. Sand grain sizes range from medium upper to very fine lower with the majority of the deposits being medium lower to fine upper (Plate 1). Individual beds vary in thickness from more than 2 meters to tens of centimeters. Cross-set thicknesses range from 5 cm to 40 cm (the average is 21 cm) with the thicker sets found at the base of the unit. At section 9, the channel deposit is made up of large scale inclined strata

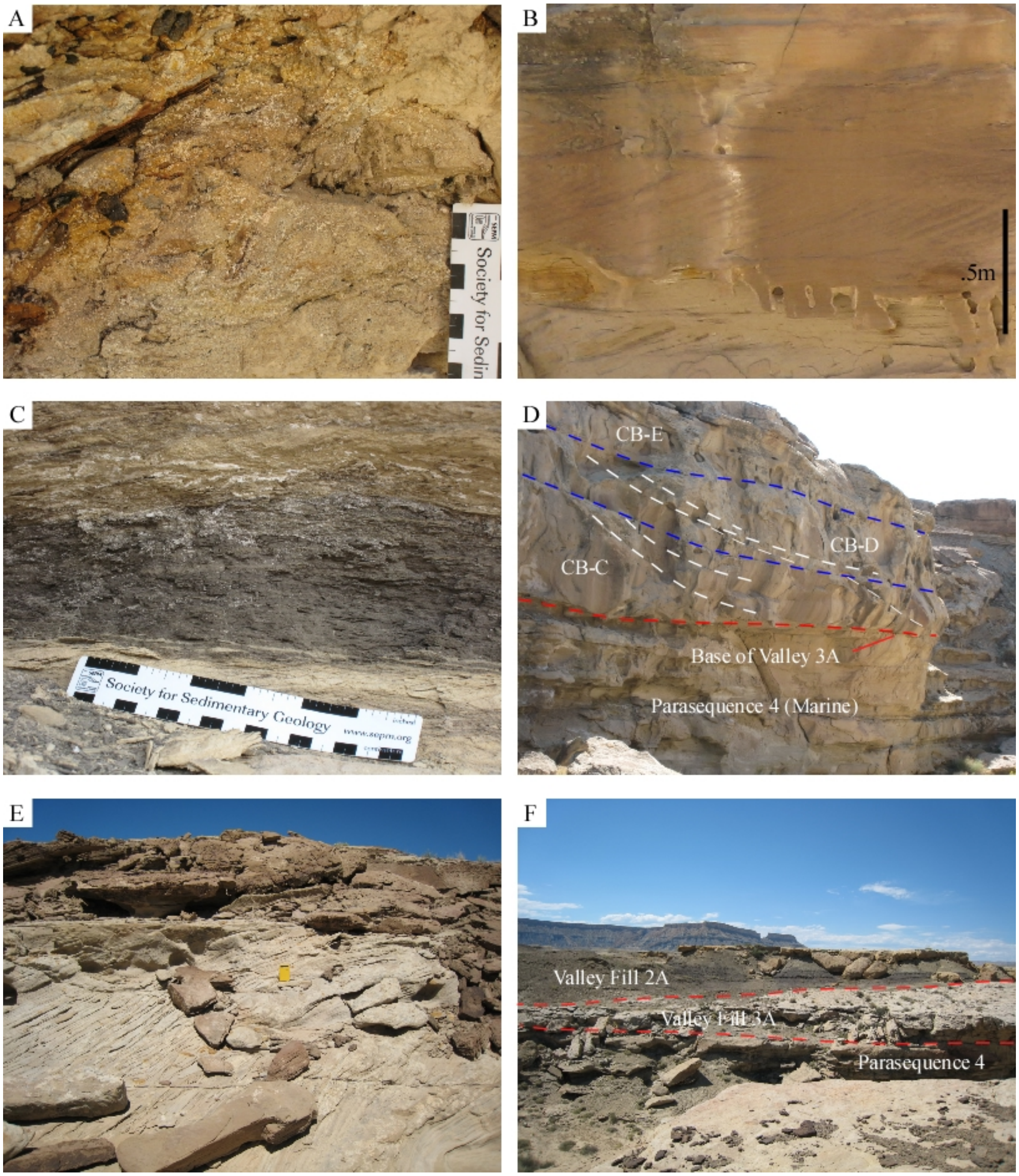

Figure 13. Outcrop photos of valley 3A. A) Lag deposits at the base of V3A. B) Dune-scale cross strata of CB-C. C) Mud drape found along the top of CB-C. D) Southerly dipping lateral accretion surfaces (3^{rd} order) within channel belts C&D. Paleocurrents here are to the west (towards the viewer). E) Large scale inclined strata of CB-E (field notebook in center of photo for scale). F) The truncation of V3A by incision of V2A above it.

migrating west with a preserved thickness of 1.4 meters. In the far northern part of this channel belt paleocurrents are northerly and accretion bedding dips westward (Fig. 12). Starting at section 12 and stretching south, multiple 5th and 3rd order surfaces appear that dip to the south (Figs. 12, 13d). Paleocurrents shift to the west across the first 5th order surface and remain westerly along the rest of the channel belt. Falling stage ripple cross-stratified sandstones and mud are found draping the bar near the middle of this channel belt.

The upper channel belt, channel belt E (CB-E), begins in the middle of the valley fill exposure just south of section 10 and runs south to the end of V3A's outcrop (Plate 1, Fig. 12). It is bounded below by a 6th order surface and above by an 8th order surface (Fig. 12). At the base of the channel belt there is a mud chip lag. The channel belt is thin, only reaching a maximum thickness of just under 2 meters (Fig. 12). Like the two channel belts that preceded it, it is mainly composed of dune-scale trough cross-stratified sandstone of facies Fl., but it has no mudstone or ripple cross-stratified sandstones preserved. Sand grain sizes range from medium lower to fine lower (Plate 1, Fig. 12). Individual beds vary in thickness from tens of centimeters to a little over a meter. In the northern part of the channel belt there are 3rd order bar accretion surfaces that dip to the south with paleocurrents towards the west (Fig. 12). At section 9, all that is preserved of CB-E is a single large cross-set over a meter high migrating west (Figs. 12, 13e). What little of this channel belt that is preserved reveals thin point bar deposits. South of section 9, the channel belt thins quickly due to the overlying valley 2A that truncates it (Figs. 12, 13f).

Interpretation

Valley 3A's deposits found in the study outcrop are resting high up on the southeastern flank of the valley and are interpreted to represent the latest stages of valley filling. The valley fill is primarily made up of laterally accreting point bars with a subordinate amount of large-scale inclined strata and sand sheets. Paleocurrents for the valley fill run primarily to the north and to the west (Fig. 9c). Evidence for sand sheets comes from the northern portions of CB-C where the entire preserved channel belt thickness is filled with one fining upward flood unit (Fig. 12). The paleocurrent direction, in conjunction with the low angle of the internal bedding surfaces, suggest that these deposits are sheet sands made formed by 3D dunes deposited along the base of the channel (Fig. 13b) (Holbrook, 2001). Large-scale inclined strata have individual cross-sets over 1 meter in height (Fig. 13e). Evidence for classifying the majority of these deposits as laterally accreting point bar deposits comes from paleocurrent directions at high angles to the dip direction of the internal bedding surfaces. A good example of this is found in CB-D south of section 12, where a laterally accreting point bar was expanding to the south (Fig 12). The presence of these point bar deposits throughout the fill points out that the fluvial system responsible for these deposits was a single thread meandering stream. These point bars are complex bars built over many flood events. However, very few ripple cross-stratified sands or mud drapes from this meandering system are preserved along the tops of these complex point bars. This is due to the significant amount scour of bar tops by overlying channel belts and, in the case of the youngest channel belt, the erosion by a younger valley. This makes estimating the depth of these channels difficult. The thickest channel belt preserved is the lowest, with a thickness of just over 5 meters (between sections 10 and 11) (Fig. 12). With a minimum erosional relief of 7.8 meters (Hilton, 2013), this means that the valley is greater than the maximum channel depth observed.

Valley 2B

Valley 2B (V2B) is located along the southern half of the study outcrop (Plate 1, Fig. 14). The exposure runs from the southern limit of the study outcrop north approx 226 meters (Fig 14, Plate 1). In the study outcrop and in the field area the highest depth of occurrence is 18.7 meters, the base of the valley is 8.7 meters above the base of parasequence 4, and it reaches a thickness of 10 meters. In the field area V2B has a minimum erosional relief of 29 meters (Hilton, 2013). Criteria used to identify this outcrop as a valley are (a) it is truncating marine deposits of parasequence 4 below (b), it is truncating the upper portion of an older valley (V3A) as well (c), its erosional relief is greater than one channel height deep and (d), the fluvial deposits onlap and downlap onto the sequence boundary. It is composed multiple channel belts that comprise tidally influenced fluvial facies as well as abandoned channel and floodplain facies (Facies Ft., Ac., Fpl., Table 1). Paleocurrents for this valley fill are predominately to the east (Fig. 9d).

The sequence boundary at this valley's base is the 8th order composite surface sequence boundary 1 (Li et al., 2010, Zhu et al., 2012). Along this undulating surface there is a pebble and mud chip lag as well as plant material (logs) (Figs. 15a, b). The outcrop is bounded above by an 8th order unconformity created by the incision of valley 1. The axis of this valley runs roughly north-south. This outcrop exposure parallels the

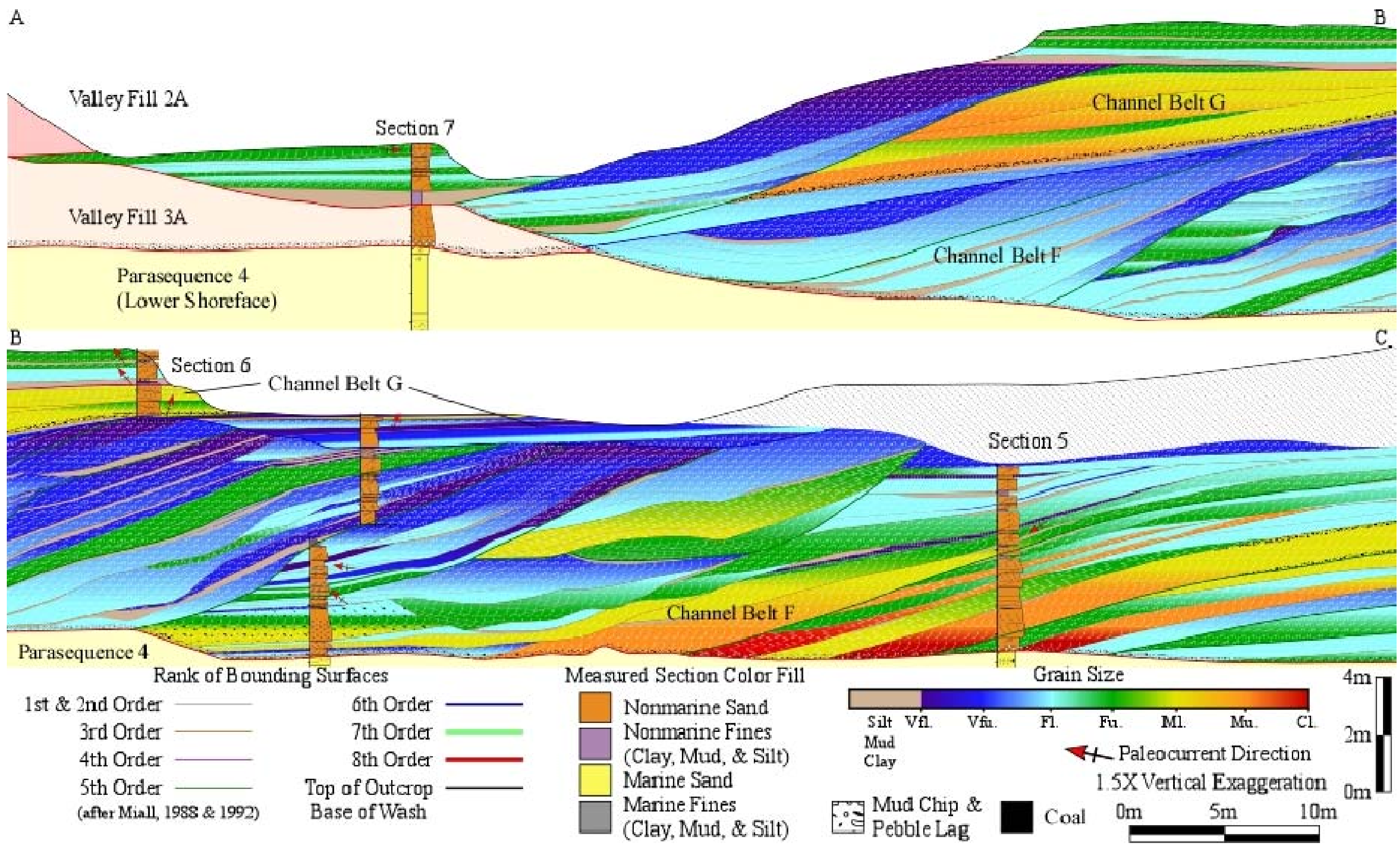

Figure 14. Detailed bedding diagram of the northern portion of valley fill 2B.

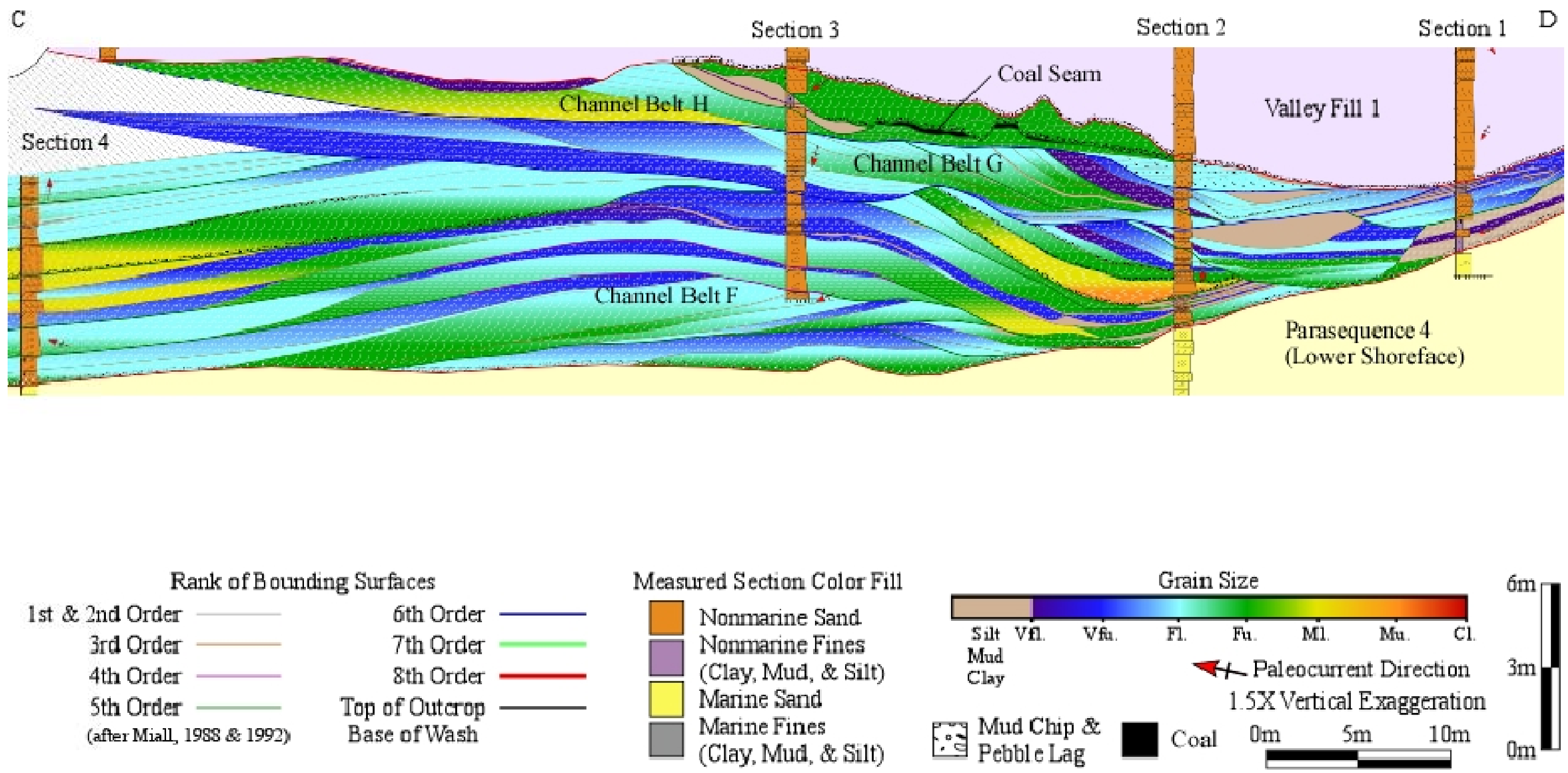

Figure 14 *continued*. Detailed bedding diagram of the southern portion of valley fill 2B.

western edge of the valley deep and cuts through the valley fill where the valley deep was widened westward (discussed in more detail below).

The lowest channel belt, channel belt F (CB-F), runs from the southern extent of the study outcrop 207 meters to the north to section 7 (Fig 14, Plate 1). It reaches a maximum thickness at section 5 to just over 7 meters and thins at the edges along the margins of the valley (Fig. 14). It is bounded below by the 8th order composite surface and above by a 6th order surface (Fig. 14). This channel belt is broken up by multiple 5th order surfaces marking the margins of channels. Internally these divisions are composed of multiple flood deposits bounded by 3rd order surfaces (Fig. 14). Flood deposits range from just over a meter to just a few centimeters thick and some have mud rip-up clasts along their bases.

This channel belt is made up of tidally influenced fluvial facies (Facies Ft., Table 1). As indicated by the abundant paleoflow reversals found within. Grain sizes range from coarse lower to very fine lower sand with abundant mud drapes (Fig 14, Plate 1). The mud drapes are commonly found as thin (cm to mm scale) deposits near the tops of flood units. However, near section 6 these mud drapes extend down to the channel floor draping the entire bar. At the southern extent of CB-F there are nested channel cuts that are aggrading as the channel migrated slightly to the south (Fig. 14). Within these nested channel cuts there is a muddy channel fill interpreted as an abandoned channel (Facies Ac., Table 1). Also, along the southern margin of this channel belt are floodplain facies (Facies Fpl., Table 1). At section 6, the valley floor rises just over a meter forming a ramp and the channel belt appears to keep climbing to the north in an aggradational fashion (Fig. 14).

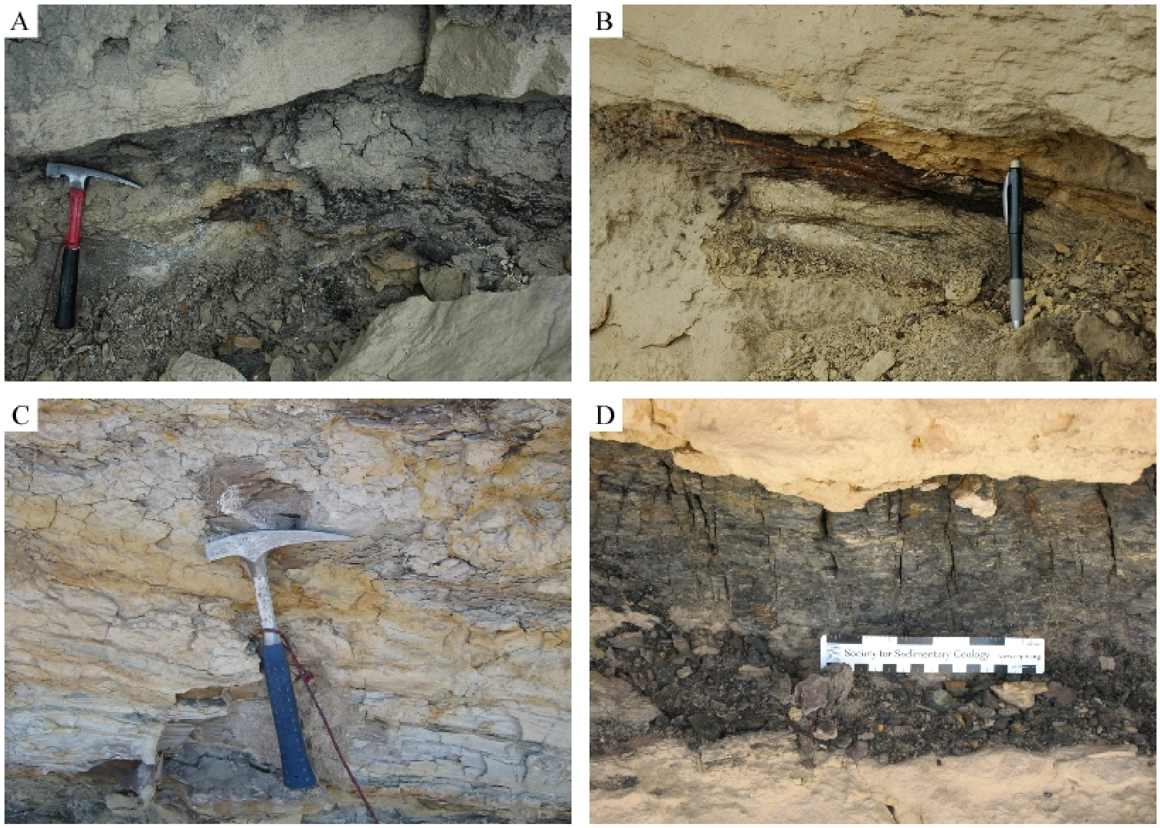

Figure 15. Outcrop close-up photographs of valley 2B. A&B) Plant debris (logs) found along the base of the valley. C) Abandoned channel fill (Facies Ac.) found along the top of CB-H. D) Coal seam found within CB-H.

The middle channel belt, channel belt G (CB-G), extends across the entire valley fill with its middle portion covered (Fig. 14). It is bounded below by an undulating 6th order surface and mainly by a 6th order surface above in the southern half. In the northern reaches it is bounded above by an 8th order composite unconformity that is the floor of the next youngest valley (between sections 6 and 7) (Fig. 14). It is significantly thinner than the lower channel belt and reaches a maximum thickness of only 4.4 meters on its northern side (Fig. 14, Plate 1). It also is composed of facies Ft and is divided by 5th order channel margins on its southern side near section 2, and its northern side between sections 6 and 7 and again at section 7. It is made up of multiple 3rd order bounded fining upward deposits that reach a maximum thickness of 1 meter. Paleocurrent directions are at high angles to the dip directions of the 3rd and 5th order bounding surfaces (Figs. 9d, 14). Grain sizes range from very fine lower to medium upper sand with mud drapes. There is a small mud-filled channel along the southern edge of the channel belt that represents facies Ac (Table 1). On the northern edge of this channel belt there is a channel fill with internal bedding surfaces that have relatively flat dips (Fig. 14). Along the top of this bar between sections 6 and 7 (Fig. 14), there are relatively flat lying deposits of ripple cross-stratified sandstone and mudstones. The mustones reach a maximum thickness of 28 centimeters and are organic rich. Paleocurrents for the sandstones are easterly.

The uppermost channel belt, channel belt H (CB-H), is exposed from half way between sections 1 and 2, to the north 67 meters (Fig. 14). It is bounded below by a 6th order surface and above by an 8th order surface, both of which are undulating. It also is made up of facies Ft subdivided into 3rd order units interpreted as flood deposits. It is thin, only reaching a maximum thickness of 2.1 meters, and is composed of fine lower to medium lower sands with mud drapes. Also present along the top of this CB-H is an abandoned channel with a coal seam just over 16 cm thick (Facies Ac., and Fpl.) (Figs. 15c, d). On top of the coal seam and abandoned channel facies lies another channel that runs from section 2 to section 3 (Fig. 14). It is up to1.6 meters thick and its base is a 5th order surface that undulates. Paleocurrents for this channel are generally northwest and internal 1st order surfaces dip in a southerly direction.

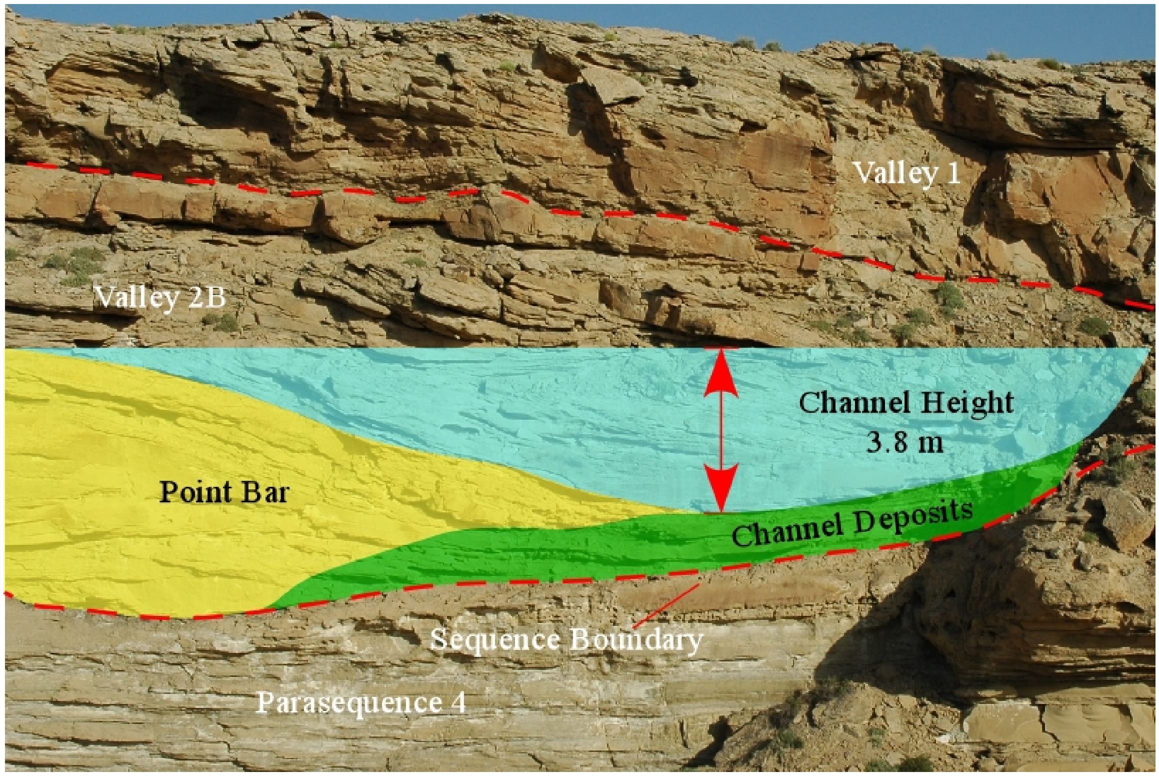

Figure 16. Estimate for channel depth within valley 2B. Picture of outcrop at sections 2 and 3 (Fig. 14).

Interpretation

Valley 2B is a tributary valley that was filled by point bar deposits from a tidally influenced single thread meandering stream. This is indicated by paleocurrent directions that are at high angles to the dip directions of the internal bedding surface. As mentioned above it is believed here that the axis of this valley runs north-south and the valley deep lies in the subsurface just to the east of the study outcrop (cliff face). Along the southern edge of the lowest channel belt the nested channel cuts give an estimated channel depth of approx. 3.8 meters (Fig. 16). Earlier it was mentioned that the height of V3A's deposits in the study outcrop reach an elevation of 24 meters above the base of parasequence 4. In the field area the elevation of V3A's deposits reaches 30.6 meters above the base of parasequence 4 (Hilton, 2013) and is marked by a rooted horizon. This is interpreted here to be V2B's interfluve. As stated earlier V2B has a minimum erosional relief of 29 meters (Hilton, 2013). Comparing this to the estimated channel depth shows that the valley depth is 7.6x the channel depth.

This valley is interpreted as a tributary valley to the main trunk valley. The first reason for calling this valley a tributary is its north-south orientation. The main trunk valley with which this valley feeds runs north-northeast which implies the tributary valley intercepts the trunk at a low angle. The second reason for interpreting this as a tributary is it incised through the interfluve deposits of the main trunk valley. This has been pointed out by Posamentier (2001) as a characteristic of tributary valleys. The last reason for this interpretation is the location of this tributary valley with respect to the trunk valley. As mentioned above, the field area is on the southeastern flank of the main valley. On the flanks of trunk valleys is where a tributary valley would be expected to be found.

This outcrop is unique in that it cuts through where the tributary river widened its valley. This process happened when the valley margin became the cut bank of the river around a point bar. Expansion with downstream translation of a point bar can result in valley widening (Martin et al., 2011). Sylvia and Galloway (2006) called these features meander scars (as seen in map view) or meander scarps (as seen from the ground within the valley) (Fig. 17). The fluvial architecture of the lowest channel belt supports the idea that this is a meander scarp. At section 3 there are 4th order bi-directionally downlapping

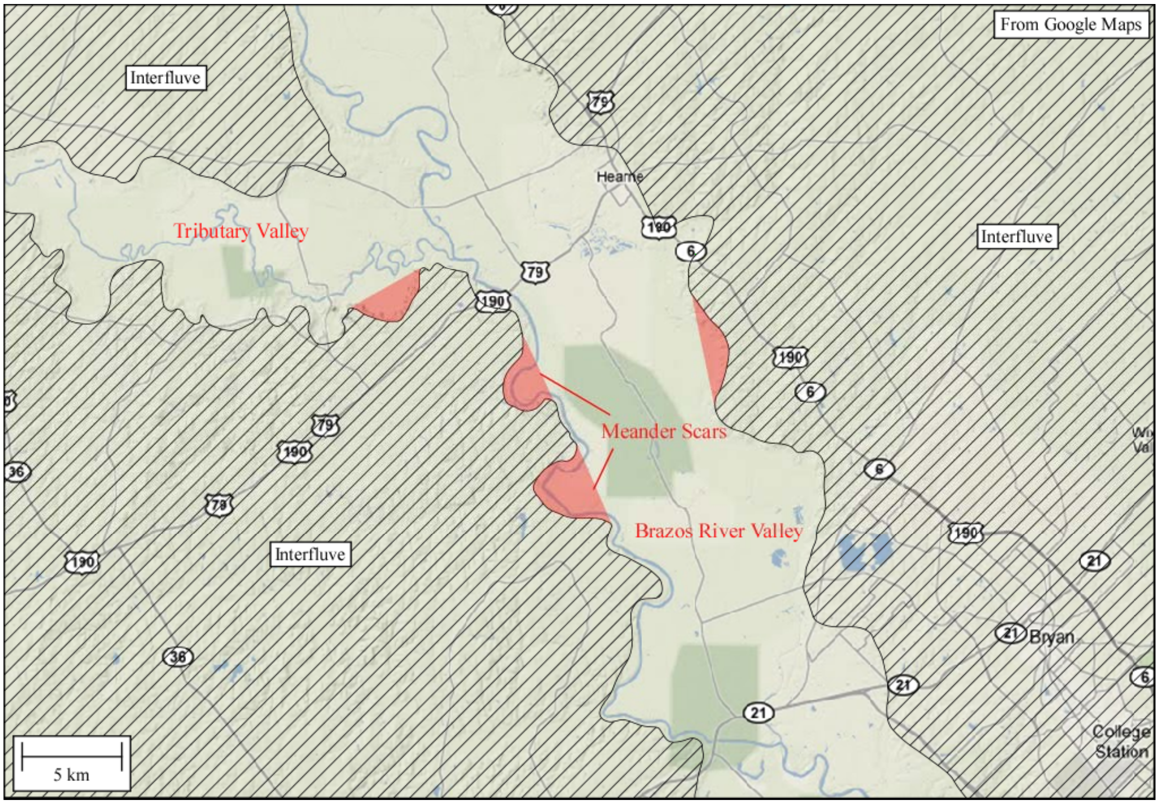

Figure 17. Map of the Brazos River valley near College Station, Texas. Red shaded areas represent areas of erosion into the valley margins. These are termed meander scars if the river presently occupies them, or paleomeander scars if the river doesn't occupy them (*sensu* Sylvia & Galloway, 2006).

surfaces denoting bar tops (Fig. 14). These bidirectional downlapping 4th order surfaces were created by a point bar expanding to the west (towards the viewer) as the river was carving out the meander scar. Along the southern edge of this point bar, paleocurrents are to the west confirming that this is the upstream edge of the point bar. As the point bar was expanding to the west it was also translating to the north. This is indicated by the abundance of laterally accreting 3rd and 5th order surfaces dipping towards the north (Fig. 14). Along the northern reaches of V2B's outcrop, paleocurrents are in an easterly direction illustrating that the river swung around and out of the meander scar. This

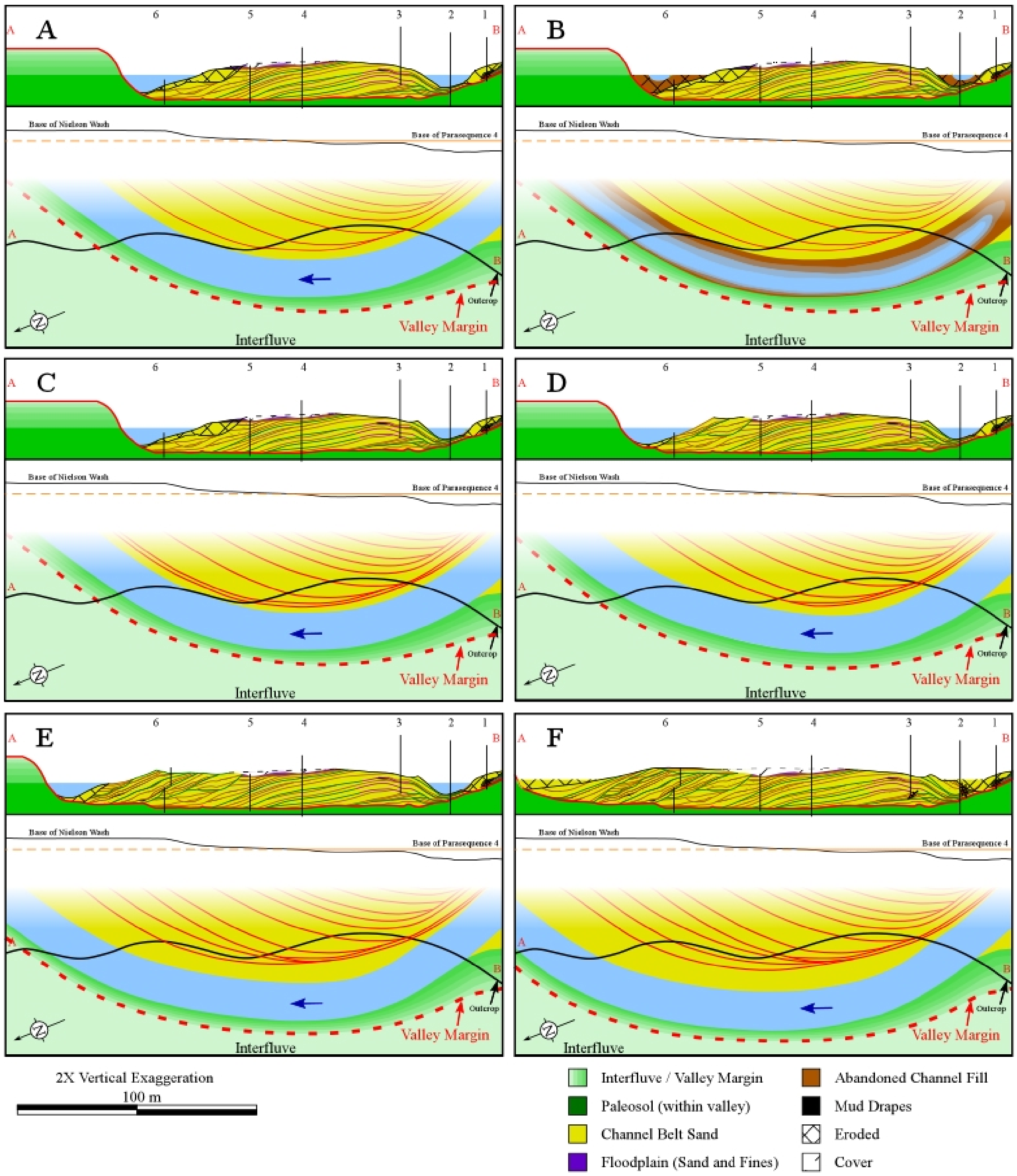

Figure 18. Model of the enlargement of valley 2B's meander scar. A) The creation of the meander scar is underway as the point bar expands and translates. B) Channel abandonment and the deposition of facies Ac. C) Channel reoccupation renews valley widening and partially erodes the abandoned channel deposits. D-F) Continued expansion and translation of the point bar as the river further widens the valley.

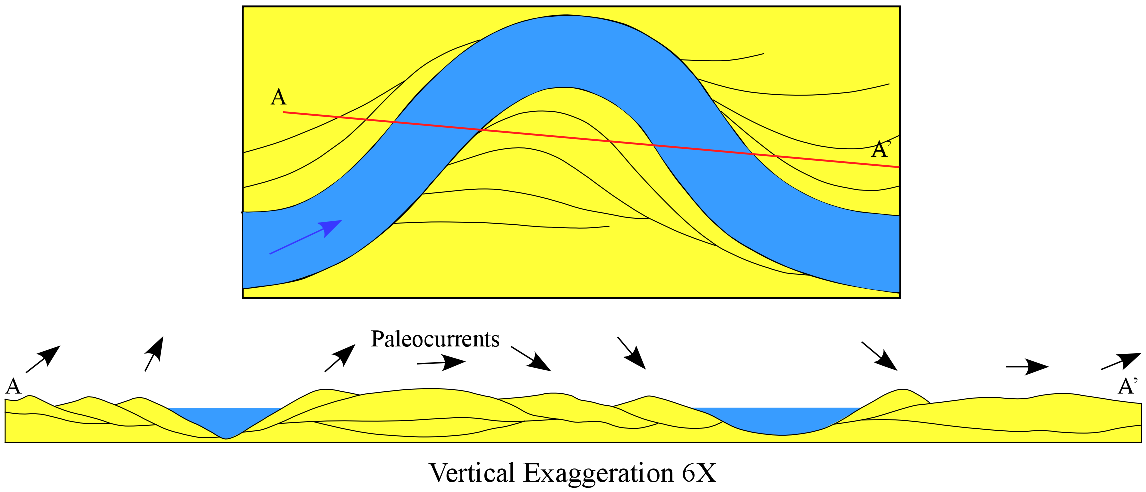

Figure 19. Modeled cross section through an expanding and translating point bar (from Bridge, 2003.

outcrop is an example of an expanding and translating point bar (Figs. 18 a-f, 19) (Bridge,2003). Further evidence that this is a meander scar comes from the fact that it did not erode into the marine deposits on the opposite side of the wash. The lowest point of this valley is below the top of the marine deposits on the on the opposite wall of the wash. If this valley were in an east-west orientation then evidence in the form of a sequence boundary would have been found on the western side of the wash.

The above described abandoned channel deposits reveal that periodically the river would either avulse, or a cutoff (either neck or chute) would form, moving the active channel out of the meander scar (Figs. 14, 18b). Reoccupation of these abandoned channels occurs when a migrating meander loop of the active channel intercepts either the channel entrance or some segment of the abandoned channel (Bridge, 2003). Along the southern margin of V2B, channel reoccupation resulted in the newly active channels partially eroding the abandoned channel deposits. A terrace was carved into the marine lower shoreface deposits of parasequence 4 and fluvial deposits of V3A along the northern margin of the meander scarp when the river reoccupied its old course (Figs. 14, 18c). This terrace formed because enough time had passed, and rates of valley filling were high enough, so that when the river returned into its old course, the base of the channel was higher. Further translation of the channel to the north reinitiated growth of the meander scarp and created the terrace (Figs. 14, 18d-f).

Valley 2A

Valley 2A (V2A) is located along the northern half of the study outcrop (Plate 1, Fig. 20). Its exposure in the study outcrop begins at section 7 and stretches north 242 meters to the end of the outcrop (Fig. 20). Like V2B, this valley is also interpreted as a tributary valley (reasons for this interpretation discussed below). This valley is bounded above by the top of the outcrop, and below by an 8th order composite surface. Just west of the study outcrop the valley floor is mostly exhumed and track of the valley deep is easily observed running north-south (Fig. 21). The preserved maximum thickness of this valley fill in the study outcrop is 3.5 meters thick (Fig. 20). This is due to the study outcrop being close to parallel with the valley axis but represents an exposure of the eastern “wing” of the valley (Fig. 22a). The top of V3A’s deposits have an elevation of 30.6 meters above the base of parasequence 4 (Ben Hilton, 2013). This means the maximum measured erosional relief (measured just west of the study outcrop) is approximately 21.3 meters. In the study outcrop the maximum erosional relief is only 11 meters (Fig. 20). In the field area Hilton (2013) measured a maximum preserved

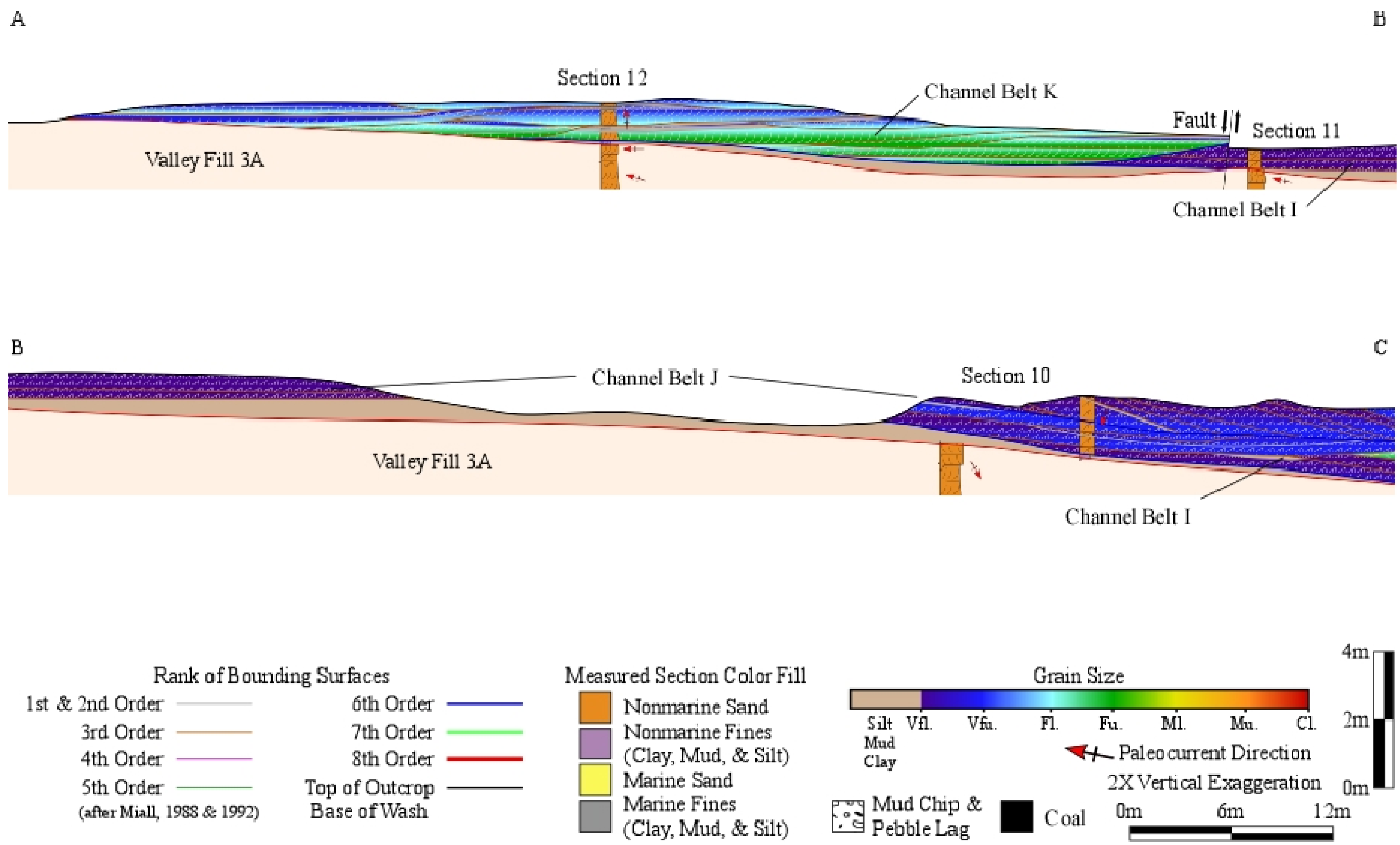

Figure 20. Detailed bedding diagram of the northern portion of valley fill 2A.

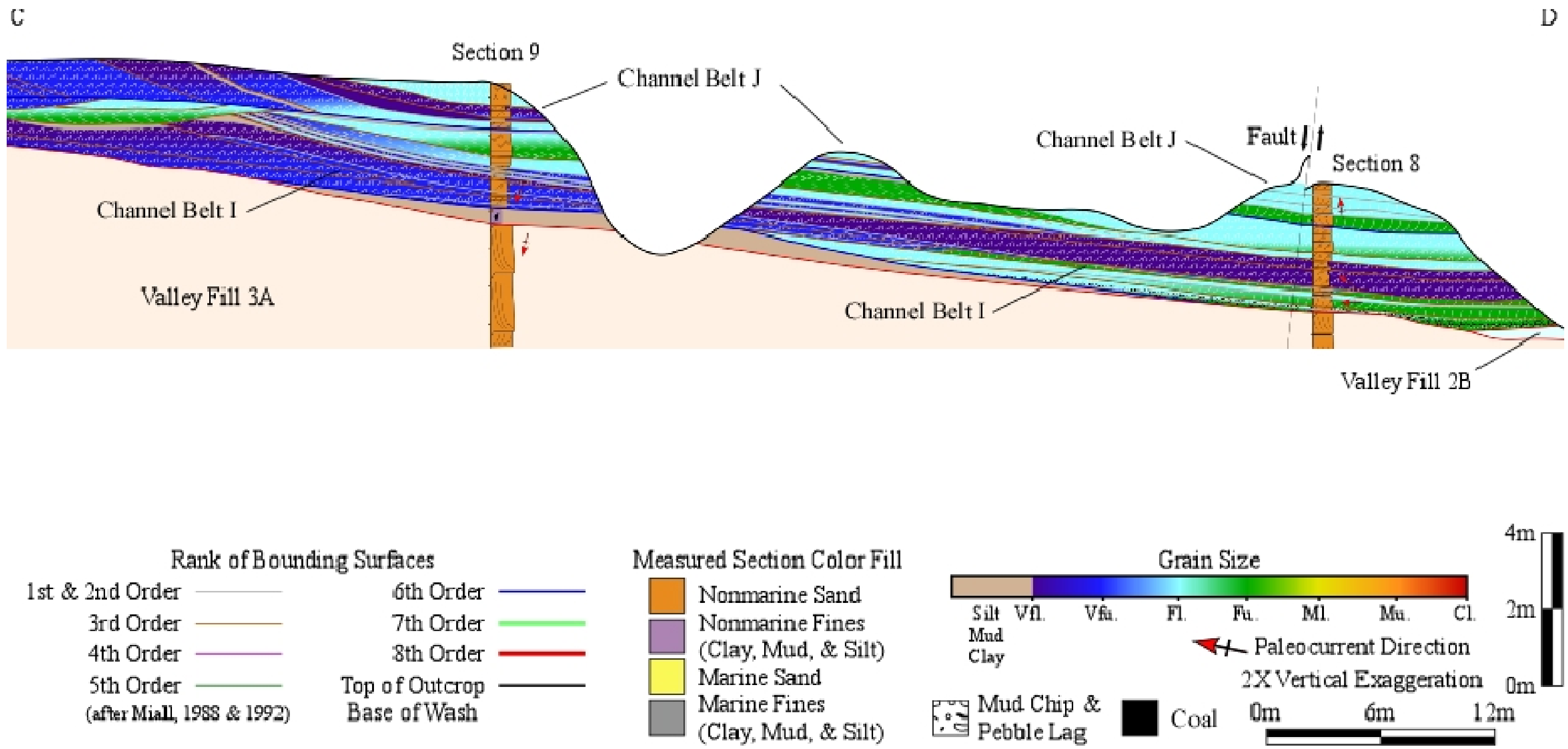

Figure 20 *continued*. Detailed bedding diagram of the southern portion of valley fill 2A.

thickness of 8.1 meters. Despite the thickness of the fill in outcrop there are three channel belts and floodplain deposits partially preserved. These channel belts are all made up of tidally influenced fluvial facies (Facies Ft., Table1). Underlying these channel deposits is a shale interpreted here to be a floodplain mudstone (Facies Fpl.) (Figs. 20, 22b). The lower shale floors the valley fill throughout most of the study outcrop (Fig. 20). It is generally thin with a maximum thickness of only 45 cm, and in places the fluvial system within this valley did scour it away completely which results in 6th order surfaces downlapping on to the valley floor (Fig. 20).

The lowest channel belt, channel belt I (CB-I), runs 173 meters from section 8 in the south to section 11 in the north (Fig. 20). CB-I is composed of facies Ft (Table 1) and is thin, reaching a maximum thickness of only 2.5 meters just to the south of section 8 (Fig. 20). This channel belt is bounded above by a 6th order surface or the surface of the outcrop, and below by a 6th order surface or an 8th order surface where it eroded through the underlying mud (Fig. 20). Grain sizes range from fine upper to very fine lower sand with mudstone lamina as well as centimeter-scale mudstone drapes (Figs. 22c, d). Internally this channel belt is composed of multiple flood deposits. The 3rd order surfaces bounding them are dipping at very low angles to the south (Fig. 20). There is an abundance of dewatering structures found within the sandstone beds of this channel belt.

The middle channel belt, channel belt J (CB-J), extends for 55 meters from section 9 to section 10 (Fig. 20). It is made up of tidally influenced fluvial facies (Ft). Grain sizes range from very fine lower to fine lower sand but are largely in the very fine range. Mud drapes are common along the tops of flood deposits. CB-J is bounded below by a 6th order surface and above by the top of the outcrop. It also is composed of

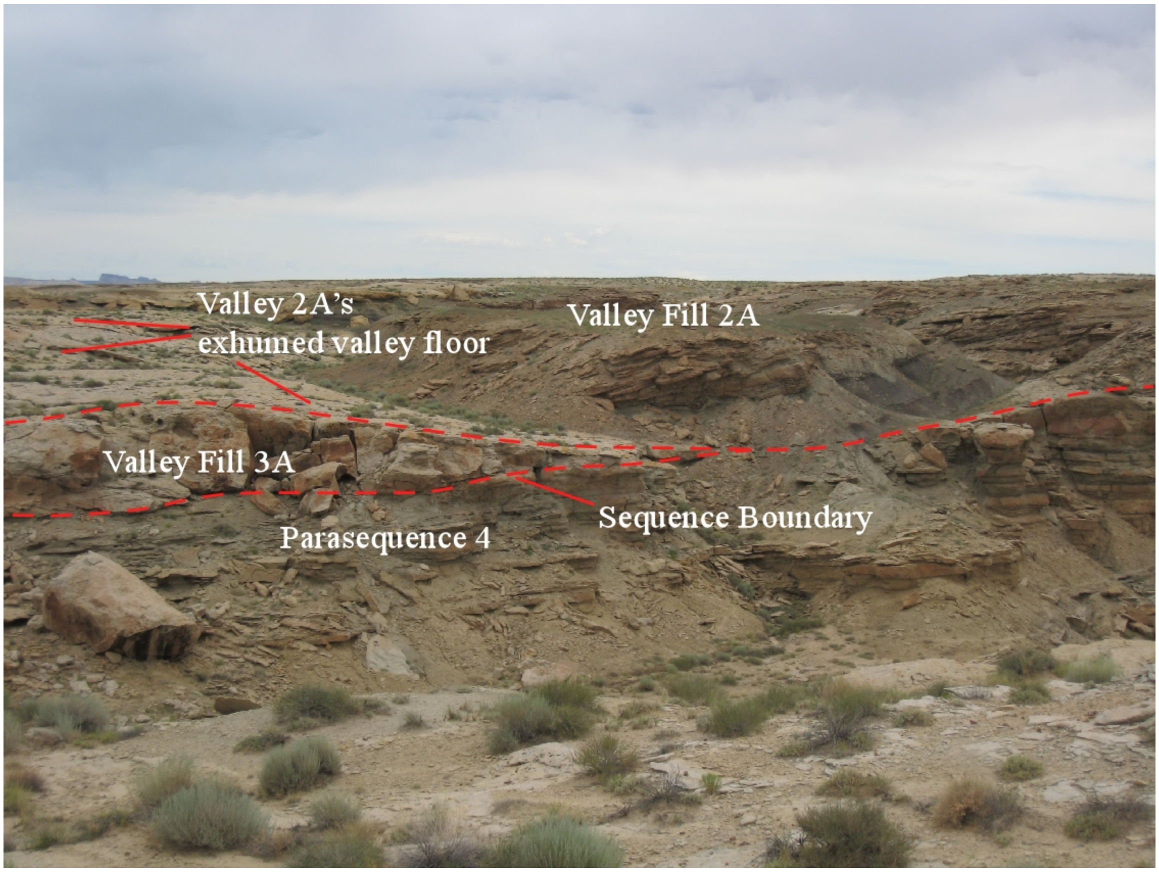

Figure 21. View to the north down the valley axis of V2A.

multiple flood deposits and the internal 3rd order surfaces dip to the south (Fig. 20). Paleocurrents in this channel belt are largely to the west.

The uppermost channel belt, channel belt K (CB-K), is found in the far northern section of the study outcrop (Fig. 20). It extends for 67 meters from section 11 to half way between sections 12 and 13 (Fig. 20). There is only a thin remnant of this channel belt left and what is preserved only reaches 1.3 meters thick. There only a few thin (< .5 meters) 3rd order bounded flood deposits within this exposure. Grain sizes range from fine upper to very fine upper sands with mud drapes common between flood units. Paleocurrents in this exposure point to the east.

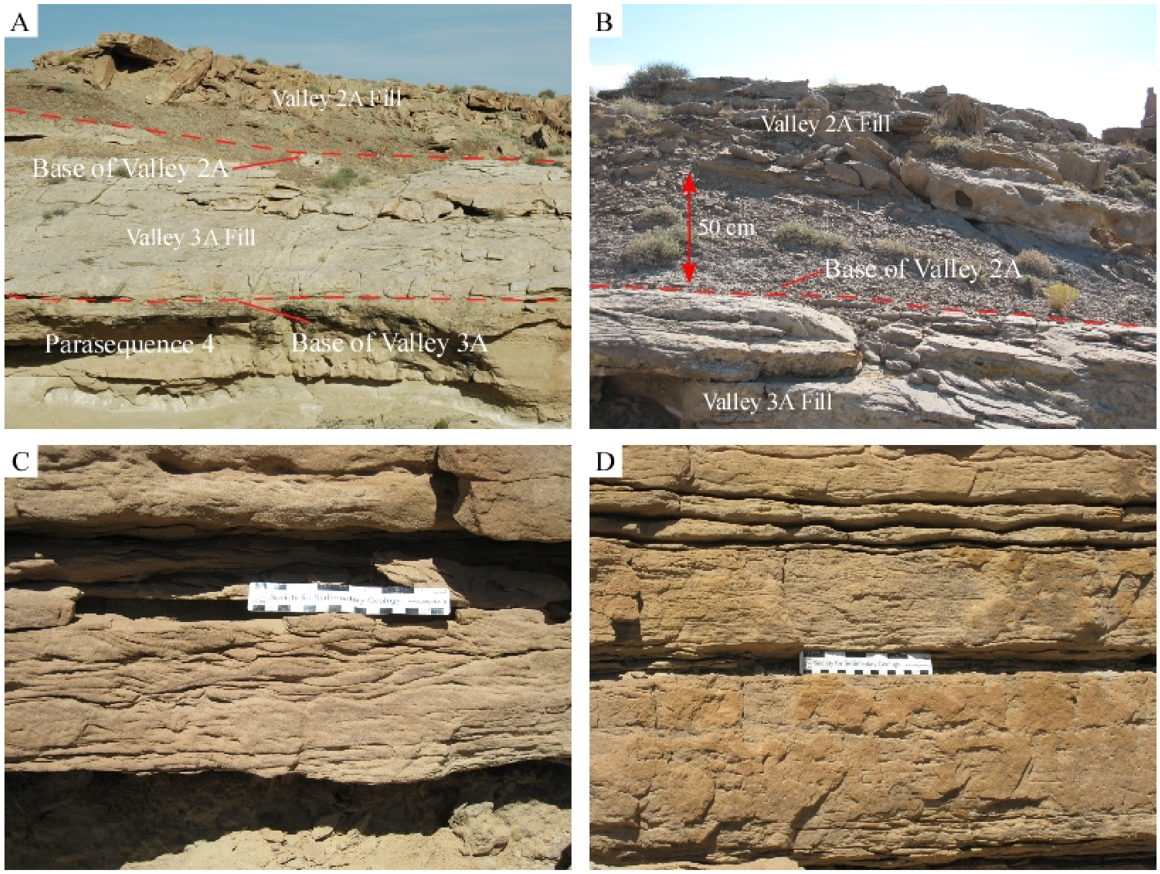

Figure 22. Outcrop close-ups of valley 2A. A) The eastern "wing" of the valley in the study outcrop. B) Photo of the floodplain fines underlying the tidally influenced fluvial deposits of valley 2A. C&D) Ripple-scale cross strata (facies Ft) with centimeter to millimeter scale mud drapes. Spaces between sandstone beds (the weathering profile) mark the location of these mudstones.

Interpretation

Valley 2A is interpreted here, like valley 2B, to be a tributary valley. Reasons for this interpretation are the same reasons V2B was interpreted as a tributary valley, which are V2A's position on the flank of the trunk valley, it incises through the trunk valley's interfluves, and the orientation of its axis is different from the trunk valley's axis. Another reason for interpreting this valley as a tributary is that it is narrower than the main trunk valley, which Posamentier (2001) points out is another characteristic of tributary valleys. This tributary valley exposure is unique in that much of the valley floor and margins are subaerially exposed. This allowed for easy identification of the valley axis which, as previously mentioned, runs north-south (Fig. 21). Another detail which becomes apparent with close examination of the valley floor, is that no fluvial deposits are resting on the base of the valley. Instead the valley floor has mud and siltstone overlying it in places that can reach thicknesses of over a meter (Figs. 23a, b). Examination of these fines along the deepest portion of the valley revealed centimeters thick massive mudstones with no bioturbation. These deposits were interpreted to be fluid muds based on the identifying characteristics described by Ichaso and Dalrymple (2009). These characteristics are that these muds are structureless and homogeneous with no evidence of grain-by-grain settling, there is no bioturbation, a minimum thickness greater than 1 cm, and they are composed of silt and clay (Ichaso & Dalrymple, 2009). Fluid muds are often found in esturarine environments (Ichaso & Dalrymple, 2009) suggesting these mudstone deposits are estuarine (Facies Em., Table 1). The fact that estuarine deposits floor the valley where once there must have been fluvial deposits means that the fluvial deposits were ravined by wave and tidal action when the valley flooded during relative sea-level rise. Immediately overlying the estuarine deposits are inclined heterolithic deposits (Facies IH., Table 1, Fig. 23c). These inclined heterolithic deposits are very tidally influenced with evidence of tidally driven flow reversals (Fig. 23d, e). These inclined heterolithic deposits were laid down as part of a bayhead delta that prograded south to north into the estuary.

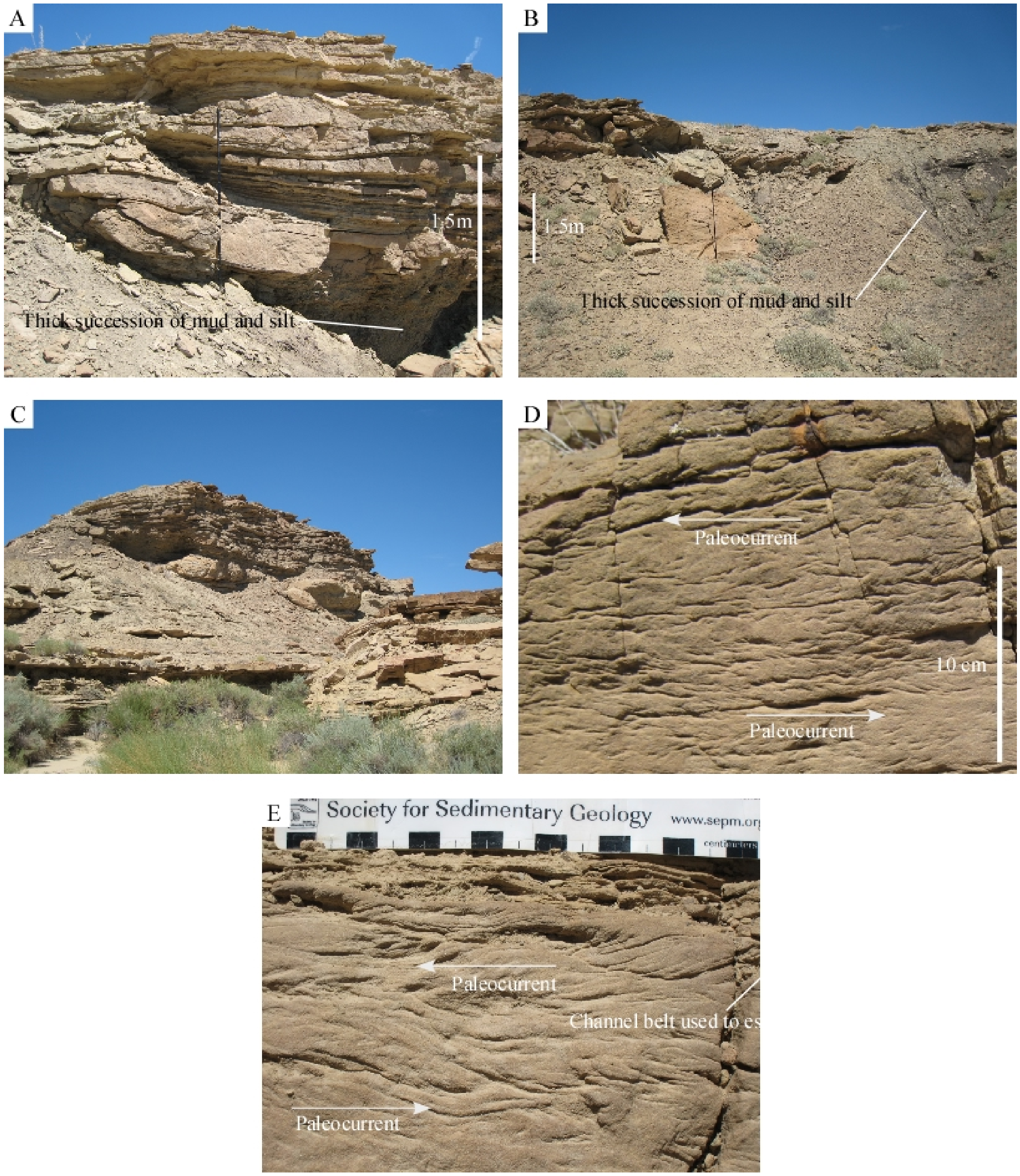

Figure 23. Outcrop close-ups of V2A. A&B) Photographs of the estuarine mudstone draping the floor of V2A. C) Inclined heterolithic strata. D&E) Examples of tidally driven flow reversals within flood units.

The deposits of the tributary valley found in the study outcrop sit above the level of these estuarine and bayhead delta deposits on the valleys eastern flank. From its lowest point of erosional relief of 11 meters near section 7, the base of the valley climbs to the north. By section 9 the height of the unconformity is 18 meters above the base of parasequence 4. The reason for this climb in the height of the unconformity above which these fluvial deposits rest is that the outcrop is angling away from the valley deep to the west. The floodplain mudstones that drape the unconformity in many locations are interpreted here to have been laid down while the top of the channel was at or near the elevation of the interfluves. When the river was in flood, the floodwaters spread out what was once the interfluve. This resulted in a succession of floodplain deposits laid down prior to the channel aggrading high enough for it to move over what once was the valleys interfluve. The height of the fluvial deposits on top of the old interfluve surface means that the channel was no longer confined to the valley. The implication here is that these deposits were laid down as the valley was in its last stages of filling. Furthermore, the thickness of the channel belts shows that the rates with which accommodation was created were slow at this time resulting in slow aggradation rates. This further attests to the idea that these deposits were laid down during the last stages of valley filling. As previously mentioned, these deposits are tidally influenced fluvial facies. Fluvial style is interpreted here to be that of a single thread meandering system. The third channel belt up from the base of the valley is clearly made up of point bar deposits based on the paleocurrent direction being at a high angle to the dip direction of the bar deposits. The dip of the internal bedding surfaces within this point bar is to the south, implying that the bar was laterally accreting in that direction as the point bar expanded south. Other deposits, such as the third channel belt up from the base of the valley, show very little dip within their internal bedding surfaces. This is interpreted here to mean that these deposits are sheet sands deposited along the base of the river channel.

Valley 1

Valley 1 is the youngest of the valley fill deposits (Li et al., 2010), and incises into the deposits of valley 2B in the southern extent of the study outcrop (Fig. 24). Valley 1 is extensive, extending south over 6 km from where it incised into the southeastern margin of valley 2 (Fig. 25) (Li et al., 2010). In the study outcrop it reaches 35 meters thick and to the south incises more deeply into parasequence 4 (Li et al., 2010). The northern exposure of valley 1 extends from the southern edge of the study outcrop 82 meters to the north ending at section 4 (Plate 1, Fig. 24). It is composed of facies Fl (Table 1). It is bounded below by an undulating 8th order composite surface, and above by the top of the outcrop (Fig. 24). This 8th order composite surface has a mud chip lag lining it. The deepest it incises is 15.9 meters from the base of parasequence 4 and at its thickest in the study outcrop it reaches 6.6 meters. There are 3 channel belts that make up this valley fill in this location.

The lowest channel belt, channel belt L (CB-L), stretches across the full 82 meters of the valley 1 exposure (Fig. 24). It is thickest on its southern flank where it reaches just over 4 meters thick. Sand grain sizes range from very fine upper to medium lower (Fig 24). Within CB-L there are no mud drapes, except for the channel on the northern margin (at section 4) (Fig. 24). It is divided by 5th order channel margins that cross cut

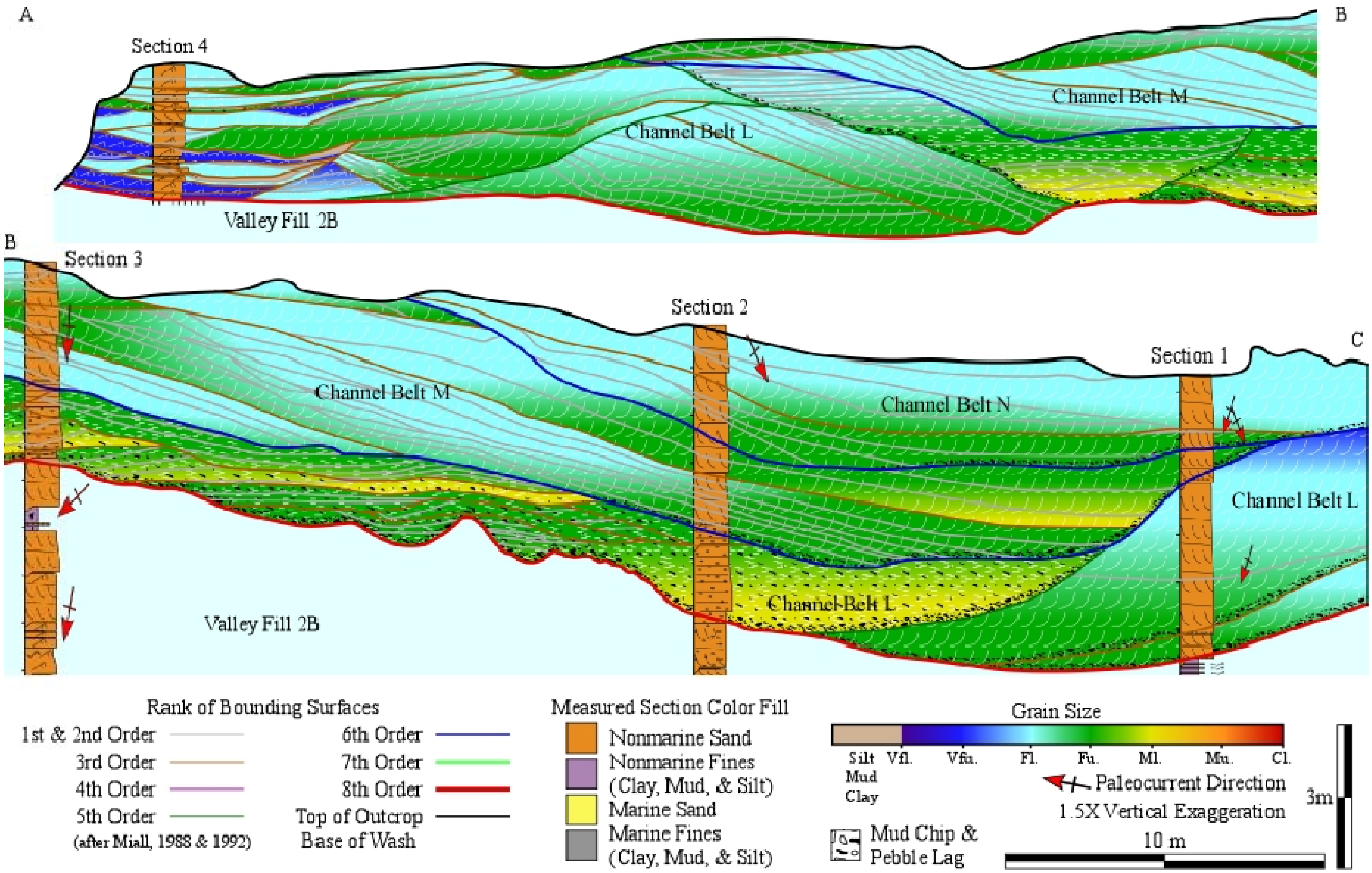

Figure 24. Detailed bedding diagram of valley fill 1.

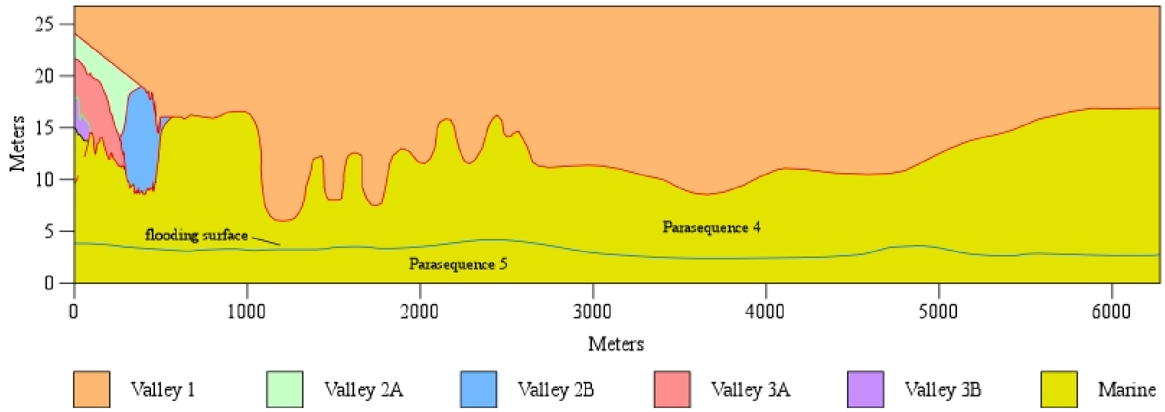

Figure 25. Cross section of the valley fills through the region (modified from Li et al., 2010). Study area is on far left where the V1 and V2 fills are located.

through the channel belt. The internal bedding is largely made up of 3rd order surfaces interpreted as bounding individual fining upward flood deposits. Between sections 1 and 3 CB-L is made up of sandstone that is rich in mud chips (Fig. 26a, and 26b). Internally this channel belt is composed of multiple 3rd order bounded flood deposits that dip in various directions (Fig. 24). Paleocurrents are generally to the west except for the far northern portion of the channel belt which has paleocurrents in a northerly direction.

The next channel belt up , channel belt M (CB-M), is approximately 62 meters wide and runs from section 1 in the south to half way between sections 3 and 4 (Fig. 24). It is bounded below by a 6th order surface which is lined with mud chips along its deepest incision on either side of section 2 (Fig. 24). Internally CB-M is made up of 3rd order bounded flood deposits that dip to the south and it is not divided by 5th order surface denoting channel margins. Individual flood deposits are up to over 1 meter thick and internally are made up of multiple southerly dipping 1st order surfaces bounding dune-

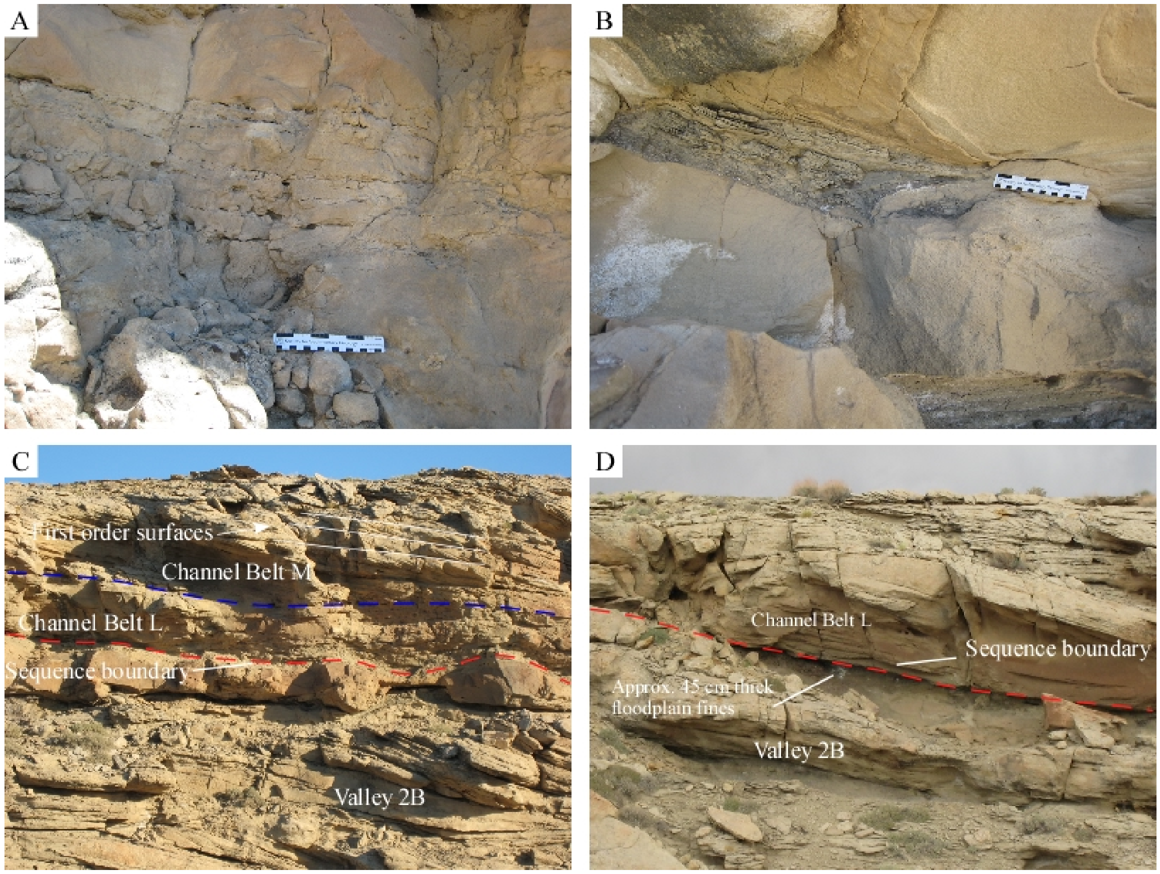

Figure 26. Outcrop photographs of valley 1. A) CB-L with extensive centimeter scale mud chips. B) Large rip-up clast within CB-L (just left of scale). C) Multiple 1st order surfaces separating dunes within CB-M. Only 3 of these surfaces illustrated (white lines). D) Location of a thick mudstone below the base of valley 1.

scale cross-sets (Fig. 26c). Paleocurrents are to the west and southwest. Sand grain sizes are from fine lower to medium lower with no apparent mud drapes.

The uppermost channel belt, channel belt N (CB-N), is very much like CB-M below it. It is bounded below by a 6th order surface with a mud chip lag and on the top by the surface of the outcrop (Fig. 24). It also is made up of multiple southerly dipping 3rd order bounded flood deposits. These flood deposits, like in CB-M immediately below, are divided by 1st order surfaces dipping to the south which bound individual dunes. Grain sizes range from fine lower to fine upper sand and paleocurrents are to the west and southwest.

Interpretation

The deposits from valley 1 were laid down during late transgression or early highstand. This is indicated by the fact that their basal elevation is 13.4 meters above the valley floor. This places these deposits in the uppermost reaches of the valley. The base of these deposits, along the sequence boundary, incises deeper into the underlying deposits of tributary valley 2B than it does the top of parasequence 4 immediately to the south (Fig. 24). This is due to the deposits of V2B being younger, less consolidated, and as a result softer than the upper shoreface deposits of parasequence 4. The basal channel belt of valley 1 found in the study outcrop is riddled with mud rip-up clasts. A clue as to the reason why comes from the top of V2B between sections 3 and 4, where there is an approximately 45 cm thick deposit of floodplain mud (Fig. 26d). Presumably these muds ran across the top of V2B. When the channel of this lower channel belt was cutting down through them during floods it incorporated them into its deposits in the form of mud chips. After this lowest channel belt was deposited the channel continued to aggrade. However the rate with which accommodation was created at the time was low enough that the successive channel belts eroded off the top of the previous channels (Fig. 24). The upper 2 channel belts (CB-M & CB-N) are very similar to one another. Both are made up of fining upward flood deposits that are composed entirely of dunes. The paleocurrents signified by these dunes are at a high angle to the dip direction of the internal bedding architecture (Fig 23). This shows that these deposits were laid down as part of a laterally accreting point bar that was expanding in a southerly direction. This, plus the absence of any confluence scours or bidirectionally downlapping braid bars, leads to the conclusion that this portion of valley 1's fill was deposited by a single thread meandering stream.

Reservoir Heterogeneity

The compound valley fill deposits found within the study outcrop display varying degrees of heterogeneity. The heterogeneity varies in magnitude both within valley fills and from valley to valley. In the study outcrop V3B is made up of 2 discreet channel belts, A & B. The older channel belt A shows no tidal influence while the younger, channel belt B, is very tidally influenced. Channel belt B displays a number of muddy elements such as double mud drapes and mud draping the foresets of dunes. These muddy elements are not thick may not act as a barrier to hydrocarbon flow, but at the very least would act as a baffle. Increasing heterogeneity in V3B is the result of rising sea levels tidally influencing fluvial backfilling of the valley. Valley 3A truncates V3B and in the study outcrop does not display as much heterogeneity. It is made up of 3 stacked channel belts with very little mudstone preserved. At the time this portion of the valley was filling relative sea-level rise was slow enough to allow each successive channel belt to erode down into the previous. This resulted in a high degree of vertical channel belt connectivity with very little mud preserved. This valley fill would make the best reservoir rock because there is very little to act as a baffle or barrier to hydrocarbon flow. Valley 2 truncates V3A and is heterogeneous. Like V3B it displays greater degrees of tidal influence as the deposits get younger. The oldest channel belt has several muddy elements such as mud draping dune foresets, mudstones preserved along the top of individual upward fining flood deposits, and mudstones that drape the entire bar. It also has abandoned channel fills (mud plugs) which were the result from avulsion or a chute or neck cutoff. The mudstones draping entire bars and the abandoned channel fills could compartmentalize this channel belt into many small containers. The next valley fill, V2A, is the most heterogeneous of the five valley fills studied here. It incises into both V3A and V2B, and the deepest portion of this valley is draped in a mudstone over a meter thick. These deposits will act as a barrier to hydrocarbon flow. Over these mudstones lie inclined heterolithic strata with abundant mudstones preserved between sandstones beds which would also act as an impedance to fluid flow. The youngest of the valley fills, V1, incises into V2B and has a low degree of heterogeneity. Also it has good sand on sand contact with V2B below. However the lowest channel belt within this valley fill is riddled with centimeter-scale mud chips most likely eroded from the top of V2B. Barton et al. (2004), point out that mud chip horizons, when altered by diagenesis, can act as barriers to hydrocarbon flow.

Sequence Stratigraphic Evolution of the Valley Systems

The Coastal Prism

Parasequence 4 is the highstand coastal prism which prograded out over the ramp margin of the Cretaceous Western Interior Basin prior to relative sea-level fall and valley incision. Valleys 1, 2, and 3 incised into this prism. The highstand coastal prism (also

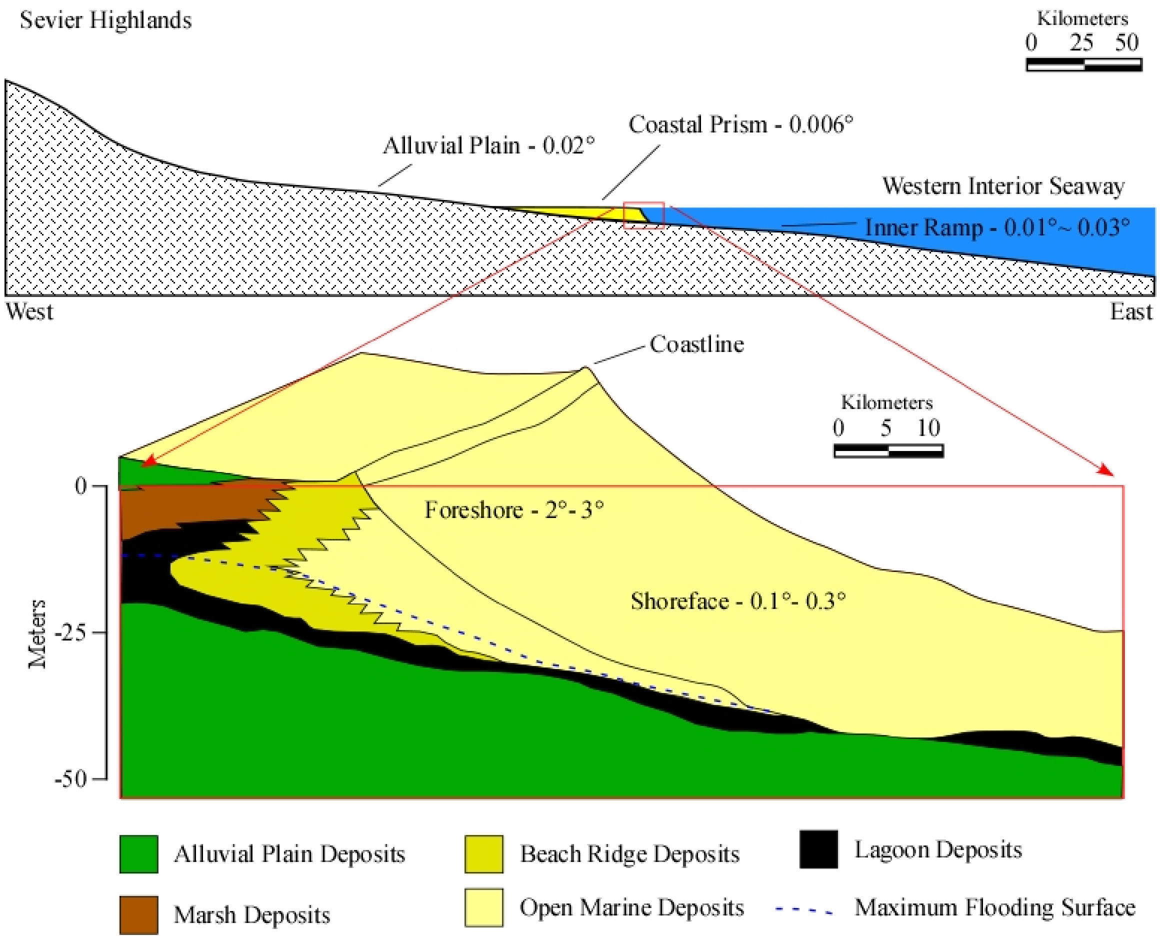

Figure 27. Top - Regional cross section from the Sevier highlands to the Western Interior Seaway illustrating the slopes of the coastal prism, alluvial plain and inner ramp (modified from Li et al., 2010). Bottom – Block diagram of the coastal prism with facies tracts and the slopes of the foreshore and shoreface (modified from Talling, 1998. Slopes are from Li et al., 2010).

known as the highstand wedge) is a prism of sediment (as seen in cross section) bounded on its landward side by the bayline (above which only fluvial processes dominate) and seaward by the shoreface (Fig. 27) (Posamentier et al., 1992). The top of the coastal prism is the relatively flat lying coastal plain (graded to sea level), and the base of the prism is bounded by the maximum flooding surface (Fig. 27) (Posamentier et al., 1992;

Talling, 1998). In the ramp setting of the Western Interior Basin these coastal prisms are generally tens of meters thick (Posamentier et al., 1992; Talling, 1998; Li et al., 2010). Rivers will incise through the coastal prism during a fall in relative sea level if the slope of the delta front/shoreface is steeper than the slope of the coastal plain (Talling, 1998). For the Ferron Sandstone of the Notom Delta, the dip of the coastal plain is calculated to be 0.006° (Fig. 27) (Li et al., 2010). The dip of clinoforms in delta fronts or shoreface deposits have dips that are typically 1 to 3 orders of magnitude steeper than that of the coastal plain (Talling, 1998; Li et al., 2010). This certainly holds true for the Notom Delta, where the dip of the delta front is calculated to be 0.14° (Li et al., 2010). This is 2 orders of magnitude greater than the slope of the coastal plain and obviously steep enough to promote valley incision (as indicated by the presence of valleys).

Holbrook et al. (2006), describe base level as a physical barrier at an elevation above which rivers cannot aggrade, and below which they cannot incise. The downstream buttress is the point to which the rivers graded equilibrium profile will be adjusted to (Holbrook et al., 2006) and in the case of the Neilson Wash valleys it is the shoreline. Holbrook et al. (2006) describe the graded equilibrium profile as existing within a "buffer zone" of numerous possible equilibrium profiles (Fig. 28). The buffer zone is bounded above by the upper buffer profile, which is the highest possible profile to which a river can aggrade, and below by the lower buffer profile, which is the lowest possible profile a river can incise down to (Holbrook et al., 2006). As the buttress (relative sea level) falls it lowers the buffer zone with it and the net effect is fluvial incision (Holbrook et al., 2006). Once the buttress falls to the elevation of the shelf/ramp, the shoreline migrates basinward across the shelf in what Holbrook et al.

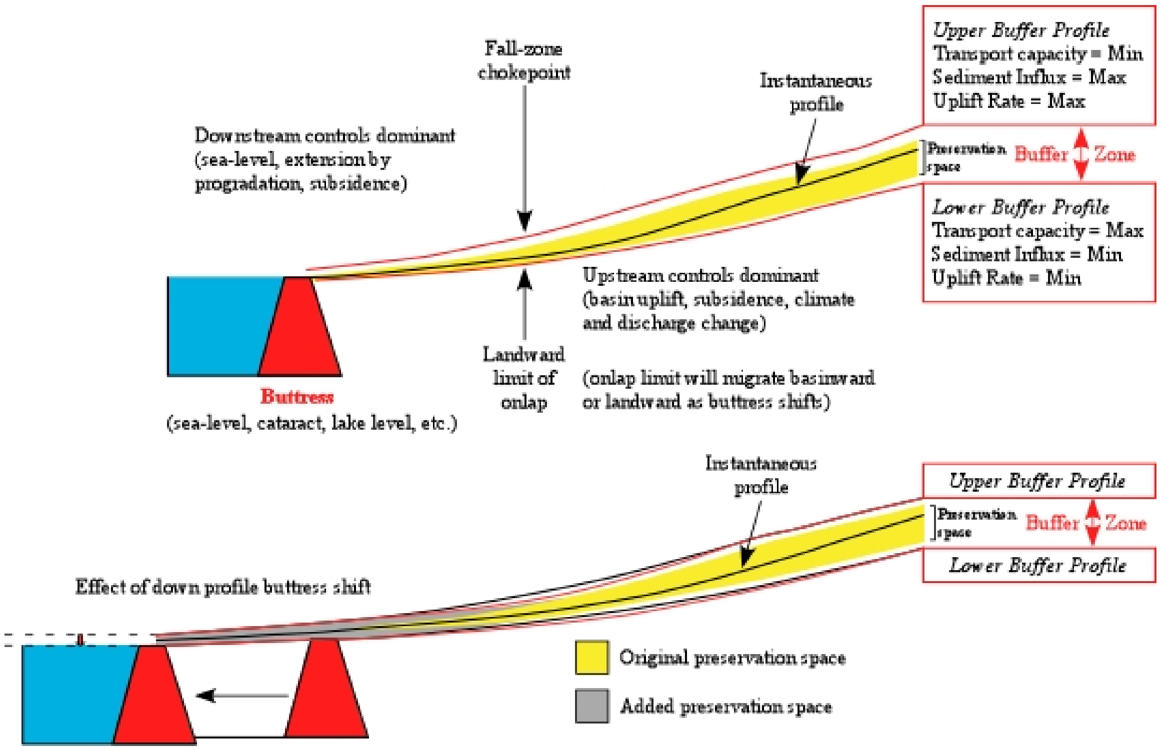

Figure 28. Top – Diagram illustrating the idea of base level buttresses and buttresses (modified from Holbrook et al., 2006 and Bhattacharya, 2011). Bottom – Diagram showing the effects of a down profile buttress shift (modified from Holbrook et al., 2006). The net effect of this buttress shift down profile is to elongate the buffer zone down dip without noticeably increasing the distance between the upper and lower buffers. Another effect of this buttress shift is the creation of additional preservation space between the elongated buffers.

(2006) call a “down-profile buttress shift” (Fig. 28). In the case of ramp settings such as the Cretaceous Western Interior Basin the slope of the shelf/ramp is low (Van Wagoner et al., 1990). The slope of the ramp upon which the Notom Delta is prograding out upon was calculated by Li et al. (2010) to be 0.01° to 0.03° (Fig. 27). When the “buttress fall” became a “down-profile buttress shift” (*sensu* Holbrook et al., 2006) during relative sea level fall, valley incision in this downdip location soon halted. This is because once

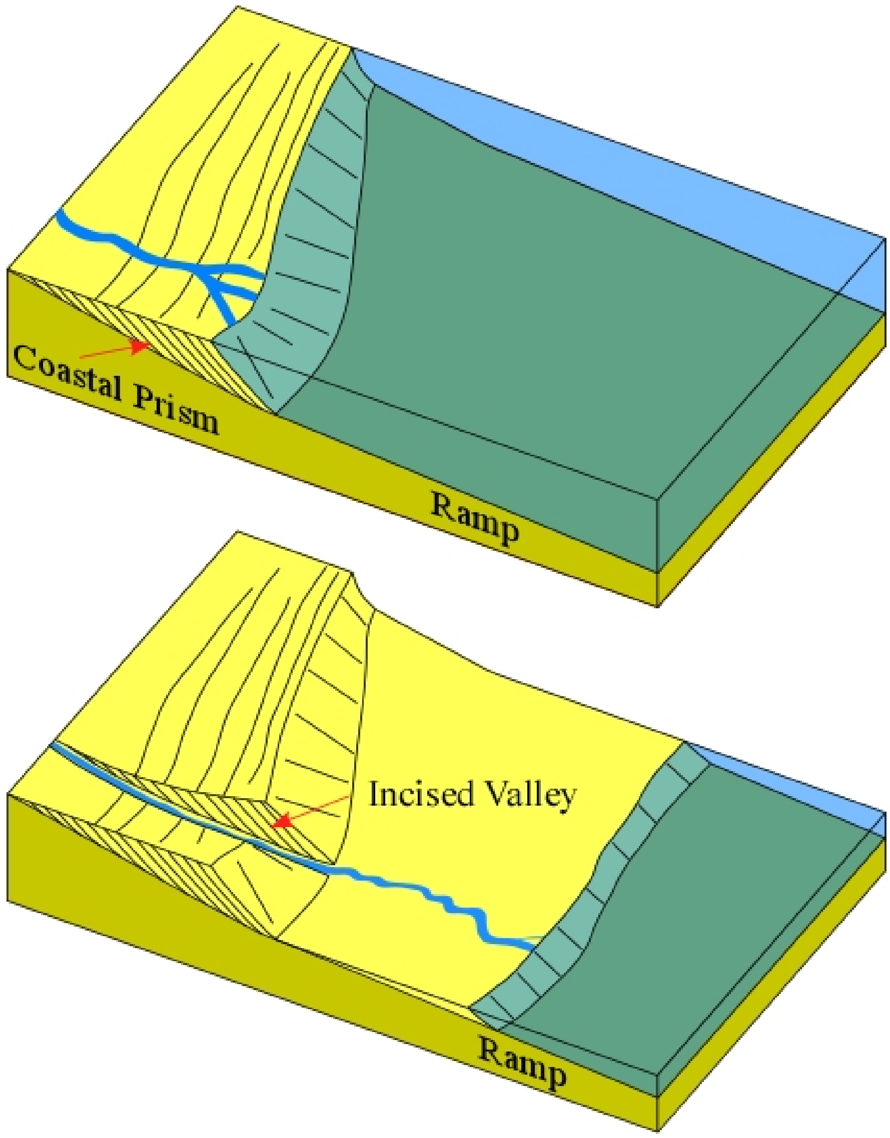

Figure 29. Block diagrams illustrating valley incision within a coastal prism in a ramp environment. Because there is no shelf slope /break there will be no nickpoint migration and valley incision across the ramp. Valley deepening will stop once the river has entrenched itself within a channel that extends to the migrating shoreline.

relative sea level fell to the point where the fluvial system was extending across the low sloping shelf (following the shoreline), the only further erosion was the river entrenching itself within a channel (Fig. 29) (Posamentier, 2001; Törnqvist et al., 2000; 2003). This puts the maximum depth of valley incision one channel height below the base of the highstand wedge (parasequence 4 in this case). However, this is not observed within the study area for this project. Research done along the westernmost outcrop exposure of the Ferron Sandstone in the region demonstrated that the valley system incised completely through parasequence 4 and into parasequence 5a (Fig. 5) (Zhu et al., 2012). Based on this information it is believed that the deepest incision made by the compound valley system is in the subsurface further to the north than the study location.

The Valley Systems

The oldest valley fill deposits found within the study area belong to valley 3B. This deposit, found along the southern flank of the trunk valley 3, represents the first episode of valley filling. As relative sea-level fell, the trunk valley incised into the lower shoreface deposits of parasequence 4 (Figs. 30a, 30b). Following lowstand, fluvial aggradation in conjunction with relative sea-level rise occurred partially filling the valley (Hilton, 2013). The motivation to divide this thin exposure of valley 3B into two channel belts was largely due to the fact that the older channel belt is not tidally influenced while the upper channel belt is. The tidally influenced fluvial deposits preserved in outcrop suggest that: (1) rising relative sea level was an influence on valley filling and, (2) these deposits may have been laid down as highstand was approached. The transition between non-tidally influenced and tidally influenced fluvial deposits within a valley fill typically takes place during marine transgressions (Shanley & McCabe, 1994; Zaitlin et al., 1994). This is believed to be true in this case based upon their elevation above parasequence 4.

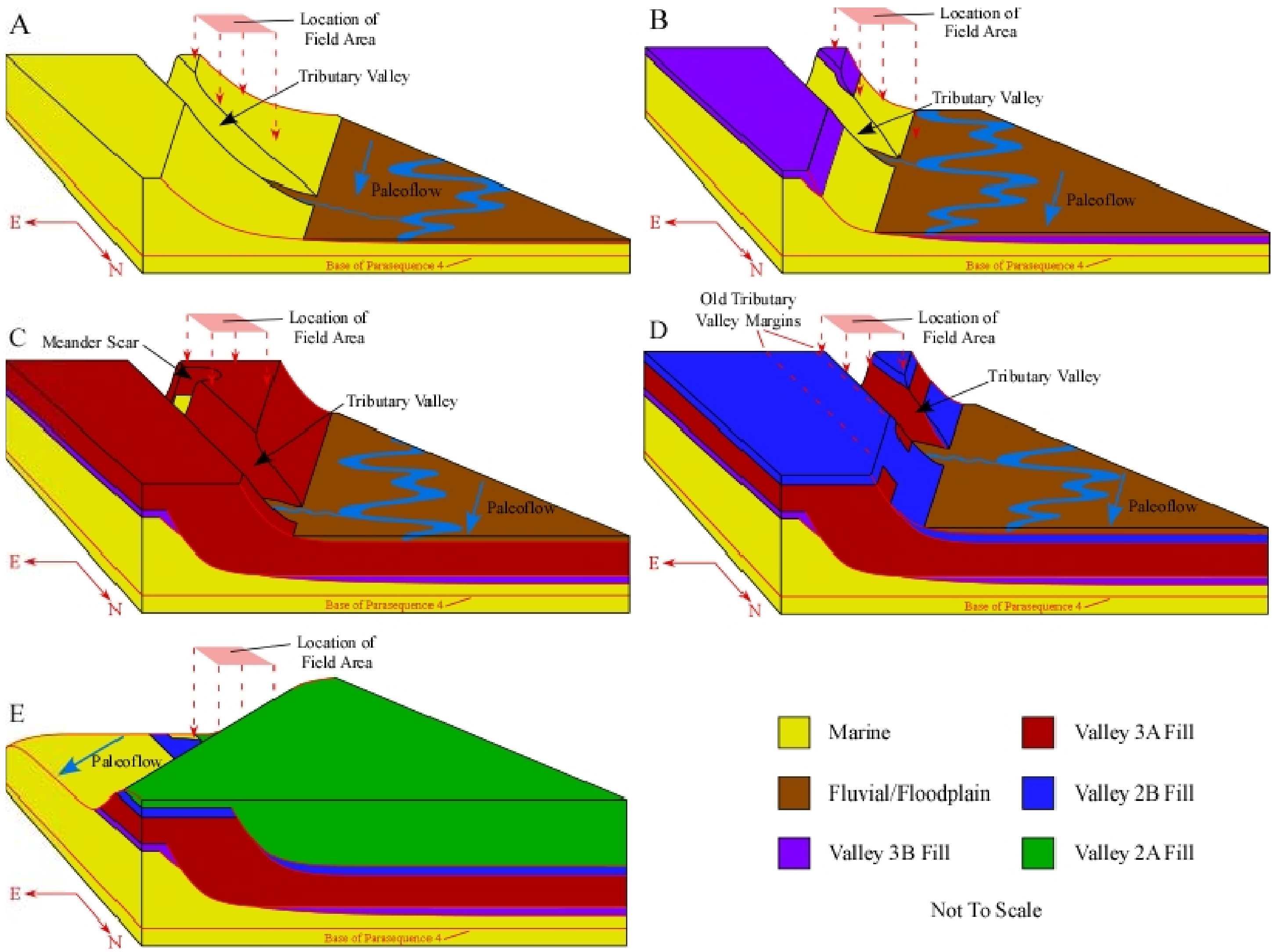

Figure 30. Block diagrams illustrating the evolution of the valley systems. Incision of Valley 3B (A), Valley 3A (B), Valley 2B (C), Valley 2A (D), and Valley 1 (E).

Sometime after deposition of the valley 3B fill, relative sea level began to fall again initiating the valley 3A cut and fill cycle. This resulted in renewed valley incision into the V3B deposits but did not erode as deep as the previous cycle (Fig. 30b). The axis of valley 3A is orientated to the north-northeast. Valley 3A deposits are fluvial (Facies fl., Table 1). The lack of tidal influence observed in the outcrop suggests that: (1) relative sea level did not return to the level of the previous highstand and, (2) sediment supply was high enough so that the river system stayed high enough in its buffer zone to be out of reach of the major effects of tidal influences. This does not mean that some tidal influence was not present in this reach of the river, just that its effects were not preserved in the outcrop. Like V3B, the deepest incision of this new valley has escaped observation within the subsurface north of the study outcrop. During relative sea-level rise the rivers aggraded and a multistory valley fill developed. The lack of bar tops or anything resembling floodplain facies suggests that the river system aggraded slowly as it migrated back and forth across the valley (Bristow & Best, 1993). The lateral extent of these channel belt deposits throughout the field area implies that this meandering river migrated rapidly across the valley is it filled (Bristow & Best, 1993). As a result of the slow aggradation rate and the high rate of channel migration there is a high degree of connectivity between these sand bodies. As a result there is very little in the way of silts, muds, or clays to act as barriers or baffles to fluid flow, if this were a reservoir. In the study area these channel deposits have eroded into the older valley 3B fill leaving the above described remnant behind (Fig. 30b). As the valley filled, the fluvial system formed an irregular unconformity, which continued into the marine deposits adjacent to the older fill deposits. That the river completely eroded the older fill deposits south of section 11, and then scoured into parasequence 4, is evidence that the river widened the valley as it filled (Fig. 14). The valley base/margin at this stage in the compound valleys evolution is now a composite surface.

After the valley filled another relative sea-level drop brought about the valley 2B cycle of incision and filling. Like the previous two cycles this one resulted in fluvial degradation within the trunk valley. However, all evidence of this cut and fill within the trunk valley is within the subsurface north of the study outcrop. What is preserved within the outcrop is a tributary valley associated with this cycle of incision and backfilling (Fig. 30c). The axis of this tributary valley is roughly north-south, with paleoflow feeding into the trunk valley to the north. As described above, the outcrop exposure of V2B is that of a point bar that formed a meander scour in the side of the tributary valley. It's likely that this tributary valley existed during the earlier two cut-and-fill events. Yet it wasn't until this cycle of valley incision and filling that the meander scarp seen in the outcrop formed. The valley 2B basal erosion surface at its deepest is 8.8 meters above parasequence 4 (Fig. 14). The deepest incision seen in the field area is associated with V3A, which is 4.8 meters above parasequence 4 (Hilton, 2013). This suggests that the inferred magnitude of relative sea-level fall may not have been as great during this cycle as the one that created valley 3A. However, it is important to note that it is unknown what the true erosional relief of valley 2B is based on this limited exposure. As mentioned earlier, the valley 2B fill is mostly that of tidally influenced fluvial facies with lesser amounts of floodplain and abandoned channel facies (facies Ft., Ac., and Fpl., Table 1). The tidal influence seen in these fluvial deposits indicates that relative sea-level rise was controlling fluvial aggradation, the architecture of the valley, and the rate of valley filling. The nearly completely preserved thickness of the lowest channel belt deposits suggests that aggradation rates early on were high. Had relative sea-level rise been slow, then in all likelihood the channel, migrating back and forth across the valley, would have returned at a lower elevation and removed more of this point bars top. Another line of evidence for a fast relative sea-level rise early on is the abandoned channel deposits described above (Fig 14, Plate 1). Blum and Aslan (2006) explain that during fast relative sea-level rises the alluvial ridge is built up rapidly. This creates floodplain lows off the flanks of the levees that, when a breach of the levee happens, capture the river. These local avulsions abandon the channel course, which then fills with finer grained material creating the abandoned channel muds and silts seen in outcrop. Fluvial aggradation during this relative sea-level rise appears to have filled the valley completely. Whether relative sea level returned to the same elevation as it was prior to initial valley incision, or came close enough for fluvial aggradation (in the absence of any base level influences) to complete valley filling, is unknown.

Prior to the next episode of valley cutting and filling it is suspected that there was an avulsion and/or migration of the tributary stream which incised valley 2B to the west. The reasoning for this is that there is no evidence of this fluvial system across the field area prior to this cycle of incision and backfilling. If this stream had been present its preserved location during the earlier cycles, then there should be another deeper unconformity found underneath it. This deeper unconformity would have been created during the valley 3A cycle during which fluvial incision created a greater amount of erosional relief. The V2A cycle of degradation and aggradation is much like the V2B cycle in that the axis of the trunk valley is still far enough to the north to not be exposed in the study area (Fig. 30d). What is found is the new incision of the tributary stream in its new position extending across the older trunk deposits. The depth of incision is not as great as the other incision events suggesting that this relative sea level fluctuation was a smaller event imprinted upon the rising limb of a larger magnitude, lower frequency sea level fluctuation. The valley axis runs roughly north-south with paleoflow to the north (Fig. 9d). As sea level rose it entered this tributary and created a tidal ravinement surface. The evidence for this is there are no fluvial deposits deposited during valley incision preserved along the valley floor. What is found flooring this valley fill is esturine mud and silt (described above). As described above, what is unique about valley 2A is that the valley floor and margins are largely exhumed and exposed on the surface. Examination of this valley floor has revealed that it is widening to the north, which possibly indicates the tributary junction with the larger trunk valley is being approached. The following relative sea-level rise filled the trunk valley and its tributary completely.

Post valley filling, the trunk stream incised an even larger and deeper valley system to the south, valley 1 (Fig. 30e). Paleocurrents in valley 1 indicate that its axis is running northeast while valley 2 (the trunk) is running north northeast (Fig. 9e) (Li et al., 2010). This is the main reason for interpreting valley 2 as a separate system, formed from its own relative sea-level fluctuations, from valley 1 (Li et al., 2010). Also, fluvial style in valley 1 differs from valley 2, in that there are thick deposits of braided fluvial sandstones at the base of valley fill 1 (Li et al., 2010). Grain sizes are larger in valley 1 as well, with thick deposits of very coarse-grained sandstones and conglomerates (Li et al., 2010). It is interpreted here that these valleys were formed from the same river system but there was a regional avulsion between the filling of valley 2 and the incision of valley 1. Given the proximity of the 2 valleys to one another it is believed that the fluvial system that incised valley 1 did incise into its older valley 2 deposits and reestablish itself within its old valley margins. Within this valley there is a vertical transition from coarser grained braided fluvial deposits to finer grained tidally influenced fluvial deposits laid down by a single thread meandering stream (Li et al., 2010). This represents the transition from lowstand to transgressive deposition as the valley was backfilled during relative sea-level rise (Li et al., 2010). The deposits of valley 1 observed in the study outcrop (Facies Fl., Table 1) represent late transgression to highstand fluvial deposition.

Discussion

High Frequency Relative Sea-level Fluctuations – Evidence for Glacioeustacy?

Valley incision by coastal plain fluvial systems is driven largely by fluctuations in relative sea level (Zaitlin et al., 1994; Blum & Aslan, 2006). This is certainly the case for the compound valley system seen in the study area. As previously described, the valley 2 system was created by multiple low magnitude cut-and-fill cycles. The compound valley system was incised into the highstand wedge of parasequence. At this downdip location within the valley there is not a lot of room for fluvial aggradation once the "down-profile buttress shift", has occurred (Fig. 28) (Holbrook et al., 2006). This means that buttress shift (i.e. relative sea level) is the main force driving fluvial aggradation within the Neilson Wash compound valley system. This is not to say that upstream controls such as discharge cannot exert some control over the equilibrium gradient of the river (Holbrook et al., 2006), but there is very little room within the thin buffer zone for upstream controls to adjust the fluvial profile (Holbrook et al., 2006). The tidal signature within the fluvial deposits, as well as the esturine deposits within valley 2A, support the idea that relative sea-level changes (buttress shift) control fluvial aggradation and degradation within this reach of the valley.

Based on the work of Zhu et al. (2012), these valley fills were assigned to sequence one, and the underlying unconformity makes up part of the composite sequence boundary 1. Sequence 1 is interpreted to have been laid down over a single 100,000 year cycle (Zhu et al., 2012). This means that the relative sea-level oscillations that prompted the excavation of the valleys are high frequency events. The high frequency and low magnitude of these cycles suggests that these events are controlled by climate change due to astronomical forcing (i.e. Milankovitch cycles) (Li et al., 2010; Zhu et al, 2012). The Neilson Wash valley system shows clear evidence that it was incised and filled during multiple sea-level fluctuations over a short time span. The data presented here does serve to add yet another example of a stratigraphically preserved signature of high frequency global sea-level fluctuations to the growing list of evidence supporting the existence of greenhouse ice sheets in the Cretaceous (Holbrook, 2001; Plint & Wadsworth, 2003; Miller et al., 2005; Li et al., 2010).

Valley Widening and the Diachroniety of Sequence Boundaries

In their 2008 paper, *Valleys that never were: Time surfaces verses stratigraphic surfaces*, Strong and Paola introduced the idea of stratigraphic and topographic valleys. Topographic valleys are the geomorphic features as they existed for a moment in time.

Stratigraphic valleys are the valleys as they appear preserved in the rock record. Stratigraphic valleys are composite features that do not resemble the amalgamated topographic valleys that they are composed of. Stratigraphic valleys are formed because the valley container is continually being modified, either by allogenic or autogenic factors, throughout an entire relative sea-level cycle (Strong & Paola, 2008; Martin et al., 2011). Modification of the valley margins during relative sea-level rise is in the form of valley widening as the valley was being filled (Strong & Paola, 2008). This is in disagreement with earlier models (i.e. Shanley and McCabe's, 1994) which suggested that once relative sea level began to rise, valley widening (excision) stopped and the valley was passively filled (Strong & Paola, 2008). Figure 31 (A thru G) illustrates the creation of a stratigraphic valley by the constant modification of the valleys perimeter through time. During relative sea-level fall the valley is incised and widening occurs through the expansion and translation of bars caused by increased sediment discharge (discussed above) (Schumm, 1993; Holbrook and Schumm, 1999; Bridge, 2003; Martin et al., 2011). As relative sea-level rises the river continues to erode the valley margin intermittently during the course of valley filling (Strong & Paola, 2008; Martin et al., 2011). As mentioned above, this is a departure from the accepted theories (e.g. Shanley and McCabe, 1994) that as soon as valleys begin to backfill all valley excision stops (Strong & Paola, 2008). With this revelation came the above discussed realization that the valley width seen preserved in outcrop was likely shaped during relative sea-level rise (Strong & Paola, 2008). Now there is an effort to understand what controls valley widening during valley filling (Martin et al., 2011).

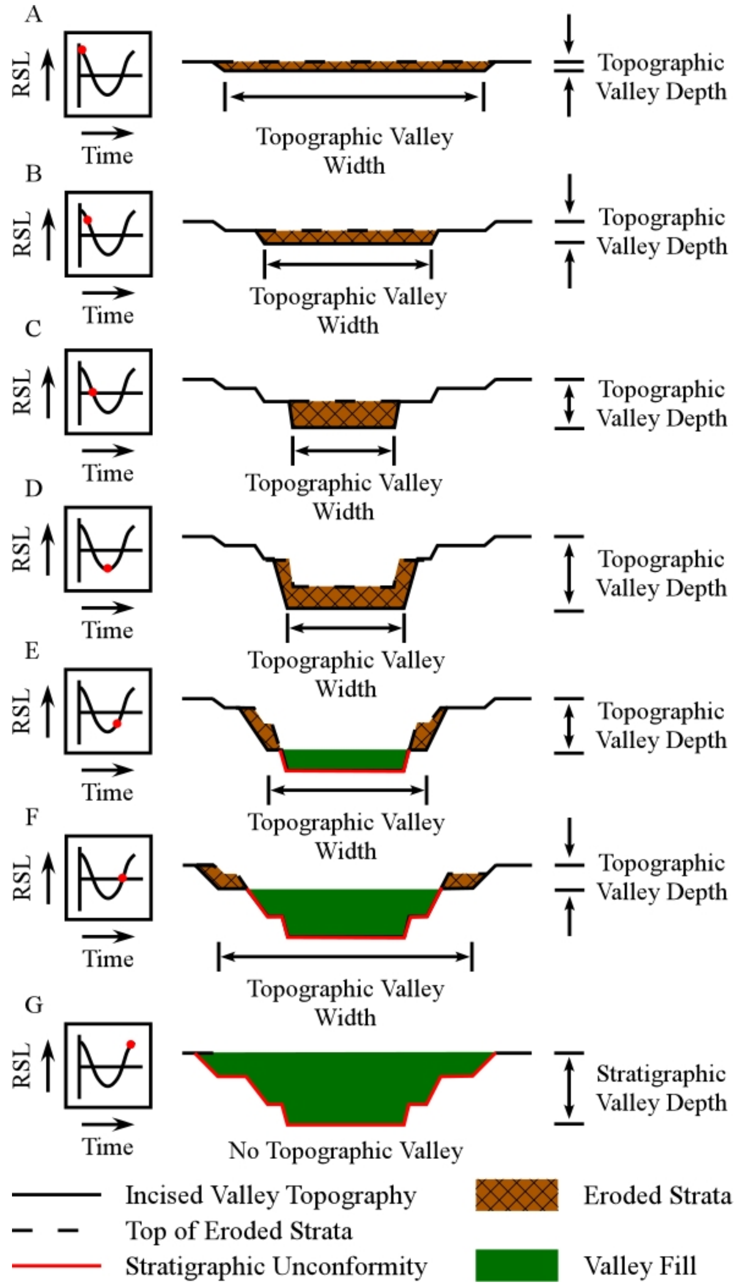

Figure 31. Model illustrating the concept of stratigraphic and topographic valleys (modified from Strong and Paola, 2008). From time A to time D fluvial incision in response to base level fall creates a topographic valley. From time E to time G rising base level forces valley filling. As the valley fills it is widening the valley erasing the old valley margins creating the stratigraphic valley preserved in outcrop. It is important to note that this model removes all traces of falling stage terraces which is not what is observed in the valley system studied here.

In order for a river to successfully widen a valley it needs to “attack” the margins of the valley (Martin et al., 2011). Attack, simply put, is the river intercepting the margin of the valley and eroding it. An effective way for this to happen is for the channel, once the river is in close proximity to a valley margin, to migrate into the valley margin around an expanding/translating bar (Martin et al., 2011). Major controls on channel migration are sediment supply, sediment type, sediment size, discharge, flood magnitude and frequency, the erodability of the floodplain, and slope of the alluvial plain/river valley (Bridge, 2003; Hook, 2007; Aswathi et al., 2008). Changes in the plan view geometry of rivers, such as expansion of a bar outwards, involves modification of the channel margins through erosion and deposition during floods (Bridge, 2003; Duan and Julien, 2010). Bankfull flow conditions are known as channel forming discharge (i.e. floods) (Bridge, 2003). Bankfull discharge is defined by Bridge (2003, p.154) as, “. . . a single discharge measure that can be assumed to represent the range in flood discharge that is responsible for the geometry of alluvial channels”. The amount of modification to the channels path during flooding events is mainly controlled by the channels power to erode and deposit sediments (Bridge, 2003). When a channel intercepts the side of a valley, the valley margin now becomes the cut bank of the river. Bar expansion can happen around a braid bar in the case of a multi-thread braided stream, or a point bar in a single thread meandering stream (Bridge, 2003; Martin et al., 2011). Bar expansion is largely an autogenic response to sediment discharge and average grain size during bankfull conditions (Bridge, 2003; Aswathi et al., 2008).

Tributary valley 2B is an outcrop example of a valley margin that was attacked multiple times during relative sea level rise. Figures 18a through 18f is a model of how the meandering tributary stream widened its valley in this location. As mentioned above, this outcrop exposure of V2B is through a meander scar caused by a westward expanding and downstream (northward) translating point bar. The lowest story of this valley fill shows that it was deposited during two distinct time periods (Fig. 18a -18f). The southern half is the oldest and was deposited during the initial incursion of the river into the valley margin (Fig. 14). Over time the river locally widened the valley as the bar expanded/translated. What is controlling the expansion/translation of this point bar is hard to determine but it's quite possible that just upstream from this location the river was creating another meander scar which increased sediment supply to this area. Another effective way to promote bar expansion is through changes in the slope of the fluvial profile (Schumm and Khan, 1972; Schumm, 1993; Bridge, 2003; Timár, 2003; Aswathi et al., 2008). Thus it is also possible that valley backfilling may have produced a slope favorable for increasing sinuosity. Fluvial widening of the valley caused by bar expansion and translation continued for some time, and created a valley floor that is progressively younger to the north (due to translation). Eventually the river avulsed to a new position out of the meander scar. This is indicated by the abandoned channel fill facies in the southern edge of the outcrop (Fig. 14), and the fact that the point bar is still preserved. Had the river migrated out of the meander scar the fluvial architecture would have been very different. In time the river reoccupied its old course through the meander scar (Fig. 18b). Enough time had passed however so now the base of the channel belt was approx. 1.1 meters higher than before due to valley filling (Fig. 32). Also significant is the fact that these younger point bar deposits are much more heterolithic suggesting that the system is more tidally influenced due to rising relative sea level (Fig. 32).

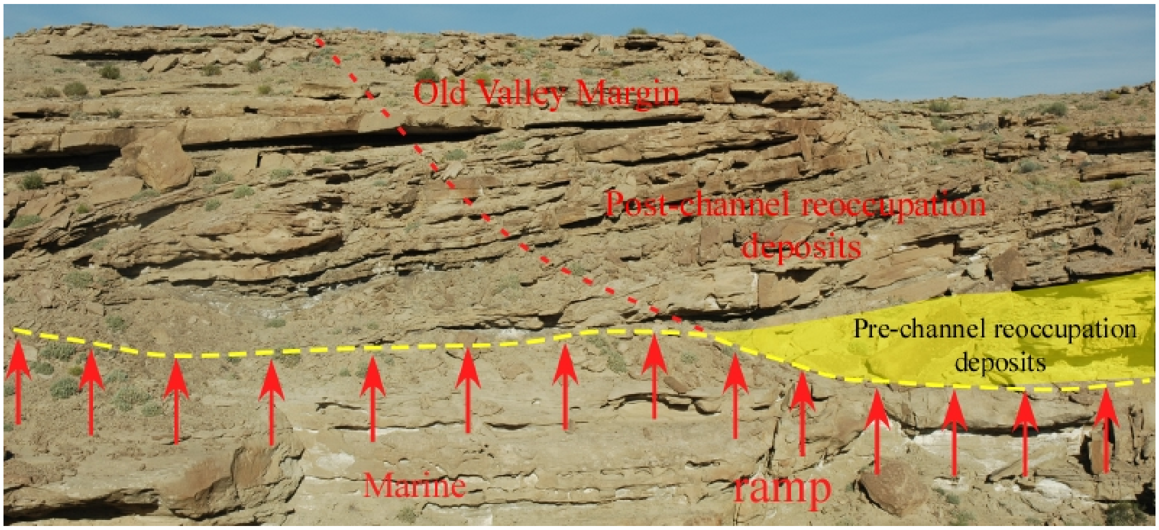

Figure 32. Outcrop photo of valley 2B illustrating the ramp formed from channel reoccupation and renewed valley widening. The ramp is 1.1 meters high measured from the base of the pre-channel reoccupation deposits (highlighted in yellow) to where the ramp stops climbing adjacent to the top of the pre-channel reoccupation deposits. Red arrows point out the base of the valley.

Expansion and translation of the point bar renewed and continued the process of locally widening the valley (Figs. 18c thru 18f). Widening of the valley here appears to be primarily the result of translation. Neilson Wash here is narrow and the point bar never expanded across the wash, as indicated by the preserved marine facies forming an interfluve on the opposite side of the modern wash. Translation of the bar elongated the meander scar northward, which created an erosional scour (the valley floor) that gets younger to the north. Also the base of the channel belt is aggrading to the north as the river was widening the valley which suggests, like the increasingly tidal nature of the deposits, that rising relative sea levels are forcing the valley to fill (Fig. 32). Each of these intermittent attacks on the valley margin is a local erosion surface known as a

Figure 33. Photograph of the southern margin of the Neckar River valley at Heidelberg, Germany. This photograph illustrates how valley margins are draped with vegetation.

diastem (Bhattacharya, 2011). The outcrop exposure of V2B is an example of how diastems amalgamate to create a time transgressive valley margin/floor. It also illustrates how over time the stratigraphic valley is created through a constantly evolving topographic valley. Furthermore, and most importantly, this exposure through V2B is an outcrop example of a valley that widened as it was filling during relative sea-level rise which helps dispel the notion that valleys are passively filled (*sensu* Shanley & McCabe, 1994).

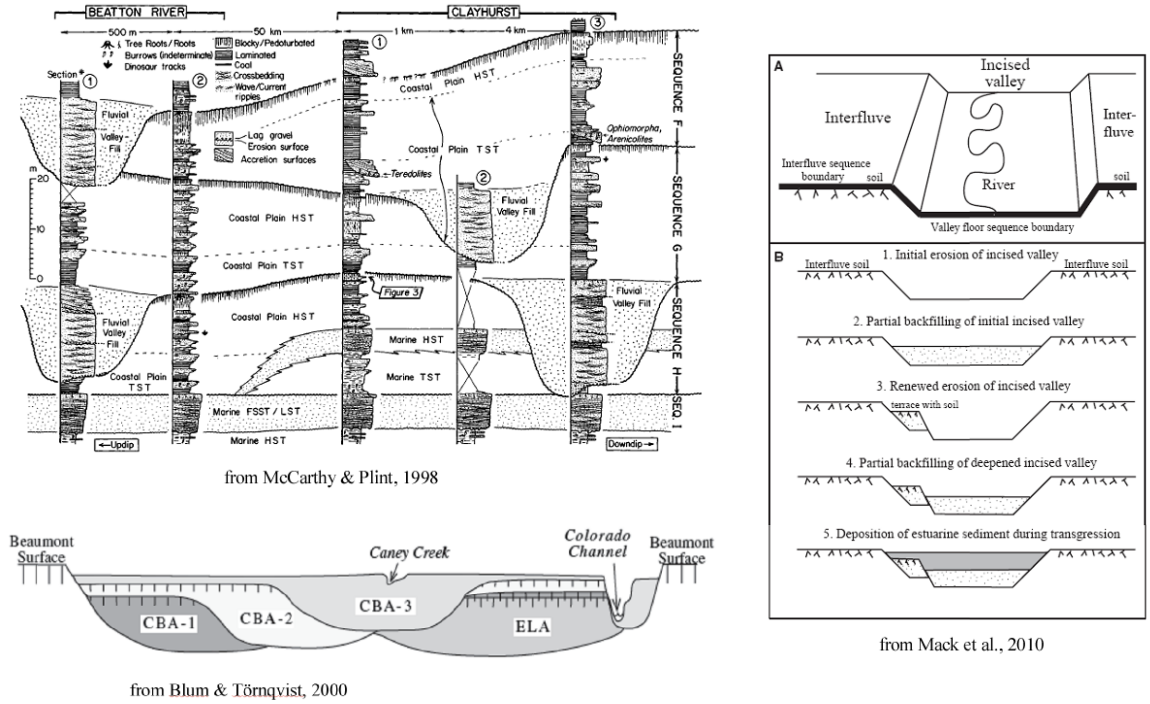

Figure 34. Examples valley models from various outcrop studies. Note that paleosols are readily identified upon the interfluves but are not observed and described along the valley margins.

Another line of evidence to support the idea that valleys can, and do widen as they are backfilled, comes from the observation of modern valleys. Along modern river valleys today there is an abundance of vegetation and soils draping the interfluves and valley margins (Fig. 33). In studies of ancient valleys paleosols and rooted horizons are commonly identified on the interfluves and used to mark sequence boundaries (McCarthy & Plint, 1998; Blum & Törnqvist, 2000; Mack et al., 2010). However, paleosols and rooted horizons are not commonly preserved in outcrop along the margins of paleovalleys (Fig. 34). If valleys were filled like the “cut-and-fill” model suggests, then there should be an abundance of soils and/or rooted horizons along the valley margins described in the literature. Were they to be commonly preserved, then valley fill deposits would not

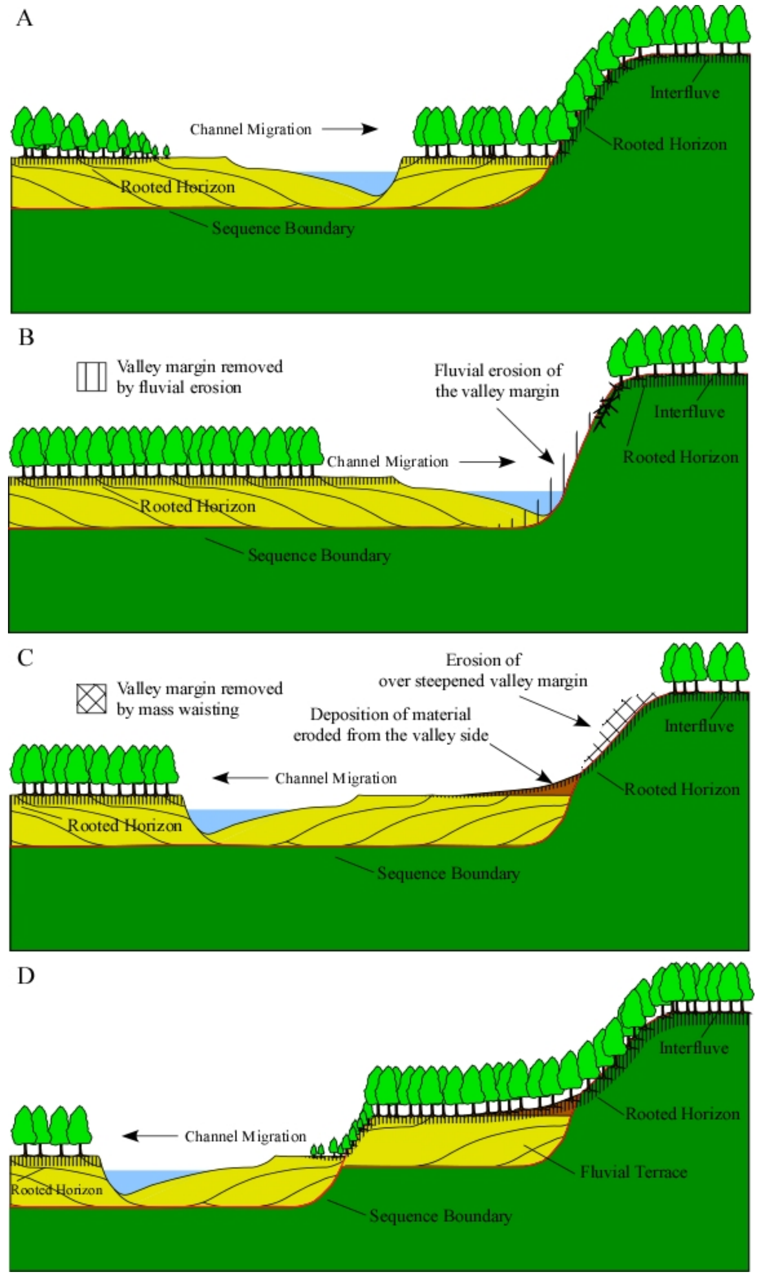

Figure 35. Model of how paleosols will not be deposited along the valley margin in the case of fluvial terrace creation. A&B) Channel migrates and eventually intercepts the valley margin eroding it. C) After eroding the valley margin the channel migrates away leaving the sequence boundary buried. Erosion of the valley margin over steepened it increasing the rate of weathering and erosion. D) Further valley incision leaves the previous channel deposits stranded as a terrace on the valley margin. (Channel belt modified from Bridge, 2003)

directly onlap onto the sequence boundary forming the valley margins. Instead, they would onlap onto either a soil horizon, or at the very least, a rooted horizon. The "sharp contact" between proximal (valley fill deposits) and distal deposits would instead be described as proximal deposits onlapping a pedogenically modified zone of distal deposits. However, this is not the case, and paleosols, along with rooted horizons, are typically missing. One possible reason these elements are missing is because the fluvial system is widening the valley as it is filling (Strong and Paola, 2008). As described above, the river periodically comes into contact with the valley margin (Strong and Paola, 2008) (Fig. 35a). When this occurs the first deposits to be eroded are the paleosols, followed by the underlying bedrock with its rooted horizon (Fig. 35b). Once the fluvial system moves away, either by avulsion or migration, the deposits that are now along the valley margins (in contact with the now modified sequence boundary) are active or passive channel fills (Fig. 35c). This doesn't mean that soils cannot be preserved along valley sides. Gupta (1997) provides an example of an incised valley with soils preserved along the margins of the valley, but this is rare in the literature.

Another line of evidence for the diachronous nature of stratigraphic valley margins come from the case of incised valleys formed over multiple cut and fill episodes (Blum & Aslan, 2006; Korus et al., 2008). Incised valleys found along coastal plains are primarily formed in response to relative sea level fluctuations (Gibling et al., 2011). Studies of Quaternary age incised valleys found along the Upper Texas Gulf Coast have shown the effectiveness of Milankovitch-scale glacioeustatic sea-level fluctuations in valley formation (Blum & Törnqvist, 2000; Blum & Aslan, 2006; Korus et al., 2008; Gibling et al., 2011). The Neilson Wash compound valley system was formed as a result

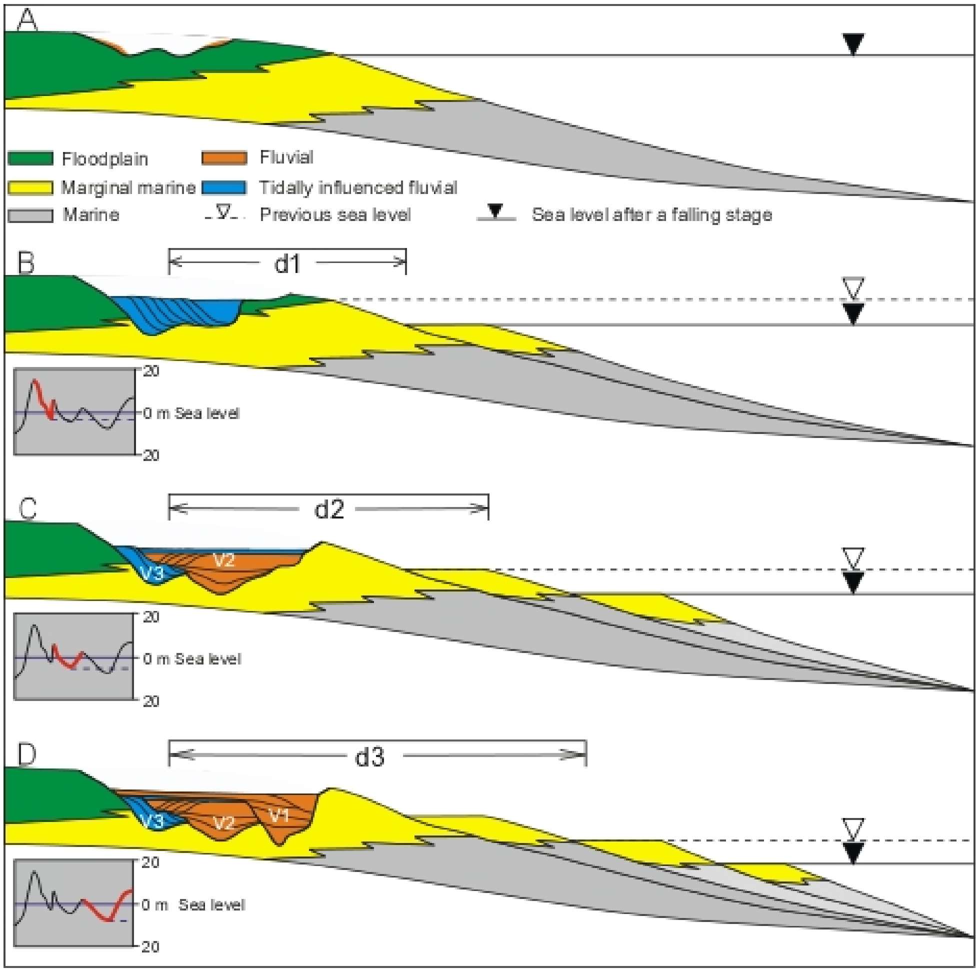

Figure 36. Diagram illustrating the stratigraphic evolution of the V1, V2, and V3 compound valley system during a stepped forced regression (from Li & Bhattacharya, 2013). A) Initial relative sea level fall and incision of valley 3. B) Valley 3 fill after relative sea level rise. C) The valley 2 cycle of incision and fill. D) The valley 1 cycle of incision and fill. Each cycle of incision and filling during this stepped forced regression results in the shoreline down stepping away from the valleys.

of multiple relative sea-level fluctuations. The compound valley system is unique in that it was created by a stepped forced regression (Fig. 36) (Li & Bhattacharya, 2013).

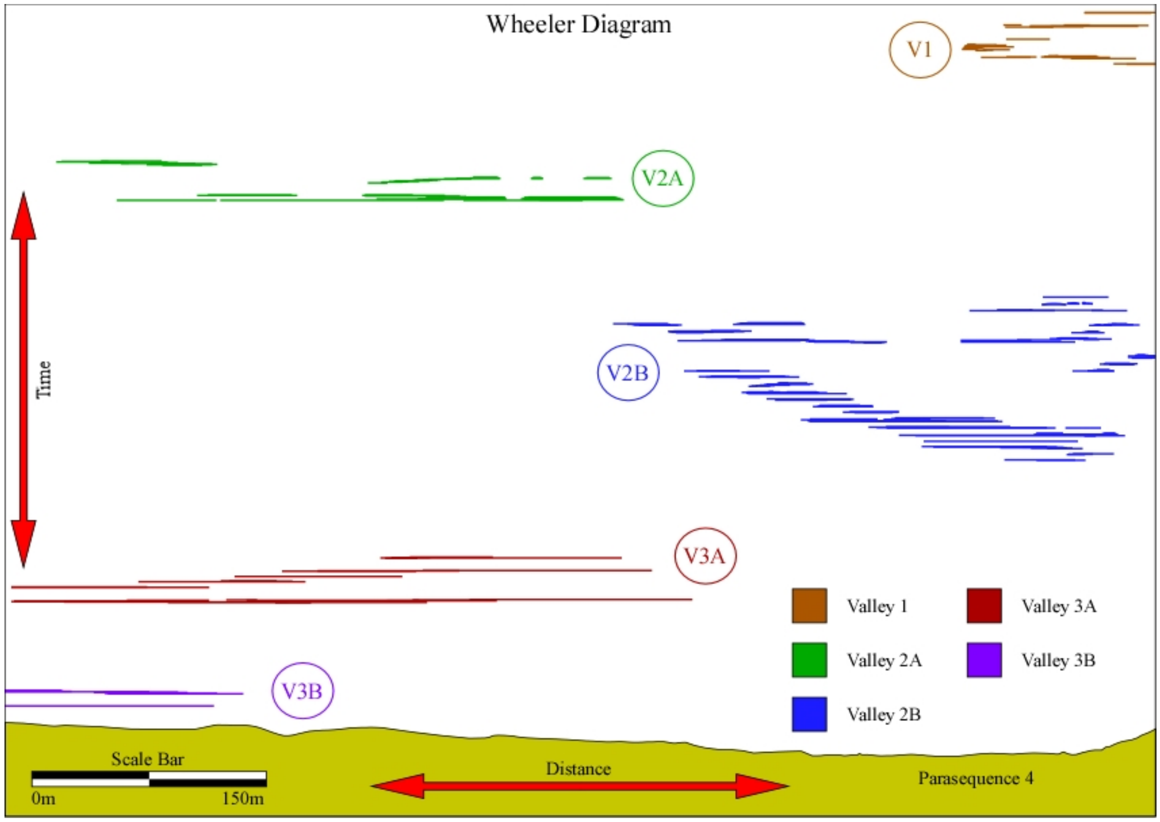

Figure 37. Wheeler diagram of the valley fills found in the study outcrop illustrating how little time is represented by the deposits of the valley fills when compared to how long it took for the multiple valleys to cut and fill. Also illustrated is the diachronous nature of the sequence boundary underlying the valleys. The entire time interval is less than 100 ka.

Evidence for this comes from the erosional relief of the valleys as well as the nature of their fills. When the unconformities that bound each of the individual valley fill deposits in the Neilson Wash compound valley are combined with one another it is apparent that the sequence boundary through the field area is highly diachronous. A Wheeler diagram of the study outcrop was constructed (fig. 37) to visualize the timing of the depositional and erosional events within the valley system (Wheeler, 1958). This technique allows the relative age of each depositional unit to be examined with respect to one another

(Bhattacharya, 2011). This is critical because there are not methods for dating deposits that are pre-Quaternary in age to a precision of << 100 ka (Bhattacharya, 2011). This Wheeler diagram was built using the detailed bedding diagram of the study outcrop. Using channel belts as the basic building blocks for the diagram, it is easily observable how these channel belt deposits were laid down over time. Also observable is the direction of lateral accretion around expanding point bars. Bhattacharya (2011) points out that when Wheeler diagrams are constructed in this fashion, as opposed to simply lumping all of the sediment within a valley fill together, there will be far more time represented in the diagram than sediment. This is certainly true for the Wheeler diagram constructed for this research. This time is the vacuity which represents sediment lost to erosion and the times of non-deposition added together (Wheeler, 1958). Archer et al. (2011) explain that, due to a lack of evidence, it is falsely assumed that for fluvial reservoir models aggradation was constant and no time gaps exist. The fact that channel belt deposits in this Wheeler diagram are floating in the vacuity, and not in contact with each other, proves that deposition was intermittent. The Wheeler diagram also illustrates just how the master erosion surface flooring the valley fill of the study outcrop developed. The fluvial systems that incised the trunk valley, as well as the tributary valleys, repeatedly modified the 8^{th} order composite sequence boundary as the valleys were incised and filled. In the Wheeler diagram of the study outcrop the valley fill reveals the position of the valleys along the exposure. The positions of each fill on the vertical axis shows the relative timing of each cut and fill cycle with respect to one another. This illustrates the time transgressive nature of the 8^{th} order composite sequence boundary flooring the compound valley system as well as the sequence of incision and

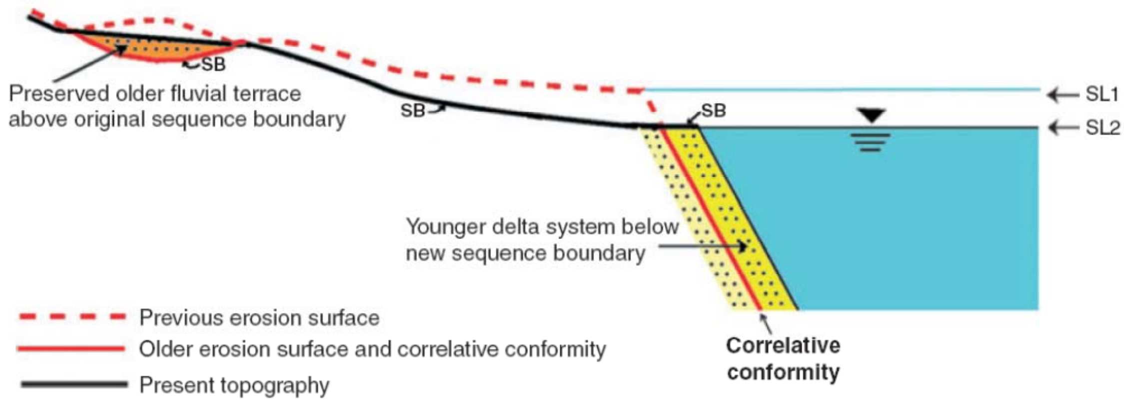

Figure 38. Cross section illustrating how fluvial terrace deposits within an incised valley can be preserved above a sequence boundary while younger falling stage deposits are preserved below (from Bhattacharya, 2011, modified from Strong & Paola, 2008).

fill events that went into its development. Combine this with the fact that along the valley margins of this system the sequence boundary is being modified during valley filling (such as with valley 2A) it is clear that this 8th order surface is highly diachronous.

Fluvial Terraces and the Chronostratigraphic Significance of Sequence Boundaries

Sequence boundaries are defined as being chronostratigraphically significant surfaces (Van Wagoner et al., 1990). The chronostratigraphic implication here is that sequence boundaries separate older deposits below the sequence boundary from younger deposits above it (Strong & Paola, 2006; Bhattacharya, 2011). However, this idea is may be incorrect if it does not take into account the stratigraphic position of falling stage deposits (Bhattacharya, 2011). Strong and Paola (2008) modeled a scenario where as relative sea level is falling, fluvial terraces are deposited along the flanks of the valley being incised (fig. 38). Later, as the shoreline migrates seaward and the river lengthens, younger delta deposits are being laid down (Strong & Paola, 2008). As relative sea level continues to fall these delta lobes are abandoned and the river will migrate seaward over their tops and erode into them (Strong & Paola, 2008). This erosion surface overlying these falling stage deltaic deposits is a highly diachronous sequence boundary that is a composite of many local erosion surfaces (*i.e.* diastems) (Strong & Paola, 2008; Bhattacharya, 2011).

Studies of incised valleys, formed by the Colorado River on the coastal plain of Texas over the last 400,000 plus years, have shown that four episodes of relative sea-level oscillations have created a compound valley much like the Neilson Wash compound valley (Blum & Törnqvist, 2000; Blum & Aslan, 2006). Each sea-level fluctuation was glacioeustatic in origin and represents 100 kyr Milankovitch cycles (eccentricity) (Reading & Levell, 1996; Blum & Törnqvist, 2000; Blum & Aslan, 2006). The resulting stratigraphic valley was created over four separate cut-and-fill events (Blum & Törnqvist, 2000; Blum & Aslan, 2006). As sea level fell during one of theses 100 kyr events, lateral migration of the river (controlled by deposition) along with episodes of aggradation and degradation (controlled by stream power and sediment supply) worked to create stepped fluvial terraces (stepped unpaired autogenic terraces *sensu* Strong & Paola, 2008) (Blum & Törnqvist, 2000; Blum & Aslan, 2006; Holbrook et al., 2006; Martin et al., 2011). In some cases, high frequency, low magnitude glacioeustatic sea-level changes are overlain upon a higher magnitude, lower frequency eustatic sea-level falls (e.g. short period Milankovitch cycles overlain upon longer period Milankovitch cycles) (Blum & Törnqvist, 2000; Blum & Aslan, 2006; Bhattacharya, 2011). This also results in a multiterraced valley (each terrace represents a single cut and fill) but in this scenario terrace formation is an allogenic response to a stepped forced regression (Blum & Törnqvist, 2000).

Whether it is autogenic or allogenic forcing that created the terraces, the end result is a paleovalley with a composite valley forming a master erosion surface bounding the entire package (Blum & Törnqvist, 2000; Blum & Aslan, 2006). The terraces themselves are areas where sediment is stored during relative sea-level fall and valley incision (Blum & Törnqvist, 2000; Blum & Aslan, 2006; Holbrook & Bhattacharya, 2012). Valley fill 3B (the oldest) represents an example of these terrace deposits preserved above the sequence boundary. As discussed above, it is interpreted here to have been deposited during a minor marine transgression associated with a stepped forced regression. Once relative sea level began falling again, and the river resumed incising, these deposits were left behind as a terrace that formed as a result of allogenic forcing, much like the Quaternary age Colorado River compound incised valley (Fig. 30c). These terrace deposits are naturally going to be older than the falling stage deposits laid down after relative sea level fall resumed. As relative sea level continued to fall, the fluvial system responsible for incising the valley would have extended out over these falling stage deposits upon the shelf/ramp and eroded into them (Strong & Paola, 2008). This erosion surface is the sequence boundary that now separates older terrace deposits above it from the younger falling stage deposits below it (Fig. 38) (Strong & Paola, 2008).

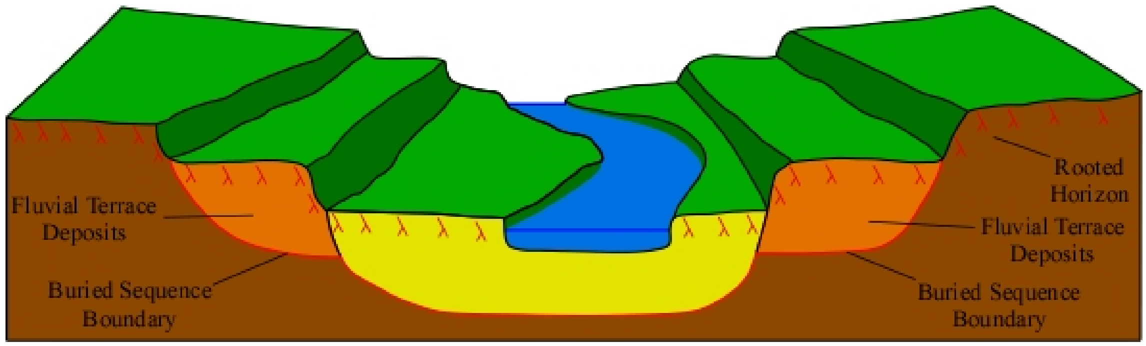

Figure 39. Block diagram of an incised valley with a flight of terraces on both sides (modified from Archer et al., 2011). The rooted horizon (vegetation) never marks the sequence boundary under, and adjacent to, the terrace deposits because the surface is buried shortly after valley excision stops.

Fluvial terraces are often described as having very low preservation potential and are not commonly described in ancient valley deposits (Plint & Wadsworth, 2003; Gibling, 2006; Holbrook et al., 2006; Archer et al., 2011). One explanation for this is they are difficult to identify due to the poor resolution of dating techniques for ancient deposits and the poor quality of the study outcrops (Plint & Wadsworth, 2003; Holbrook et al., 2006; Archer et al., 2011). As discussed earlier, missing paleosols and rooted horizons from valley margins in outcrop might be the result of river widening during the backfilling of valleys. However, another explanation for these phenomena could be that these paleosols were never present draping stratigraphic valley margins. This can only happen if the valley margin sequence boundary was buried during valley incision and was never subaerially exposed. As mentioned above, this would happen if the valley margin was covered in flights of terraces formed during base level fall (Fig. 39). These deposits bury the valley bounding sequence boundary and prevent vegetation from taking hold along them. The fact that stratigraphic valley margins are not commonly draped in paleosols may mean that terraces deposits are more common than previously believed.

As discussed previously, the sequence boundary that is the floor and margins of this valley system is highly diachronous. This is due to the compound valley being created over multiple cut and fill cycles as well as modifications to each individual valleys margin over time such as in the case of valley widening during valley backfilling. It is the nature of sequence boundaries to constantly evolve over time until burial. Because they are constantly being modified and extended seaward during falling stage, it is highly likely that there will be older proximal deposits preserved above the sequence boundary while younger distal deposits are below. Unfortunately the falling stage deposits that were laid down along the ramp/shelf are not preserved due to erosion. However, evidence of falling stage forced regressive deposits ius observed in the older marine parasequences (Fig. 5) (Zhu et al., 2012). The preservation of terrace deposits within the Neilson Wash compound valley system suggests that sequence boundaries do not always separate younger deposits above from older deposits below. This is because lowstand had not been attained yet during this stepped forced regression and the younger falling stage deposits would have been be overlain by the sequence boundary (Strong & Paola, 2008; Bhattacharya, 2011). This relationship of older terrace deposits above the sequence boundary, while there are younger falling stage deposits preserved below it, is in disagreement with the definition of a sequence boundary and suggests that the defining characteristic of sequence boundaries as chronostratigraphic significant is not valid (Strong & Paola, 2008; Bhattacharya, 2011).

Conclusions

Outcrops of the Ferron Sandstone along Neilson Wash show an example of a compound valley fill that incised into the marine parasequences of the highstand prism. The field area adjacent to the study outcrop is unique in that it sits near the junction of a trunk valley and tributary valleys. The compound valley system was created over multiple cut and fill episodes. Valleys show a significant abrupt basinward shift in deposition, (2) truncation, (3) valley fill deposits downlap onto the valley floor or onlap the valley margins, (4) regionally mappable interfluves, (5) the presence of smaller tributary valleys (in the case of the trunk valley). Comparing the incision depth of the valley vs. the height of the river channel is further proof that these are valleys. Proof that these are indeed discreet valleys comes from several lines of evidence: (1) cross cutting relationships of each valleys basal erosional surface, (2) the degree of tidal influence found, (3) the maximum depths of valley incision and, (4) from the differing orientations of the valleys.

Valley excision removes the old topographic valley margins and replaces them with the stratigraphic margins seen in outcrop. This suggests that the sequence boundaries encasing the valley are strongly time transgressive. The margin of valley 2B is an outcrop example of one that was modified during the time the valley was backfilling. The outcrop of V2B is an exposure through a meander scarp formed over time as the river widened the valley as it filled. Further evidence for this process of valley widening during backfilling can be found in the lack of paleosols along ancient valley margins. One explanation for this is that valleys widen as they are filled and stripped away all evidence of vegetation. The compound valley system is believed to be the result of several high frequency sea-level fluctuations, suggesting that they are the result of glaceoeustatic Milankovitch cycles (Zhu et al., 2012). The multitude of relative sea-level fluctuations resulted in a regional composite sequence boundary. The Wheeler diagram of the study outcrop illustrates that only three of the valleys modified this sequence boundary. However, across the field area it was found that all 3 of these valleys incised into parasequence 4 at some point and modified the sequence boundary. Because individual valleys (formed and filled during one sea-level cycle) can widen as they are filled this means the sequence boundary is modified during that entire cycle. In the case of the Neilson Wash compound valley the sequence boundary has the potential to be modified through each cut and fill cycle. The net effect is a strongly time transgressive sequence boundary that was modified throughout the life of the compound valley.

Sequence boundaries are defined as surfaces separating older deposits below it from the above younger deposits requiring chronostratigraphic significance. Strong and Paola (2008) describe a scenario where as relative sea level falls, younger, distal falling stage deposits are placed below the sequence boundary. In the non-marine realm, older terrace deposits within incised valleys are preserved above the same sequence boundary. As described earlier, valley 3B is a terrace deposit preserved on the flank of a younger valley. This terrace deposit also sits on top of the composite sequence boundary. These deposits were older than the falling stage delta deposits laid down at the time valley 3A was incising. Unfortunately these falling stage deposits have been eroded away so there can be no correlation between the sequence boundary and the age of the deposits above and below it. However, the presence of an older terrace deposit above the sequence boundary does help to support the idea that sequence boundaries are not chronostratigraphically significant.

References

Archer, S. G., Reynisson, R. F., and Schwab, A. M., 2011, River terraces in the rock record : An overlooked landform in geological interpretation?, *in* Davidson, S. K., Leleu, S., and North, C. P., eds., From River to Rock Record: The Preservation of Fluvial Sediments and their Subsequent Interpretation: SEPM, Special Publication 97, p. 63–85.

Ardies, G.W., Dalrymple, R.W., and Zaitlin, B.A., 2002, Controls on the geometry of incised valleys in the Basal Quartz unit (Lower Cretaceous), Western Canada Sedimentary Basin: Journal of Sedimentary Research, v. 72, p. 602–618.

Armstrong, R. L., 1968, Sevier orogenic belt in Nevada and Utah: Geological Society of America Bulletin, v. 79, p. 429-458.

Aswathi, M. V., Vijith, H., and Setheesh, R., 2008, Factors influencing the sinuosity of Pannagon River, Kottayam, Kerala, India: An assessment using remote sensing and GIS: Environ Monit Assess., 138, p. 173-180.

Barton, M. D., Tyler, N., and Angle, E. S., 2004, Facies architecture and permeability structure of valley fill sandstone bodies, Cretaceous Ferron Sandstone, Utah: *in* T. C. Chidsey, Jr., R. D. Adams, and T. H. Morris, eds., Regional to Wellbore Analog for Fluvial-Deltaic Reservoir Modeling; the Ferron Sandstone of Utah: AAPG Studies in Geology 50, p. 383-403.

Bhattacharya, J. P., 2011, Practical problems in the application of the sequence stratigraphic method and key surfaces: integrating observations from ancient fluvial–deltaic wedges with Quaternary and modelling studies: Sedimentology, v. 58, p. 120–169.

Bhattacharya, J. P., MacEachern, J. A., 2009, Hyperpycnal rivers and prodeltaic shelves in the Cretaceous seaway of North America: Journal of Sedimentary Research, v. 79, p. 184-209.

Bhattacharya, J. P., Tye, R. S., 2004, Searching for modern Ferron analogs and application to subsurface interpretation, *in* T. C. Chidsey, Jr., R. D. Adams, and T. H. Morris, eds., Regional to Wellbore Analog for Fluvial-Deltaic Reservoir Modeling; the Ferron Sandstone of Utah: AAPG Studies in Geology 50, p. 39-57.

Bhattacharya, J.P. and Walker, R.G., 1991, Allostratigraphic subdivision of the Upper Cretaceous Dunvegan, Shaftesbury, and Kaskapau Formations in the subsurface of northwestern Alberta: Bull. Can. Petrol. Geol., 39, 145–164.

Blum, M. D., and Aslan, A., 2006, Signatures of climate vs. sea-level change within incised valley-fill successions: Quaternary examples from the Texas Gulf Coast: Sedimentary Geology, v. 190, p. 177–211.

Blum, M.D., and Törnqvist, T.E., 2000, Fluvial response to climate and sea-level change: a review and look forward: Sedimentology, v. 47 (Supplement), p. 1–48.

Blum, M. D., 1993, Genesis and architecture of incised valley fill sequences: a late Quaternary example from the Colorado River, Gulf Coastal Plain of Texas: *in* Weimer, P., and Posamentier, H.W., eds., Siliciclastic Sequence Stratigraphy, Recent Developments and Applications: AAPG Memoir 58, p. 259–283.

Boyd, R., Dalrymple, R.W., and Zaitlin, B.A., 2006, Estuary and incised valley facies models, *in* Posamentier, H.W., and Walker, R.G., eds., Facies Models Revisited: SEPM, Special Publication 84, p. 171–234.

Bridge, J.S., 2003, Rivers and Floodplains: Oxford, U.K., Blackwell Science, 491 pp.

Bridge, J. S., 2006, Fluvial facies models: Recent developments, *in* Posamentier, H.W., and Walker, R.G., eds., Facies Models Revisited: SEPM, Special Publication 84, p. 81–168.

Bristow, C.S., and Best, J.L., 1993, Braided rivers: perspectives and problems, *in* Best, J.L., and Bristow, C.S., eds., Braided Rivers: Geological Society of London, Special Publication 75, p. 1–11.

Catuneanu, O., Willis, A.J. and Miall, A.D., 1998, Temporal significance of sequence boundaries: Sedimentary Geology, v. 121, p. 157–178.

DeCelles, P. G., 2004, Late Jurassic to Eocene evolution of the Cordilleran thrust belt and foreland basin system, western U.S.A.: American Journal of Science, v. 304, p. 105-168.

DeCelles, P. G., and Coogan, J. C., 2006, Regional structure and kinematic history of the Sevier fold-and-thrust belt, central Utah: GSA Bulletin, v. 118, p. 841-864.

Duan, J. G., Julien, P. Y., 2010, Numerical simulation of meandering evolution: Journal of Hydrology, 391, p34-46.

Fielding, C.R., 2010, Planform and facies variability in asymmetric deltas: facies analysis and depositional architecture of the Turonian Ferron Sandstone in the Western Henry Mountains, South-Central Utah, U.S.A.: Journal of Sedimentary Research, v. 80, p. 455–479.

Gardner, M. H., 1995, Tectonic and eustatic controls on the stratal architecture of mid-Cretaceous stratigraphic sequences, central western interior foreland basin of North America, *in* S. L. Dorobek and G. M. Ross, eds., Stratigraphic Evolution of Foreland Basins: SEPM, Special Publication No. 52, p. 243–281.

Garrison, J. R. Jr., and van den Bergh, T. C.V., 2004, High-Resolution Depositional Sequence Stratigraphy of the Upper Ferron Sandstone Last Chance Delta: An Application of Coal-Zone Stratigraphy, *in* T. C. Chidsey, Jr., R. D. Adams, and T. H. Morris, eds., Regional to Wellbore Analog for Fluvial-Deltaic Reservoir Modeling; the Ferron Sandstone of Utah: AAPG Studies in Geology 50, p.125-192.

Garrison, J. R. Jr., and van den Bergh, T. C. V., 2006, Effects of sedimentation rate, rate of relative rise in sea level, and duration of sea-level cycle on the filling of incised valleys: examples of filled and "overfilled" incised valleys from the upper Ferron Sandstone, Last Chance Delta, east-central Utah, U.S.A., *in* R. W. Dalrymple, D. A. Leckie, and R. W. Tillman, eds., Incised Valleys in Time and Space: SEPM Special Publication No. 85, p. 239-279.

Gibling, M.R., Fielding, C.R., Sinha, R., 2011, Alluvial valleys and alluvial sequences: towards a geomorphic assessment, *in* Davidson, S.K., Leleu, S., North, C. eds., From River to Rock Record: The Preservation of Fluvial Sediments and Their Subsequent Interpretation: SEPM Special Publication, 97, p. 423–447.

Gibling, M. R., 2006, Width and thickness of fluvial channel bodies and valley fills in the geological record: A literature compilation and classification: Journal of Sedimentary Research, v. 76, p. 731-770.

Gupta, S., 1997, Tectonic control on paleovalley incision at the distal margin of the early Tertiary Alpine foreland basin, southeastern France: Journal of Sedimentary Research, v. 67, p. 1030-1043.

Hilton, B. D., 2013, 3D allostratigraphic mapping and facies heterogeneity of a compound, tributary incised valley system, Turonian Ferron Sandstone, Notom Delta, South-Central Utah: University of Houston, Master's Thesis, 132 pp.

Holbrook, J.M., 2001, Origin, genetic interrelationships, and stratigraphy over the continuum of fluvial channel-form bounding surfaces: an illustration from middle Cretaceous strata, southeastern Colorado: Sedimentary Geology, v. 144, p. 179–222.

Holbrook, J. M., and Bhattacharya, J. P., 2012, Reappraisal of the sequence boundary in time and space: Case and considerations for an SU (subaerial unconformity) that is not a sediment bypass surface, a time barrier, or an unconformity: Earth-Science Reviews, v. 113, p. 271-302.

Holbrook, J.M., and Schumm, S.A., 1999, Geomorphic and sedimentary response of rivers to tectonic deformation: A brief review and critique of a tool for recognizing subtle epeirogenic deformation in modern and ancient settings: Special issue on Tectonics of Continental Interiors: Tectonophysics, v. 305, p. 287–306.

Holbrook, J. M., Scott, R. M., and Oboh-Ikuenobe, F. E., 2006, Base level buffers and buttresses: A model for upstream versus downstream control on fluvial geometry and architecture within sequences: Journal of Sedimentary Research, v. 76, p. 162-174.

Hook, J. M., 2007, Complexity, self-organisation and variation in behavior in meandering rivers: Geomorphology, v. 91, p. 236-258.

Ichaso, A. A., and Dalrymple, R. W., 2009, Tide- and wave-generated fluid mud deposits in the Tilje Formation (Jurassic), offshore Norway: Geology, v. 37, p. 539-542.

Imbrie, J., Hays, J.D. and Martinson, D.G., 1984, The orbital theory of Pleistocene climate: support from a revised chronology of the marine oxygen isotope record, *in* Berger, A.L. ed., Milankovitch and Climate: Dordrecht, The Netherlands. Reidel Publishing Company, p. 269–305.

Korus, J. T., Kvale, E. P., Eriksson, K. A., and Joeckel, R. M., 2008, Compound paleovalley fills in the Lower Pennsylvanian New River Formation, West Virginia, USA: Sedimentary Geology, v. 208, p. 15-26.

Le Clair, S. F., and J. S. Bridge, 2001, Quantitative interpretation of sedimentary structures formed by river dunes: Journal of Sedimentary Research, v. 71, p. 713–716.

Li, W., Bhattacharya, J.P. and Campbell, C., 2010, Temporal evolution of fluvial style in a compound incised-valley fill, Ferron ''Notom Delta'', Henry Mountains Region, Utah (USA): Journal of Sedimentary Research, v. 80, p. 529–549.

Li, Y., and Bhattacharya, J. P., 2013, Facies architectural study of a stepped, forced regressive compound incised valley system in the Ferron Notom Delta, Southern Central Utah, U.S.A.: Journal of Sedimentary Research, v. 83, p. 206-225.

Mack, G. H., Tabor, N. J., and Zollinger, H. J., 2010, Palaeosols and sequence stratigraphy of the Lower Permian Abo Member, south-central New Mexico, USA: Sedimentology, v. 57, p. 1566-1583.

Martin, J., Cantelli, A., Paola, C., Blum, M., Wolinsky, M., 2011, Quantitative modeling of the evolution and geometry of incised valleys: Journal of Sedimentary Research, v. 81, p. 64-79.

Mattheus, C. R., Rodriguez, A. B., Green, D. L., Simms, A. R., Anderson, J. B., 2007, Control of upstream variables on incised-valley dimension: Journal of Sedimentary Research, v. 77, p. 213-224.

McCarthy, P.J. and Plint, A.G., 1998, Recognition of interfluves sequence boundaries: Integrating paleopedology and sequence stratigraphy: Geology, v. 26, p. 387–390.

Miall, A.D., 1988, Reservoir heterogeneities in fluvial sandstone: Lessons from outcrop studies: American Association of Petroleum Geologists, Bulletin, v. 72, p. 682–687.

Miall, A., D., 1992, Alluvial deposits, *in* Walker, R. G., and James, N. P., eds., Facies Models: Geological Association of Canada, p. 119-142.

Miall, A., D., 2006, Reconstructing the architecture and sequence stratigraphy of the preserved fluvial record as a tool for reservoir development: A reality check: American Association of Petroleum Geologists, Bulletin, v. 90, p. 989–1002.

Miller, K. G., Wright, J. D., and Browning, J. V., 2005, Visions of ice sheets in a greenhouse world: Marine Geology, v. 217, p. 215-231.

Montgomery, S. L., Tabet, D. E., and Barker, C. E., 2004, Coalbed gas in the Ferron Sandstone Member of the Mancos Shale: A major Upper Cretaceous play in central Utah, *in* T. C. Chidsey, Jr., R. D. Adams, and T. H. Morris, eds., Regional to Wellbore Analog for Fluvial-Deltaic Reservoir Modeling; the Ferron Sandstone of Utah: AAPG Studies in Geology 50, p.501-528.

Pang, M., and Nummedal, D., 1995, Flexural subsidence and basement tectonics of the Cretaceous Western Interior basin, United States: Geology, v. 23, p. 173-176.

Peterson, F., and R. T. Ryder, 1975, Cretaceous rocks in the Henry Mountains region, Utah and their relation to neighboring regions, *in* J. E. Fassett and S. A. Wengerd, eds., Canyonlands Country: Four Corners Geological Society Guidebook, 8th Field Conference, p. 167-189.

Plint, A. G., and Wadsworth, J. A., 2003, Sedimentology and palaeogeomorphology of four large valley systems incising delta plains, Western Canada foreland basin; implications for mid-Cretaceous sea-level changes: Sedimentology, v. 50, p. 1147–1186.

Plint, A. G., and Wadsworth, J. A., 2006, Delta-plain paleodrainage patterns reflect small-scale fault movement and subtle forebulge uplift: Upper Cretaceous Dunvegan Formation, Western Canada Foreland Basin, *in* Dalrymple, R. W., Leckie, D. A., and Tillman, R. W., eds., Incised Valleys in Time and Space: SEPM, Special Publication 85, p. 219-238.

Posamentier, H.W., 2001, Lowstand alluvial bypass systems: Incised *vs*. unincised: American Association of Petroleum Geologist, Bulletin, v. 85, p. 1771–1793.

Posamentier, H.W., Allen, G.P., James, D.P. and Tesson, M., 1992, Forced regressions in a sequence stratigraphic framework: concepts, examples, and exploration significance: American Association of Petroleum Geologist, Bulletin, v. 76, p. 1687–1709.

Reading, H. G., and Levell, B. K., 1996, Controls on the sedimentary rock record, *in* Reading, H. G., ed., Sedimentary Environments: Processes, Facies, and Stratigraphy: Oxford, U.K., Blackwell, p. 14-15.

Ryer, T. A., Anderson, P. B., 2004, Facies of the Ferron Sandstone, East-Central Utah, *in* T. C. Chidsey, Jr., R. D. Adams, and T. H. Morris, eds., Regional to Wellbore Analog for Fluvial-Deltaic Reservoir Modeling; the Ferron Sandstone of Utah: AAPG Studies in Geology 50, p. 59-78.

Schumm, S.A., 1993, River response to baselevel change: implications for sequence Stratigraphy: Journal of Geology, v. 101, p. 279–294.

Schumm, S.A., and Ethridge, F.G., 1994, Origin, evolution and morphology of fluvial valleys, *in* Dalrymple, R.W., Boyd, R., and Zaitlin, B.A., eds., Incised-Valley Systems: Origin and Sedimentary Sequences: SEPM, Special Publication 51, p. 11–27.

Schumm, P. S., and Khan, H. R., 1972, Experimental study of channel patterns: GSA Bullitin, V. 83, p. 1755-1770.

Sethi, P.S., and Leithold, E.L., 1994, Climatic cyclicity and terrigenous sediment influx to the early Turonian Greenhorn Sea, southern Utah: Journal of Sedimentary Research, v. 64, p. 26–39.

Shanley, K.W., and McCabe, P.J., 1994, Perspectives on the sequence stratigraphy of continental strata: American Association of Petroleum Geologists, Bulletin, v. 78, p. 544–568.

Strong, N., and Paola, C., 2008, Valleys that never were: Time surfaces versus stratigraphic surfaces: Journal of Sedimentary Research, v. 78, p. 579-593.

Sylvia, D. A., and Galloway, W. E., 2006, Morphology and stratigraphy of the late Quaternary lower Brazos valley: Implications for paleo-climate, discharge and sediment delivery: Sedimentary Geology, v. 190, p. 159-175.

Talling, P.J., 1998, How and where do incised valleys form if sea level remains above the shelf edge?: Geology, v. 26, p. 87–90.

Timár, G., 2003, Controls on channel sinuosity changes: a case study of the Tisza River, the Great Hungarian Plain: Quaternary Science Reviews, v. 22, p. 2199-2207.

Tornqvist, T.E., Wallinga, J., Murray, A.S., de Wolf, H., Cleveringa, P., de Gans, W., 2000, Response of the Rhine–Meuse system (west-central Netherlands) to the last Quaternary glacio-eustatic cycles; a first assessment: Global and Planetary Change, v. 27, p. 89-111.

Törnqvist, T. E., Wallinga, J., Busschers, F. S., 2003, Timing of the last sequence boundary in a fluvial setting near the highstand shoreline—Insights from optical dating: Geology, v. 31, p. 279-282.

van Heijst, M. W. I. M., and Postma, G., 2001, Fluvial response to sea-level changes: a quantitative analogue, experimental approach: Basin Research, v. 13, p. 269–292.

Van Wagoner, J.C.,Mitchum JR., R.M., Campion, K.M., and Rahmanian, V.D., 1990, Siliciclastic Sequence Stratigraphy in Well Logs, Core, and Outcrops: Concepts for High Resolution Correlation of Time and Facies: American Association of Petroleum Geologists, Methods in Exploration Series, no. 7, 55 pp.

Wellner, R. W., and Bartex, L. R., 2003, The effect of sea level, climate, and shelf physiography on the development of incised-valley complexes: A modern example from the East China Sea: Journal of Sedimentary Research, v. 73, p. 926–940.

Wheeler, H.E., 1958, Time stratigraphy: American Association of Petroleum Geologists Bulletin, v. 42, p. 1047–1063.

Zaitlin, B.A., Dalrymple, R.W., and Boyd, R., 1994, The stratigraphic organization of incised valley systems associated with relative sea-level change, *in* Dalrymple, R.W., Boyd, R., and Zaitlin, B.A., eds., Incised-Valley Systems: Origin and Sedimentary Sequence: SEPM, Special Publication 51, p. 45–60.

Zhu, Y., Bhattacharya, J.P., Li, W., Lapen, T.J., Jicha, B. R., Singer, B. S., 2012, Milankovitch-scale sequence stratigraphy and stepped forced regressions of the Turonian Ferron Notom deltaic complex, south-central Utah, U.S.A.: Journal of Sedimentary Research, v. 82, p. 723-746.


8
7
6
5
4
3
2
1
South
Base of Neilson Wash
Base of Parasequence 4
Base of Parasequence 4
13
12
11
10
9
North
Base of Neilson Wash
1.5x Vertical Exaggeration
Base of Parasequence 4
Base of Parasequence 4
Map of Study Outcrop within Neilson Wash
Study Outcrop
Measured Sections
Map from USGS topo., Factory Butte Quadrangle
Measured Section Symbols
Trough Cross Stratification
Ripple Cross Stratification
Climbing Ripples
Planar Rippled Cross Stratification
Planar Cross Stratification (Loose Spacing Between Lines)
Laminated (Tight Spacing Between Lines)
Hummocky Swaley Cross Stratification
Soft Sediment Deformation (De-watering Structures)
Mud Chips
Pebble & Mud Chip Lag
Root Traces / Paleosols
Plant Debris
Leaf Imprints
Fish Scales
Bioturbation (Bioturbation Index 0 - 2)
Bioturbation (Bioturbation Index 2 - 4)
Bioturbation (Bioturbation Index 4 - 6)
Massive Sandstone (No Symbol)
Paleocurrent direction with respect to outcrop orientation
Up is towards the outcrop and down is away
Measured Section Color Fill
Nonmarine Sand
Nonmarine Fines (Clay, Mud, & Silt)
Marine Sand
Marine Fines (Clay, Mud, & Silt)
Fill Symbols
Trough Cross Stratification
Ripple Cross Stratification
Climbing Ripples
Planar Cross Stratification
Laminated
Planar Rippled
Massive Sandstone (No Symbol)
Coal
Paleosol
Mud Chips
Pebble Lag
Cover
Rank of Bounding Surfaces
(after Miall, 1988 & 1992)
1st & 2nd Order
3rd Order
4th Order
5th Order
6th Order
7th Order
8th Order
Scale Bar
50 meters
Grain Size Fill
Clay
Silt
Vfl.
Vfu.
Fl.
Fu.
Ml.
Mu
Cl.
Plate 1 - Fluvial Architecture of the Neilson Wash Compound Valley System with Mapped and Interpolated Grain Size Variability.
By
Christopher Eric Campbell
May, 2013
1.5 x Vertical Exaggeration